UFRJ

UNIVERSIDADE FEDERAL DO RIO DE JANEIRO
INSTITUTO DE QUÍMICA
PROGRAMA DE PÓS-GRADUAÇÃO EM CIÊNCIA DE ALIMENTOS

LAIDSON PAES GOMES

ESTUDO DO EFEITO DA SONICAÇÃO NA PRODUÇÃO DE BIOPLÁTICOS DE QUITOSANA: ATIVIDADE ANTIMICROBIANA E COMPORTAMENTO REOLÓGICO

Rio de janeiro

2015

Laidson Paes Gomes

ESTUDO DO EFEITO DA SONICAÇÃO NA PRODUÇÃO DE BIOPLÁTICOS DE QUITOSANA: ATIVIDADE ANTIMICROBIANA E COMPORTAMENTO REOLÓGICO

Tese de Doutorado apresentada ao Programa de Pós-Graduação em Ciência de Alimentos da Universidade Federal do Rio de Janeiro, como requisito parcial à obtenção do título de Doutorado em Ciências.

Orientadores: Prof.ª Drª Vânia M. Flosi Paschoalin
Prof.° Dr° Eduardo M. Del Aguila

Rio de Janeiro
2015

LAIDSON PAES GOMES

ESTUDO DO EFEITO DA SONICAÇÃO NA PRODUÇÃO DE BIOPLÁTICOS DE QUITOSANA: ATIVIDADE ANTIMICROBIANA E COMPORTAMENTO REOLÓGICO

Tese de doutorado apresentada ao programa de pós-graduação em Ciência de Alimentos da Universidade Federal do Rio de Janeiro, como parte dos requisitos para obtenção do grau de Doutor em Ciências.

Aprovada em:26 de novembro de 2015.

Banca Examinadora

Prof.ª Drª Vânia M. Flosi Paschoalin-IQ/UFRJ

(Orientadora)

Prof.º Drº Eduardo M. Del Aguila-IQ/UFRJ

(Coorientador)

Prof.ª Drª Maria H. Rocha Leão- EQ/UFRJ

Prof.ª Drª Lourdes M. Correa Cabral-EMBRAPA

Prof.ª Drª Rossana M. da Silva Moreira Thiré-COPPE/UFRJ

Prof.º Drº Lucio Mendes Cabral-FF/UFRJ

AGRADECIMENTOS

A minha família, Nellio R. B. Gomes (pai), Jussiara P. Gomes (mãe) e Thaiga P. Gomes (irmã) pelo imenso apoio em todos esses anos de estudo e principalmente por ser a referência de educação, caráter, honestidade e profissionalismo fundamental para minha formação pessoal, permitindo chegar a esse estágio.

Ao prof° Joab T Silva (*in memorian*) pela sua incapacidade de dizer não aos alunos em busca de estágio, que após de diversas tentativas em diferentes laboratórios foi o primeiro a me dizer "sim" e permitir que eu iniciasse minha carreira cientifica.

A minha orientadora prof[a] Vânia M. F. Paschoalin pelos esforços depositados em mim, dando todo auxílio possível para o meu desenvolvimento e crescimento profissional, principalmente pela confiança no meu trabalho e no meu potencial, permitindo a minha participação na elaboração de projetos de pesquisa e do desenvolvimento dos mesmos em diferentes grupos de pesquisas sediados em variados países (Brasil, Portugal e Inglaterra).

A meu orientador e amigo prof° Eduardo M. Del Aguila, por esses oito anos de orientação e amizade, onde com toda paciência me ensinou na prática o que é e como se faz ciência. Além de me apoiar e ajudar a enfrentar todas as etapas difíceis no decorrer desses anos de convivência.

A prof[a] Cristina T. Andrade por todos esses anos de parceria bem produtivos, pela confiança e indicação para trabalhar com grupo de pesquisa na Universidade do Porto e pela disponibilidade de todos os seus orientados em me ajudar.

A prof[a] Maria P. Gonçalves, por ser essa pessoa fantástica, dona de muito conhecimento e generosidade, pela ótima recepção e auxilio tornando simples e rápida a adaptação a Universidade do Porto, por todas as historias e curiosidade sobre Portugal antes da criação do Brasil durante nossos almoços e de toda orientação no desenvolvimento do projeto.

A Hiléia K. S. Souza e José M. Campiña por me recebem como uma família, tornando minha adaptação muito fácil a Cidade e Universidade do Porto, além do empenho e parceria direta no desenvolvimento do projeto.

Aos meus amigos Artur, Claudio, Diego, Gabriel, Leandro, Pedro e Thiago que sempre me apoiaram e acreditaram no meu potencial, apesar de nunca entenderem o que eu realmente

fazia há tantos anos na faculdade, acreditando ser uma coisa muito legal e que era algo muito difícil.

A todos os meus amigos que estão e que passaram pelo LAABBM (Analy, Giseli, Patrícia, Cyntia, Karine, Val, Wilson, Julia, Diego, Davi e Rafael Luiz), que ajudaram no meu desenvolvimento e crescimento profissional dentro desses oito anos, por tornarem o ambiente de trabalho agradável e divertido e principalmente por aturarem minhas piadas e meu temperamento muitas vezes "reclamão"

A Nathalia Sales por ser um ouvido incansável de minhas historias, pelas alegrias e tristezas partilhadas e por me estimular e fazer parte das minhas evoluções durante "o segundo semestre".

As amizades que construí na cidade do Porto (Julia, Marina, Raissa, Norton, Muriel, Fernanda e Bonna), que tornaram a adaptação à vida nova muito simples e divertida, além de estamos sempre juntos nos apoiando e nos auxiliando nos momentos de dificuldade.

A Nastassia Porto por todo o tempo de convivo, por ser uma referência para o meu crescimento, me fez acreditar no meu potencial e me estimulando a ser sempre maior, mostrando um mundo de possibilidades e que eu era capaz de alcançar objetivos que acreditava estarem muito distantes da minha realidade.

A Fundação Carlos Chagas Filho de Amparo à Pesquisa do Estado do Rio de Janeiro (FAPERJ, Rio de Janeiro, Brazil), ao Conselho Nacional de Desenvolvimento Científico e Tecnológico (CNPq, Brasília, Brasil), a Coordenação de Aperfeiçoamento de Pessoal de Nível Superior (CAPES, Brasília, Brasil) pelo Programa Institucional de Bolsas de Doutorado Sanduíche no Exterior, PDSE; Proc nº 18935/12-5.

RESUMO

GOMES, Laidson Paes. Produção de nanopartículas de quitosana: sua atividade antimicrobiana e a complexação de fibras/nanopartículas na produção de filmes. Rio de Janeiro, 2015. Tese de (Doutorado em Ciência de Alimentos) Programa de Pós-Graduação em Ciência de Alimentos, Universidade Federal do Rio de Janeiro, Rio de Janeiro, 2015.

A aplicação de materiais em nano escala e nanoestruturas é uma área emergente, uma vez que estes materiais podem proporcionar soluções para desafios tecnológicos e ambientais, com o objetivo de preservar o meio ambiente e os recursos naturais. A quitosana é um polissacarídeo natural obtido a partir da *N*-desacetilação da quitina. A quitosana vem sendo largamente utilizada nas indústrias de alimentos e de bioengenharia, com proposito de encapsular ingredientes ativos em alimentos, na imobilização de enzimas, e como um veículo para libertação controlada de fármacos. As propriedades biológicas e químicas mais importantes são a sua biodegradabilidade, biocompatibilidade e bioatividade. Nanopartículas à base de quitosana vem sendo preparadas por diferentes métodos e várias aplicações vêm sendo desenvolvidas para estes produtos. Neste estudo, avaliou-se a degradação de fibras de quitosana (NS) em solução utilizando sonda de ultrassom durante diferentes períodos de tempo (S(*ts*)= 5, 15 and 30min) formando NPs (nanoprtículas), que foram caracterizadas por espalhamento de luz dinâmico (DLS), as soluções foram misturadas em diferentes proporções NS/S(*ts*) 3:7, 1:1 e 7:3. A partir de cada mistura NS/S(*ts*), foram preparados filmes que tiveram suas propriedades mecânicas, de barreira, sensibilidade à humidade, a transparência, a permeabilidade ao vapor de água (WVP) e a cor dos biofilmes avaliados. A morfologia dos filmes foi investigada por microscopia de força atômica (AFM) e microscopia eletrônica de varredura (MEV). Os resultados indicam que, através do controle das condições de sonicação e proporção da mistura, é possível ajustar a viscoelasticidade e aspecto morfológico das misturas em níveis intermédios em relação aos seus componentes individuais, com a mesma distribuição de graus de polimerização e sem a incorporação de aditivos ou plastificantes. Os resultados mostraram que foi possível modificada e controlada WVP, propriedades mecânicas e de barreira ao ajustar a proporção de mistura dos filmes produzidos. As análises cor e opacidade demonstraram uma boa transparência dos filmes com L coordenar $\geq$ 91. As imagens obtidas por AFM e SEM mostrou a presença de partículas em torno de 10-300 nm, e uma boa morfologia para os filmes produzidos a partir das mistura. As soluções coloidais mostraram partículas com raio hidrodinâmico (*Rh*) no intervalo de 220-3000 nm, e os valores de potencial zeta na gama de 24-25 mV, demonstrando uma estabilidade moderada. As atividades antimicrobianas da quitosana com diferentes distribuições de massa molar foram testadas contra patógenos alimentares. Foi avaliado o potencial zeta, a concentração mínima inibitória (MIC), a concentração mínima bacteriana (MBC), atividade antibacteriana *in vitro* e a integridade da membrana celular foi investigada contra *Escherichia coli*. Os estudos demonstram que as partículas de menor tamanho apresentam melhor atividade antimicrobiana com mesmos valores para MIC e o MBC (0,2 mg/mL) sobre a bactéria testada *Escherichia coli*.

Palavras-chave: Quitosana, Ultrassonicação, Nanopartículas, Biofilme, Atividade antimicrobiana.

ABTRACT

GOMES, Laidson Paes. Produção de nanopartículas de quitosana: sua atividade antimicrobiana e a complexação de fibras/nanopartículas na produção de filmes. Rio de Janeiro, 2015. Tese de (Doutorado em Ciência de Alimentos) Programa de Pós-Graduação em Ciência de Alimentos, Universidade Federal do Rio de Janeiro, Rio de Janeiro, 2015.

The use of nanoscale materials and nanostructures is an emerging area, since these materials may provide solutions to technological and environmental challenges in order to preserve the environment and natural resources. Chitosan is a natural polysaccharide prepared by the *N*-deacetylation of chitin. It has been widely used in food and bioengineering industries, including the encapsulation of active food ingredients, in enzyme immobilization, and as a carrier for controlled drug delivery. The most significant biological and chemical properties are its biodegradability, biocompatibility and bioactivity. Chitosan-based nanoparticles have been prepared by various methods. Falta alguma coisa. In this study, it was evaluated the chitosan-fibril (NS) degradation using sonication for different time of periods (S(*ts*)=5, 15 and 30min), forming NP (nanoparticles) that were evaluated by dynamic light scattering (DLS). Mixed solutions of NS/S(*ts*) at different ratios 3:7, 1:1 and 7:3 were used for preparing blend films by the knife coating method. The NS/S(*ts*) films had their mechanical, barrier properties, moisture sensitivity, transparency, water vapor permeability (WVP) and color were evaluated. The morphology of films was investigated by atomic force microscopy (AFM) and scanning electron microscopy (SEM). The results indicate that, through the control of the sonication conditions and mixture ratio, it is possible to adjust the viscoelasticity and morphological aspects of the mixtures at intermediate levels relative to their individual components, with the same distribution of degrees of polymerization and without the incorporation of additives or plasticizers. The results showed that it was possible modified and controlled the WVP, mechanical and barrier properties by adjusting the mixing ratio in the films produced. The color and opacity analyses demonstrated a good transparency of films with L coordinate ≥ 91. The images obtained by AFM and SEM showed the presence of particles around 10-300 nm, and a good morphology for the films produced by mixing. The colloids solutions showed particles with hydrodynamic ray (*Rh*) in the range 220–3000 nm, and zeta potential values in the range 24–25 mV, exhibiting a moderate stability. The zeta potential of chitosans and chitosan particles was around 25 mV.The minimum inhibitory concentration (MIC), minimum bacterial concentration (MBC), *in vitro* antibacterial activity and the integrity of cell membrane were investigated against *Escherichia coli*. The antimicrobial studies showed that smallest particles have a high antimicrobial activity presenting similar concentrations for MIC and MBC (0.2 mg/mL) upon the tested bacteria (*E. coli*).

Keywords: Chitosan, Ultrassonication, Nanoparticles, Biofilms, Antimicrobial activity.

SUMÁRIO

LISTA DE FIGURAS

CAPITULO I

CAPITULO II

CAPITULO III – ESTUDO ORIGINAL 1

CAPITULO IV– ESTUDO ORIGINAL 2

CAPITULO V – ESTUDO ORIGINAL 3

LISTA DE TABELAS

CAPITULO I

CAPITULO II

CAPITULO III – ESTUDO ORIGINAL 1

CAPITULO IV– ESTUDO ORIGINAL 2

LISTA DE ANEXOS

ANEXO I

Subimissão da revisão para **International Journal of Polymer Science** - CHITOSAN NANOPARTICLES: PRODUCTION BY GREEN CHEMISTRY, PHYSICOCHEMICALPROPERTIES AND APPLICATIONS IN FOOD PRESERVATION

ANEXO II

Artigo para **Food Hydrocolloids** - TWEAKING THE MECHANICAL AND STRUCTURAL PROPERTIES OF COLLOIDAL CHITOSANS BY SONICATION

1 INTRODUÇÃO

Com o avanço do conceito da química verde que busca formas mais ecológicas e menos agressivas ao meio ambiente na síntese e produção de macromoléculas vem sendo propostas. A utilização de biopolímeros pode ser uma boa alternativa na substituição de derivados do petróleo. A quitosana é uma macromolécula oriunda do processo de desacetilação da quitina, que é o segundo polissacarídeo mais abundante na natureza. A conversão da quitina em quitosana confere a essa molécula características que se enquadram no conceito de química verde, incluindo características como serem atóxicas biodegradáveis, biocompatíveis e apresentarem potencial antimicrobiano natural. Na ultima década vem crescendo de forma exponencial o número de trabalhos que apresentam diferentes aplicações para esses polímeros. A indústria de alimentos vem enfrentando problemas com as embalagens convencionais, tais como plásticos e seus derivados que são eficientes na conservação de alimentos, porém causam grande impacto ao meio ambiente e adicionam um custo significativo ao produto final. A quitosana aparece como opção na substituição desses materiais devido a suas características já destacadas e a possibilidade de produção da mesma a partir de rejeitos da indústria pesqueira (quitina oriunda do exoesqueleto de crustáceos). Outro ponto importante na produção de biofilmes comestíveis a base de quitosana é sua alta atividade antimicrobiana natural contra microrganismos patogênicos e deteriorantes, incluindo fungos e bactérias Gram negativas e positivas. Porém os biopolímeros apresentar propriedades mecânicas e de barreira relativamente pobres, o que atualmente limitam a sua utilização industrial. Em especial a sua baixa propriedade de barreira a humidade devido à sua natureza hidrofílica. No entanto sido implementada a ideia de que essas propriedades podem ser melhoradas através da utilização de nanocompósitos. A formação de um nanocompósito para melhorar as propriedades térmicas, mecânicas e de barreira tem provado ser uma alternativa promissora. Com isso a utilização de macromoléculas biológicas como a quitosana como base de embalagens bioativas vem se tormando um modo promissor e eficaz da manutenção da qualidade dos produtos alimentícios.

2 REVISÃO BIBLIOGRÁFICA

2.1 CAPITULO I

CHITOSAN NANOPARTICLES: PRODUCTION BY GREEN CHEMISTRY, PHYSICOCHEMICAL PROPERTIES AND APPLICATIONS IN FOOD PRESERVATION (Submetido para **International Journal of Polymer Science**)

Laidson Paes Gomes, Vânia M. F. Paschoalin and Eduardo Mere Del Aguila*

Universidade Federal do Rio de Janeiro, Instituto de Química - Av. Athos da Silveira 149, Cidade Universitária – 21949-909, Rio de Janeiro, RJ - Brazil.

*Corresponding author

Mailing address:

Instituto de Química, Universidade Federal do Rio de Janeiro

Av. Athos da Silveira Ramos 149 – Centro de Tecnologia – Bloco A - sala 545

Cidade Universitária - 21941-909

Rio de Janeiro, RJ, Brazil

Phone: +55 21 39887362

Fax: +55 21 39887266

E-mail: emda@iq.ufrj.br

Abstract

Biologically active biomolecules such as chitosan and its derivatives have significant potential in the food industry in view of contaminations associated with food products and the increasing concerns in relation with the negative environmental impact of conventional packaging materials. Chitosan is a biopolymer derivative of chitin, obtained from the waste of industrial fishing activities. Its unique chemical structure as a linear polycation with high charge density, reactive hydroxyl and amino groups, as well as extensive hydrogen bonding, confer a wide range of applications to this compound. It is economical and easily available and offers real potential for applications in the food industry due to its particular physico-chemical properties, short time biodegradability, biocompatibility with human tissues, antimicrobial and antifungal activities. These characteristics produce versatile substance that give this biopolymer high potential for applications in food preservation. Meanwhile, food nanotechnology as a new technology is in need of reviews regarding potentially adverse effects, as well as its many positive effects. In this review, we aim to cover some of the developments in chitosan nanotechnology by green chemistry and its applicability to the food industry using its natural antimicrobial activity due to variations in polymer molecular weight and degree of deacetylation.

Keywords: nanoparticles, chitosan, antimicrobial activity, coating, food preservation

2.1 INTRODUCTION

In the last years, the sustainable development concept has obtained important politic and social attention due to the application of “green technologies” and the use of “green products”, that contribute to sustainability through the decreasing of environmental degradation, by establishing the best ways to synthesize and obtain products necessary for the development of different areas, while at the same time reducing impacts on the environment (DAHL; MADDUX; HUTCHISON, 2007).

Green chemistry explores chemistry techniques and methodologies that reduce or eliminate the use or generation of feedstock, products, by-products, solvents, reagents, etc., that are hazardous to human health or to the environment (RAVEENDRAN; FU; WALLEN, 2003).

Solvent-free organic reactions are an important part of green chemistry and make it possible to reduce the consumption of solvents unfriendly to the environment and allow for the use of scaled down reaction vessels. Avoiding a certain solvent reduces the number of components in a reaction, stops any solvent emission problems, and circumvents any solvent recycling requirements. It is known that the best solvent is no solvent, but, if a solvent is needed, then water is usually recommended, and catalysis in aqueous biphasic systems is an industrially attractive methodology, which has found broad applications (SHELDON, 2005).

Two decades ago, however, a new approach to polymer synthesis has been developed, employing enzymes as catalysts (enzymatic polymerization) for a review, see (KOBAYASHI; UYAMA; KIMURA, 2001). *In vitro* enzymatic catalysis has been extensively used in the organic synthesis area as a convenient and powerful tool (JONES, 1986; WONG; WHITESIDES, 1994) showing several advantages, including high efficiency, recyclability, the ability to operate under mild conditions, and environmental friendliness (BAXTER et al., 2005).

Natural biopolymers are attractive for different applications in improving human health, aiding in drug or vaccine production or even in the production of food preservatives and additives, since these compounds have inherently biocompatible and biodegradable structures, are safe, and also are more easily accepted by health surveillance regulatory and inspection institutions.

All biopolymers are produced in living cells by enzymatic catalysis. Research on finding new enzymes and on the mechanisms of enzymatic reactions have been among the most important central topics in fields such as biochemistry, organic chemistry, medicinal chemistry, pharmaceutical chemistry and polymer chemistry (BRUICE, 2002).

Currently, many thousands of enzymes are commercially available and some of them have suffered modifications for industrial applications. Generally, oxidoreductases, hydrolases and isomerases are relatively stable, and some isolated enzymes among these are conveniently used as catalysts in a practical manner in chemical, food and pharmaceutical industrial plants.

All *in vivo* enzymatic reactions involve the following characteristics: (i) high catalytic activity (high turnover number), (ii) reactions under mild conditions with regard to temperature, pressure, solvent, pH of the medium, etc., bringing about energetic efficiency, and (iii) high reaction selectivity of regio-, enantio-, chemo-, and stereo regulations, giving rise to perfectly structure-controlled products. If these *in vivo* characteristics could be

obtained for *in vitro* enzymatic polymer synthesis, we may expect the following outcomes: (a) perfect control of polymer structures, (b) creation of polymers with new structures, (c) a clean and selective process without forming byproducts, (d) a low loading process that saves energy, and (e) biodegradable properties of product polymers in many cases. These are indicative of "green" nature of *in vitro* enzymatic catalysis for developing new polymeric materials (KOBAYASHI; MAKINO, 2009), and in the polymer area the interest regarding green chemistry is increasing.

Chitin is the second most abundant natural polymer in the world, after cellulose. It is comprised of N-acetilglycosamines units bound by β-(1→4) linkages. The first *in vitro* synthesis of chitin was accomplished in 1995 via ring-opening polyaddition of a chitobiose oxazoline derivative monomer (a disaccharide) catalyzed by chitinase (EC 3.2.1.14), a glycoside hydrolase of chitin working in its reverse reaction (KOBAYASHI; SAKAMOTO; KIMURA, 2001; SATO, H. et al., 1998).

Chitin is found in three different crystalline forms; α, β and γ, dependent on the arrangement of the individual chitin chains. In α-chitin, the most common chitin form, the chains are arranged in an antiparallel way, and are densely packed with both inter- and intramolecular hydrogen bonding, which explains the inability of α-chitin to swell in water and also why α-chitin is the most rigid chitin form (BAXTER et al., 2005; CARREAU, 1972; SOUSA et al., 2013). In β-chitin, the chains are packed in a parallel way (BORGES; CAMPIÑA; SILVA, 2013; BORMAN, 1990), resulting in a looser packing which can incorporate small molecules into the crystal lattice to form various crystalline complexes. The high degree of hydration and reduced packaging tightness give more flexible and soft chitinous structures, as can be seen when comparing insect cuticles composed of β- versus α-chitin. γ -chitin, the third and most controversial form of chitin, consists of two parallel strands which alternate with a single antiparallel strand.

Commercial chitin can be found with various average degrees of acetylation (DA) ranging from the fully acetylated to the totally deacetylated products. When containing higher degrees of acetylation, this polymer is soluble in very few solvents, which limits its application. Production is usually performed in heterogeneous conditions, and, because of this then, the residual acetyl substituent distribution depends on the source of chitin, on the conditions of deacetylation and on the degree of residual acetylation. It is clear that the solubility of these polymers directly depends on the average degree of acetylation but also on the distribution of the acetyl groups along the chains (BRUGNEROTTO et al., 2001).

The main application of chitin is involved with its structural modification, forming chitosan by the deacetylation process. The derivative biopolymer Chitosan (CS) is formed, when the deacetylation of chitin units is ≥60%. This compound shows higher solubility than chitin and can, after glycosidic bond hydrolysis, form olygossacharids with variable molecular weights.

2.1.1 **Chitosan (CS)**

Chitosan is primarily produced from chitin, which is widely distributed in nature, mainly as the structural component of arthropod exoskeletons (including crustaceans and insects). Structurally, chitin is an insoluble linear mucopolysaccharide (Fig. 1) consisting of repeated *N*-acetyl-D-glucosamine (Glc*N*Ac) units linked by β-(1→4) glycosidic bonds (fig. 1). The totally deacetylated chitosan molecule structure has an $–NH_2$ group and two –OH in each glycosidic residue, showing a polycationic character formed by $–NH_3^+$ radicals when in pH solutions inferior to its pKa, with $–NH_3^+$ radicals (SHUKLA, SUDHEESH K. et al., 2013). The relative amount of these two monomers (2- amine and 2- acetamide) can be modified between the chitosans, depending on the extraction and production methods and the organisms used for the extraction. The production of polymers with different physical-chemical characteristics, due to the degree of deacetylation (DD), is a consequence of the amount of deacetylated radicals (2-amine) present in the sample, varying between 60 and 95%.

The depolymerization of chitosan molecules forms oligomers with variable amounts of 2-amino and 2-acetoamido units, producing low molecular weight *chitosan* (LMWCS) ranging from 5000 to 10000 Da, which changes viscosity and pKa, among other parameters (KITTUR; VISHU KUMAR; THARANATHAN, 2003).

CS is insoluble in both, organic solvents or water. It can, however, be readily dissolved in weak acidic solutions, due to the presence of amino groups. The solubilization occurs by protonation of the $–NH_2$ on the C-2 position of the D-glucosamine repeat unit, when the polysaccharide is converted to a polyelectrolyte in acidic media (SCHRAMM, 1994). To obtain a soluble product, the deacetylation degree (DD) of CS should reach 80–85% or higher (KRAJEWSKA, 2005).

The removal of the acetate radical from the chitin molecule monomers can be carried out by different methods, such as chemical hydrolysis, often performed using acids such as

HCl, nitrous acid, phosphoric acid, and hydrofluoric acid, or alkaline treatments or enzymatic deacetylation (GOMES, LAIDSON P. et al., 2014).

The conversion of chitin to chitosan conducted by acid treatment is not used due to the breakage susceptibility of the glycoside bonds of the polymer, since oligomers obtained in his way are not bioactive, due to molecule destructuration and the possibility of environmental contamination and the creation of toxic chemical compounds (KIM, S.-K.; RAJAPAKSE, 2005).

The most common method for chitosan synthesis is the deacetylation of chitin using NaOH, which requires chitin exposure to severe temperature and NaOH concentration conditions. This process has significant yield, but higher degrees of deacetylation require more severe treatment conditions. To obtain chitosans with a degree of deacetylation of 85 to 92%, chitin should be exposed to harsh alkaline conditions, which can degrade. At the same time, there is large consumption of water and energy, as well as impacts on the environment due the large volume of discarded solvents (TAN et al., 2015).

Enzymes are used for an increasing range of applications. In fact, enzyme-catalyzed processes have been gradually replacing chemical processes in many areas of the industry, because they save energy, water and chemicals, help improve product quality, and, furthermore, present valuable environmental benefits. These benefits are becoming more important at a time of increasing awareness regarding sustainable development, green chemistry, climate change and organic production (KANG; LIANG; MA, 2014). Different hydrolytic enzymes able to catalyze the cleavage of glycoside bonds in chitosan have been isolated (AZIZ et al., 2012; LECETA et al., 2013). Cellulase, pectinase, pepsin, papain, neutral protease, lipase, and α-amylase show the ability to hydrolyze chitosans, at comparable activity levels but with different specificities (GOMES, LAIDSON P. et al., 2014; MUZZARELLI, R. A. A.; TOMASETTI; ILARI, 1994; RONCAL et al., 2007).

These enzymes are obtained from different organisms and their use for the deacetylation of chitin has been explored in order to improve process efficiency and control over the physicochemical characteristics of the formed products. These enzymes are capable of reducing chitin crystallinity and assay conditions can be adjusted to produce chitosan macromolecules with different molecular weights (MW) between 4.0-10.0 kDa. Moreover, if enzymes able to promote deacetylation of 2-acetamido monomers are associated to this process, chitosans presenting different molecular weights and different degrees of

deacetylation can be obtained (DEL AGUILA et al., 2012; GOMES, LAIDSON P. et al., 2014)

When the enzymatic conversion is compared to the commonly used chemical method, in addition to environmental impacts, such as higher power consumption and the generation of large amounts of toxic waste, the products formed during in the alkaline hydrolysis method are heterogeneous, with variable MW and DA (TSIGOS et al., 2000).

The homogeneity in size and degree of deacetylation of the formed chitosans is very important for the subsequent application of the generated product, and the higher the product uniformity, better market value will be, since they may be used in several different types of applications (BEANEY; LIZARDI-MENDOZA; HEALY, 2005).

The growing number of scientific papers and patents regarding chitosan and its applications demonstrates a surprisingly high level of research on this biopolymer, both in basic and in applied science.

The growth in the number of publications related to applications of chitosan in different subject areas in the last 15 years is exponential: in early 2015, 5475 publications were available, approximately twice the number of publications observed for 2009 (2848). Eleven years ago, not even one thousand publications were available per year (838), demonstrating the exponential increase of the study and importance of this biopolymer (fig. 2).

Areas of particular application regarding chitosan in the past 15 years are the pharmaceutical industry, such as tissue engineering and drug transport, of 20 and 21%, respectively. However, the versatility of chitosan application can be demonstrated by the diversity of uses in many areas, ranging from purification of water contaminated with metal ions to the formation of nanotubes and use as an antimicrobial agent. This versatility contributes directly to the exponential growth of studies conducted with this macromolecule, which is intrinsically related to new applications of this biopolymer (fig . 3).

2.1.2 **Chitosan bioactivities**

Many biological activities have been reported for CS, such as antimicrobial, anticancer, antioxidant, and immunostimulant effects that are dependent on its physico-chemical properties (Table 1). Food applications have already been approved by the Food and Drug Administration in Japan, Italy and Finland (KEAN; THANOU, 2010). Chitosan has not been

officially proclaimed a GRAS by the FDA in United States for use in food, although this regulatory agency has approved chitosan for medical uses, such as bandages and drug encapsulation.

2.1.2.1 Antimicrobial activity of chitosan

Among the different CS bioactivities, perhaps the most applicable in the food production chain is its antimicrobial activity, and this will be the focus of this review. The antimicrobial activity of CS is influenced by several factors, which can be classified into four categories (a) microbial factors related to the species of the target organism and cell age; (b) intrinsic factors such as the density of positive charges, molecular weight, concentration, hydrophilic/hydrophobic characteristics and chelating potential of chitosan; (c) physical state and water solubility and (d) environmental factors, such as ionic strength of the medium, pH, temperature and time of exposure to the pathogen (KONG et al., 2010).

2.1.2.2 Degree of deacetylation (DD) of chitosan

The DD is the great importance because chemical behaviors, such as solubility and acid-base behavior, of both chitin and chitosan, depends considerably on this characteristic (SORLIER et al., 2001). The DD is a parameter defined by routine analyses performed for quality control on chitin and chitosan preparations and is essential for studying their chemical structure, properties, and structure property relationships. If the DD is known, many properties can be predicted.

Several spectroscopic methods are able to determine the DD, with the most usual being X-ray diffraction (ZHANG, Y. et al., 2005), infrared spectroscopy (KASAAI, MOHAMMAD R., 2008) and nuclear magnetic resonance (solid or liquid–state) (KUMIRSKA et al., 2010).

The antimicrobial activity of chitosan is directly proportional to its DD (LIU, X. D. et al., 2001). Increases in the DD cause an increase in the number of amine groups in the chitosan macromolecule with an increase in the number of amino protonated groups (NH^{3+}) in acid media and complete dissolution in water, which results in the higher possibility of interaction between chitosan and the cell walls of negatively charged microorganisms (S. SEKIGUCHI; Y. MIURA; H. KANEKO, 1994). Generally, yeasts and fungi are chitosan-sensitive microorganisms, followed by Gram-positive bacteria, and, finally Gram-negative

bacteria (ING et al., 2012). The antimicrobial activity is higher at pH 6.0 (chitosan pKa = 6.2) when a higher number of amine groups are in the form of free bases when compared to pH 7.5 (KENDRA; HADWIGER, 1984). Other studies tested chitosans with different DD, 92.5 % and 85 %, and observed that polymers with higher deacetylation (high DD) were more effective in controlling microorganism growth (SIMPSON et al., 1997).

2.1.2.3 Molecular Weight – MW

Molecular weight is also of fundamental importance; generally chitosans with lower molecular weights and lower degrees of deacetylation exhibit greater solubility and faster degradation than their high molecular weight counterparts. Detailed characteristics of chitosan for biomedical applications are well described in a comprehensive review, where, due to the presence of the reactive functional group, chitosans were modified into various forms, such as thiolated, carboxyalkyl, bile acid-modified, quaternized (N, N, N-trimethyl chitosan; TMC), sugar-bearing and cyclodextrinlinked chitosans (COTTER; HILL; ROSS, 2005) The main methods used to determine the molecular weight of chitin and chitosan are viscosimetry (KASAAI, MOHAMMAD R., 2007), light scattering (SORLIER et al., 2003), gel permeation chromatography (GOMES, LAIDSON P. et al., 2014), osmometry and sedimentation equilibrium by ultracentrifugation (CÖLFEN; BERTH; DAUTZENBERG, 2001).

It has been shown that low molecular weight chitosans (LMW -CS) of less than 10 kDa have greater antimicrobial activity compared to high molecular weight chitosans (CS - HMW) ranging between 10 and 500 kDa (UCHIDA; M. IZUME; A. OHTAKARA, 1989). Studies with hydrochloride D-glucosamine (a chitosan monomer), however, were not effective in inhibiting bacterial growth. This suggests that the antimicrobial activity of chitosan is related not only to the cationic nature of the deacetylated glucosamine, but also with the chain length of the biopolymer (BLAGODATSKIKH et al., 2013).

Although some results about the bactericidal activity of low molecular weight chitosans are comparable, it has been reported that, depending on the bacteria strain, the conditions of the biological assays and the physico-chemical characteristics (MW and DD) of the chitosan in question, the results are not always in agreement. Studies with a 9.3 kDa chitosan have shown this macromolecule to inhibit *E. coli* growth, while a 2.2. kDa chitosan promotes the growth of this same bacteria (TOKURA et al., 1997). On the other hand, a 4.6 kDa chitosan was most active against Gram positive bacteria, yeast and fungi (TIKHONOV et

al., 2006). Thus, results with LMW-CS are still somewhat controversial and unclear, indicating that more studies are required on the inhibition mechanisms of LHW-CS.

2.1.2.4 Effect of pH

It has been shown that the antimicrobial activity of chitosan and chitosan-based films increases in lower pH. One theory postulates that the positive charge of the amine group (NH^{3+}) at lower pH values than the pKa (pH<6.3), at which this functional group carries 50% of its total electric charge, allows for interactions with negatively charged microbial cell membranes, a phenomenon which may cause leakage of intracellular constituent (HELANDER et al., 2001). However, even if this is a well recognized explanation regarding the antimicrobial effects of chitosan, there is no direct evidence demonstrating this behavior against bacteria.

2.1.2.5 Solubility properties

Although chitin and chitosan have been confirmed as being attractive biomacromolecules with relevant antimicrobial properties, their applications are somewhat limited due to both being water-insoluble. Water-soluble chitosan derivatives can be obtained by the introduction of permanent positive charges in the polymer chains, resulting in a cationic polyelectrolyte characteristic independent of the pH of the aqueous medium. This can be accomplished, for example, by the quaternization of the nitrogen atoms of the amino groups. According to Xie et al. 2002 (XIE et al., 2002), at neutral pH, the degree of protonation of NH_2 is very low, so the repulsion of NH^{3+} is weak. Under such conditions, the intermolecular and intramolecular hydrogen bonds result in a hydrophobic micro-area in the polymer chain, creating hydrophobic and hydrophilic portions, favoring the structural affinity between the bacteria cell wall and the derivative. In another study, the cell supernatants of *S. aureus* exposed to a water-soluble chitosan derivative in deionized water suggested that the water-soluble chitosan produced by the Maillard reaction may be a promising commercial substitute for acid-soluble chitosans (CHUNG; YEH; TSAI, 2011).

2.1.2.6 Derivatization

Chitosan-derivatives are usually obtained by chemical modifications of the amino or hydroxyl (especially at the C6 position in the chitosan backbone) groups, in order to improve their physicochemical properties (MARTINS et al., 2013). Some authors report that the bactericidal activity of chitosan-derivatives is stronger than that of unmodified chitosan. Jia *et al* (2001)(JIA; SHEN; XU, 2001) demonstrated that the *N*-propyl-*N*,*N*-dimethyl chitosan presents a bactericidal activity against *E. coli* 20 times higher than that of chitosan with 96% deacetylation, but with different MWs. Other authors reported that the antimicrobial activity of *N*,*N*,*N*-trimethyl chitosan (TMC) is ca. 500 times higher than that of unmodified chitosan. It has also been reported that other chitosan-derivatives, such as hydroxypropyl chitosan, *O*-hydroxyethylchitosan and carboxymethyl chitosan, among others, also exhibit significant antimicrobial activity (JIA et al., 2001; SUN et al., 2014).

2.1.2.7 Temperature and Storage

For commercial applications, it would be practical to prepare chitosan solutions in bulk and store them for further use. During storage, specific chitosan, viscosity or MW characteristics might be altered. Therefore, the altered viscosity of a chitosan solution must be monitored, since it may influence other functional properties of the solution. The stability of chitosan solutions (MW of 2025 and 1110 kDa) and their antibacterial activity against Gram-positive (*Listeria monocytogenes* and *S. aureus*) and Gram-negative (*Salmonella enteritidis* and *E. coli*) bacteria were investigated at 4 °C and 25 °C after 15-week storage (NO et al., 2006).

2.1.2.8 Microbial species

Chitosan exerts an antifungal effect by suppressing sporulation and spore germination (HERNÁNDEZ-LAUZARDO et al., 2008). In contrast, antibacterial activity is a complicated process that differs between Gram-positive and Gram-negative bacteria due to different cell surface characteristics. . In several studies, stronger antibacterial activity was apparent against Gram-negative bacteria when compared to Gram-positive bacteria (CHUNG et al., 2004), while in another study Gram-positive bacteria were more susceptible, perhaps as a consequence of the Gram-negative outer membrane barrier (ZHONG et al., 2008).

2.1.3 **The use of nanotechnology in chitosan production**

Nanoscience is an emerging field that deals with interactions between molecules, cells and engineered substances, such as molecular fragments, atoms and molecules. In terms of size constraints, the National Nanotechnology Initiative (NNI) defines nanotechnology in dimensions of roughly 1 to 100 nanometers (nm) (TOMASIK; ZARANYIKA, 1995), but in a broader range this can be extended up to 1000 nm. Particles found in this range appear to be optimal for achieving a number of important tasks, such as nano-carriers, including alterations of a drug's reactivity, strength, electrical properties, and, ultimately, its behavior *in vivo*. There is great interest in developing new nanodelivery systems for drugs that are already on the market, especially cancer therapeutics (CHO, K. et al., 2008).

The major goals in designing nanoparticles (NP) as a delivery system are to control particle size, surface properties and the release of pharmacologically active agents in order to achieve the site-specific action of the drug at the therapeutically optimal rate and dose regimen.

Nanoparticles can be prepared from a variety of materials such as proteins, polysaccharides and synthetic polymers. The application potential of a nanoparticle depends on certain factors, such as type of material (REN et al., 2009), particle shape (WANG, R. H.; XIN; TAO, 2005) and concentration (KIM, B. et al., 2003). The intrinsic properties of nanoparticles are determined predominantly, by their size, composition, crystallinity and morphology, as mentioned previously (NADANATHANGAM VIGNESHWARAN et al., 2006). The chemical composition of NP, their surface shape, charge, hydrophobicity, size (NEL et al., 2006) and the presence or absence of functional groups or other chemical compounds (MAGREZ et al., 2006) are important features that define the future applications of these compounds.

Nanoparticles have been most frequently prepared by three methods: (a) dispersion of preformed polymers; (b) polymerization of monomers; and (c) ionic gelation or coacervation of hydrophilic polymers. However, other methods, such as supercritical fluid technology (REVERCHON; ADAMI, 2006) and particle replication in non-wetting templates (PRINT) (ROLLAND et al., 2005) have also been described in the literature for application in the production of nanoparticles. The latter was claimed to maintain absolute control of particle size, shape and composition, which could set an example for the future mass production of nanoparticles in the industry (ASHOKKUMAR; GRIESER, 1999).

Over time various applications have been developed using nanoparticles prepared from either synthetic polymers or natural polymers. Among natural polymers, chitosans are widely explored for their biomedical and pharmaceutical applications (OCHEKPE; OLORUNFEMI; NGWULUKA, 2009).

CS has been explored as a material of choice to form nanoparticles for the last decade. Chitosan properties have been enhanced by making them nanoparticles. The unique character of NP, such as small size and quantum size effect could result in chitosan nanoparticles (CSNP). They are simple and inexpensive to manufacture, can be scaled-up in the production process, and have unique sizes and large surface-to-volume ratio. They are mucoadhesive and hydrophyllic in nature and, because of this; they provide good protection to encapsulated drugs, increasing their clearance time and stability in the body.

Although CS alone is considered safe for oral administration, its properties may change completely upon chemical modifications. Moreover, it is well-known that the pharmacokinetic properties of a drug or excipient change considerably when included in a nanoparticulate system. Thus, the *in vivo* fate is decided by the size, charge and surface modifications of the NPs. This, in turn, can alter the toxicity profile of the NP itself, as these properties influence the way the NPs interact with different types of cells, thus modifying their cellular uptake, absorption through the gastrointestinal tract, tissue distribution and excretion. This is the reason that the generally recognized as safe (GRAS) status of CS does not apply for nanoparticulate formulations and depends primarily upon the conditions of intended use (KEAN; THANOU, 2010).

In addition, the molecular weight and degree of deacetylation of chitosan also affect its pharmacokinetic properties and toxicity. Thus, each and every derivative should be assessed individually, both in free form and in nanoparticulate form. A recently published review by Kean and Thanou in 2010 (KEAN; THANOU, 2010) has summarized all the current findings related to CS toxicity.

Different methods have been used to prepare chitosan nanoparticles (CSNP), and the selection of the method depends on factors such as particle size requirement, thermal and chemical stability of the active agent, reproducibility of the release kinetic profiles, stability of the final product and residual toxicity associated with the final product (AZEVEDO et al., 2013). The main chitosan nanoparticles preparation methods are emulsion cross linking, emulsion- droplet coalescence, coacervation/ precipitation, ionotropic gelation, reverse micelles, template polymerization and self-assembly polyelectrolytes (BASTOS et al., 2010).

However, the selection of any of these methods depends on the nature of the active molecule, as well as the type of the delivery device.

From a technical point of view, it is extremely important that chitosan be hydro soluble and positively charged. These properties enable this polymer to interact with negatively charged polymers, macromolecules and even with certain polyanions upon contact in aqueous environment (PATEL, J.; JIVANI, 2009).

Even though chitosan nanoparticles appear to be safe in laboratory-scale studies, the knowledge of the risks involved in real-world applications leaves much to be desired, since there are some cases in which the use of chitosan nanoparticles has been questionable (KUZMA; ROMANCHEK; KOKOTOVICH, 2008). However, the use of these particles on the macroscale is questionable, as nanomaterials exhibit novel properties due to their extremely small size, high surface area, and reactivity (MELO, 2008; OBERDÖRSTER; OBERDÖRSTER; OBERDÖRSTER, 2005). Therefore, the consequences of releasing them into the environment must be assessed.

The early findings of these particles in favor of human use at the nanolevel are promising signs for their possible safe environmental applications. However, some doubts have been aroused with regard to the use of nanoencapsulated food additives and nanocoated films in food packaging (PERERA; RAJAPAKSE, 2014). However, complete toxicity effects have not yet been studied and more exposure assessments are required in order to obtain a better picture of the relationship between nanoparticle applications and their health risks. Most of the time, the risks regarding nanoparticles are assessed with their chemical composition and, to date, no widely accepted or well-defined risk assessment methods or test strategies exist explicitly designed for nanoparticles (CONG et al., 2011). It is, thus, important to gather more information regarding health and environmental risks associated with nanoparticle applications, in order to identify the proper risk assessment strategies–and implement regulatory policies to ensure the safety of these nanomaterials.

2.1.4 **Ultrasound applied to chitosan**

In the polymer area, there is also increasing interest in green chemistry, in order to design chemical products and processes that reduce or eliminate the use or generation of hazardous substances, particularly if nanoparticles will be used in human beings. Correlation between structure-property and structure-activity are often employed in the production, such as enzymatic desacetylation and other non-classical activation methods developed in

accordance with ‘green chemistry’ requirements. Ultrasonic irradiation offers important potential for the conversion of biomass raw materials such as polymeric carbohydrates to useful lower weight molecules (GOMES, LAIDSON P. et al., 2014; KANG et al., 2014; SAVITRI et al., 2014) .

The application of ultrasound is one of the most economical and simple tools for the degradation of long polymeric macromolecules. Through temperature, frequency and intensity control and polymer concentrations, the extent of the degradation is mainly determined by the sonication time (*ts*) (BAXTER et al., 2005; KASAAI, MOHAMMAD R; ARUL; CHARLET, 2008). The scission of the polymeric chains for production the polymers with molecular mass within a ts-dependent distribution can be produced in this way.

The ultrassonication technique was applied by Gallant et al 1972 (SOUSA et al., 2013) and Degrois et al 1974 (DEGROIS et al., 1974), who were the first one to study the ability of this technique in degrading starch granules. Ultrasonication is a common tool for the preparation and processing of polymer nanoparticles. It is particularly effective in breaking up aggregates and in reducing the size and polydispersity of nanoparticles (BERNE; PECORA, 1976). The physical stability and *in vivo* distribution of nanoparticles are affected by their mean size, polydispersity, and surface charge density (BODMEIER; MAINCENT, 1998). Despite the wide-spread applications of ultrasonication in nanotechnology, its effects on chitosan nanoparticles are not well understood, although there have been several reports on the ultrasonication of chitosan polymers.

High-intensity ultrasonication produces acoustic cavitation, which generates short-lived hot spots with intense local heating of 5000 °C, pressures of 1000 atm, and heating and cooling rates above 1010 K/s (SUSLICK; PRICE, 1999). These, along with free-radical formation, may mediate redox reactions and intramolecular regroupings in samples (ELPINER, 1964). Cavitation also generates rapid streaming of solvent molecules around the cavitation bubble, as well as shock waves during bubble collapse, which in turn generate very large shear forces (TANG, E. S. K.; HUANG; LIM, 2003).

Recent studies have further investigated the effects that ultrasound treatments can cause in polymer macromolecules, changing properties such as chemical composition, size, shape, surface charge density, hydrophobicity (NEL et al., 2006), polydispersity and the presence or absence of functional groups or other chemical agents (MAGREZ et al., 2006) when subjected to different treatment conditions (IZIDORO et al., 2011). Other studies have demonstrated that it is possible to improve the solubility, swelling power and the the capacity of water absorption of starch samples after ultrasound treatment (24W with 40 % amplitude

and a frequency of 20kHz) (SOUZA, H. K. S. et al., 2013). The characterization of nano products obtained by ultrasonication is extremely important to determine their possible applications.

Several methods have been developed for the production of chitosan nanospheres, such as ionotropic gelation, spray drying , emulsification, coacervation, and more recently, ultrasonication (SINHA et al., 2004). The development of stable chitosan nanospheres is limited by the ionic interaction between chitosan and the anionic compound, which may be an alginate, tripolyphosphate (TPP) , carrageenan or polyelectrolyte (KIM, S. et al., 2013).

Most–importantly, previous evidence on the ultrasonic degradation of chitosan supports that scission occurs mainly through the β-(1→4) linkage and that DD remains barely unaffected even for long sonication times (BAXTER et al., 2005; LI, J.; CAI; FAN, 2008).

2.1.5 **Evaluation of the antimicrobian activity of chitosan**

The antimicrobial potential of chitosan has been observed in different developmental stages in fungi, such as micelial growth, sporulation, spore viability and germination and the production of virulence factors. The antimicrobial activity of chitosan is further associated to physico-chemical characteristics (molecular mass, deacetylation degree and solution pH), also depends on the target organism and its developmental phase (DINA RAAFAT et al., 2008; TSAI; SU, 1999).

The natural antimicrobial properties of chitosan and its derivatives have resulted in their extensive use as commercial disinfectants, since some chitosans and derivatives have an advantage over other types of disinfectants due to their high antimicrobial activity, broad spectrum of activity and low toxicity to mammalian cells, allowing for their discard with less damage to the environment and its derivatives (LU et al., 2013a).

It has been shown that the difference between the antimicrobial potential of chitosan-based films and their derivatives may be directly involved with variations in particle size, film thickness and the structure of the matrix-forming fibers. Another study determined the structure and particle size of two different films, with particles between 74-500 μm (resembling a flake), and particles between 37-63 μm (resembling a sphere) where the antimicrobial activity of the film against *S. aureus* was higher in the film with smalled-sized, spherical shaped particles, which provides greater specific surface (TAKAHASHIA et al., 2008)

Some studies describe the CS mechanism of action as a result of the interaction between the chitosan macromolecules, that are positively charged, and the membranes of the microbial cells, that are negatively charged, with breakage occurring and, consequently, leakage of intracellular components, including proteins (JUNG et al., 1999; LIU, H. et al., 2004). The CS interacts with the cell membrane, altering its permeability (LEUBA; STOSSEL, 1986) and also acting as a chelating agent selectively binding to trace metals, thus inhibiting the production of toxins and microbial growth. CS also activates various defense processes in the host tissue (EL GHAOUTH et al., 1992), acting as a binding agent to water and as an inhibitor of several enzymes.

Another described mechanism of inhibition is the interaction between the positively charged chitosan with the cellular DNA of fungi and bacteria, which consequently inhibits the RNA and protein syntheses. This mechanism occurs only with low molecular weight chitosans (LMW-CS) which can penetrate microorganism cells. This mechanism of action is still controversial, but could explain the inhibition of Gram-positive and Gram-negative bacteria and fungi, establishing a similar mechanism of action for all, regardless of cell membrane structure, due to ionic interactions with DNA (SUDARSHAN, N. R.; HOOVER, D. G.; KNORR, D., 1992).

On the other hand, the mechanism for antibacterial activity appears to be different when considering Gram-positive and Gram-negative bacteria, due to the different characteristics of each type of cell membranes. Still, many researchers have demonstrated that there were no significant differences between antibacterial activities (WANG, X.; DU; LIU, 2004). Based on the available evidence, it seems that bacteria in general are less sensitive to the antimicrobial activity of chitosan than fungi, since their growth occurs at pH $\leq$ 6.0 (ROLLER; COVILL, 1999) It is believed that the observed differences are attributed to the characteristics of each of the studied microorganisms, mainly with regard to the growth phase of the cell, since the charge of the microbial cell surface varies depending on this parameter (BAYER; SLOYER, 1990; TSAI; SU, 1999).

Chitosan molecular weight and deacetylation degree may contribute together to the solubility of this biopolymer, thus explaining seemingly controversial results. The modification of the molecular weight changes the content of N-acethylglucosamine units in chitosan, which have both an intramolecular and intermolecular influence, resulting in chitosans with different conformations. However, increasing chitosan solubility implies in control of the deacetylation of the residues, which is sometimes a low yield process (KURITA; KAMIYA; NISHIMURA, 1991).

Chitosan definitely demonstrates a strong inhibitory effect on microorganism the growth at low pHs, since this antimicrobial activity is weakened with increasing pH (KONG et al., 2008), due to the low protonation of amino groups, which also influences in decreasing the solubility of the biopolymer (AIEDEH; TAHA, 2001; PAPINEAU et al., 1991).

The different physical states and molecular weight of chitosan and its derivatives provide distinct mechanisms of antibacterial action. Low molecular weight chitosans and water-soluble ultrafine nanoparticles can penetrate bacteria cell walls, binding with DNA and inhibition of mRNA synthesis that occurs through chitosan penetration in microorganism nuclei and interference with mRNA and protein synthesis (SUDARSHAN, N. R. et al., 1992). High molecular weight and water soluble chitosans and solid chitosans, including larger nanoparticles, in turn interact with the cell surface and alter cell permeability (LEUBA; STOSSEL, 1986), resulting in or forming an impervious layer around the cell, thereby blocking the transport of essential solutes into the cell (CHOI et al.; EATON et al., 2008).

2.1.6 **Application of antimicrobial activity in the food industry**

It is accepted that chitosan nanoparticle-based films can be effectively used in the food industry, as they provide various benefits, including good edibility, biocompatibility with human tissues, an aesthetically pleasing appearance, barrier properties against pathogenic microorganisms, atoxicity non-polluting, and low cost (GAVHANE; GURAV; YADAV, 2013). Their applications are listed in the table 1.

Food companies are looking for strategies to make their products healthier without compromising quality and consumer perception. Biopolymer nanoparticles are being studied for their ability to protect and target the delivery of bioactive ingredients, and/or to design foods with novel physicochemical or sensory attributes. An important area of current research is the identification of new sources of biopolymers and new types of preparation methods that can be used to fabricate biopolymer particles with novel or improved functional attributes. However, it is also important that the ingredients and processing methods used be economically feasible for large-scale production. In addition, the biopolymer particles produced must be compatible with food and beverage matrices, must protect encapsulated ingredients during food storage, and must release them in an active form at the desired site of action.

2.1.6.1 Food crops

Chitosan can be used primarily as a natural seed treatment and plant growth enhancer, and as an ecologically friendly biopesticide substance that boosts the innate ability of plants to defend themselves against fungal infections (EL-SAWY et al., 2010). Chitosan applications for plants and crops are regulated by the EPA, and the USDA National Organic Program regulates its use on organic certified farms and crops (LINDEN et al., 2000). EPA-approved, biodegradable chitosan products are allowed for use outdoors and indoors on plants and crops grown commercially and by consumers (USDA; EPA, 2007).

Chitosan has prevented numerous pre- and post- harvest diseases on various horticultural commodities. Microscopical observations indicate that chitosan had a direct effect on the morphology of chitosan-treated microorganisms reflecting its fungistatic or fungicidal potential. In addition to a direct microbial activity, other studies strongly suggested that chitosan induced a series of defense reactions correlated with enzymatic activities (KATIYAR et al., 2014).

The foliar application of chitosan in pepper plants decreased transpiration and reduced water use by 26-43%, while maintaining biomass production and yield. Hence, chitosan might be an effective antitranspirant to conserve water use in agriculture (BITTELLI et al., 2001; HIRANO et al., 1990) reported that coating seeds with depolymerized chitosan or its oligosaccharides typically increased chitinase activity in seedlings by 30-50%, unless the seeds had a hard cuticle. A low molecular weight chitosan (5 kDa) induced the accumulation of phytoalexins in plant tissue, decreased the total content and changed the composition of free sterols, producing adverse effects on infesters, activating chitinase, beta-glucanase, lipoxygenases and stimulating the generation of reactive oxygen species (VASYUKOVA et al., 2001).

Chitosan had been shown to increase the production of glucanohydrolases, phenolic compounds and the synthesis of specific phytoalexins with antifungal activity, and also reduces macerating enzymes such as polygalacturonases, pectin metil esterase etc (YANG, Y. et al., 2000) studied maize seeds and reported that chitosan concentrations at 2-4 g/litre resulted in positive effects on endogenous hormone content, alpha-amylase activity and chlorophyll content in seedling leaves.

In addition, Chitosan also induced structural barriers, for example, inducing the synthesis of a lignin-like material. For some horticultural and ornamental commodities, chitosan increased harvested yield, due to its ability to form a semipermeable coating, and

extends the shelf life of treated fruit and vegetables by minimizing the rate of respiration and reducing water loss. Other studies showed that chitosan at 0.1 or 0.5% increased leaf area, leaf dry weight and leaf length of soybean, lettuce and rice, whereas chitosan at 0.1% showed positive effects on leaf area, leaf length and dry weight of tomato (CHIBU, 2000). As a nontoxic biodegradable material, as well as an elicitor, chitosan has the potential to become a new class of plant protectant, assisting towards the goal of sustainable agriculture (HERNÁNDEZ-LAUZARDO et al., 2008).

2.1.6.2 Food preservation

Coatings based on chitosan were used as an antifungal agent and in enhancing the germination and quality of artichoke seeds. The effect of the formulation and thickness on seed germination (G%), fungi activity and vegetative growth were studied by Ziani et al, 2009 (ZIANI et al., 2009). Results indicated significant differences between treatments on seed germination and it was observed that all chitosans reduced the number of fungi strains and increased plant growth.

In another study, apples (*Malus domestica* Borkh. cv. Gala) were heat-treated at 38°C for 4 days (heat treatment) before or after being coated with 1% chitosan. The heat treatment + chitosan treated fruit showed the lowest respiration rate, malondialdehyde, membrane leakage, ethylene evolution and the highest firmness and consumer acceptance among the treatments (SHAO et al., 2012).

In other studies, when applied on wounded wheat leaves, chitosan induced lignification and, consequently, restricted the growth of nonpathogenic fungi in wheat. Chitosan also inhibited the growth of *A. flavus* and aflatoxin production in liquid cultures, pre-harvest maize, and groundnut, and also enhanced phytoalexin production in germinating peanut (CUERO; OSUJI; WASHINGTON, 1991). In addition, Chitosan also improved the microbiological quality of fresh cut broccoli (MOREIRA; ROURA; PONCE, 2011).

2.1.6.3 Food technology

Chitosan films have shown potential to be used as a packaging material for the quality preservation of a variety of foods. It has also been widely used in antimicrobial films to provide edible protective coating, and in the dipping and spraying of food products due to its antimicrobial properties.

In a review, Dutta et. al., 2009 (DUTTA et al., 2009) aimed to highlight various preparative methods and antimicrobial activities including the mechanism of the antimicrobial action of chitosan-based films. The optimisation of the biocidic properties of these so called biocomposite films and the role of biocatalysts in the improvement of quality and shelf life of foods has been discussed elsewhere. The use of chitosan-based edible films could be a promising technique to preserve the microbial quality of pork meat hamburgers. Its importance in the modulation of the oxygen permeability of films in order to avoid the undesirable effects of metmyoglobin (MtMb) formation was studied by Vargas et al., 2011 (VARGAS; ALBORS; CHIRALT, 2011), promoted by the lower oxygen partial pressure in the surface of the coated hamburgers. The addition of sunflower oil to chitosan-based films yielded glossier films and led to an improvement in the water vapour barrier properties when acetic acid was used as a solvent to prepare the films. Juice clarification had been successfully carried out for apple, carrot, grape, lemon, orange and pineapple juices by Rungsardthong et al. 2006 (RUNGSARDTHONG et al., 2006).

2.1.6.4 Active food packaging

Although conventional packaging materials, such as plastics, are effective for food preservation, they have created many serious environmental problems. The use of environmentally friendly, cost-effective packaging materials has gained considerable attention from scientists, and the use of bio-based active films appears to be a better solution in respect to these requirements (AIDER, 2010). The use of chitosan nanoparticle-based edible films has been reported on many occasions (DE MOURA et al., 2011). The versatility of chitosan nanoparticles has generated a wide range of applications in the food industry. The main focus has been to develop chitosan-based films to be used as packaging material to act against bacteria and fungi, to improve shelf life by preserving the food and maintaining food quality.

The interest in edible coatings is on the rise due to their ability to reduce fruit respiration and transpiration rates, and increase storage time and consistency retention (DEBEAUFORT; QUEZADA-GALLO; VOILLEY, 1998; VELICKOVA et al., 2013; VU et al., 2011). In order to achieve this purpose, their potential non-toxic, biodegradable, antimicrobial, low relative cost of production and the approval of its use as a food additive by the "*United States Food and Drug Administration"* (USFDA) were tested (KNORR, 1986).

The use of chitosan decreased the respiration rate and production of ethylene in raspberries (TEZOTTO-ULIANA et al., 2014), and has a great selective permeability to

respiratory gases, acting as a passing barrier for O_2 (ELSABEE; ABDOU, 2013). This control of gases between the fruit and the environment reduces respiration rates, 1-carboxylic-1-aminocyclepropane oxidase and syntases enzyme action, which are highly influenced by the presence O_2 (COLINET et al., 2010). The reduction of mass loss with chitosan use was also related to the formation of a selective barrier around the surface of the fruit, improving moisture loss and reducing respiration and the main metabolic processes that lead to loss of water (HAN et al., 2004; HONG et al., 2012).

Edible coatings consisting solely of chitosan or a combination of chitosan with other biopolymers, such as sodium caseinate, were applied to carrots, cheese and salami (MOREIRA, MARIA DEL ROSARIO et al., 2011). The sodium caseinate/chitosan films inhibited bacteria and yeast and can be applied to different food matrices. In other studies, acetic or propionic acid were incorporated into a chitosan matrix in bologna ham, baked ham and fresh salmon (SCHIRMER et al., 2009).

The application of high concentrations of chitosan is considered effective in the control of fruit colouring, decreasing fruit darkening and maintaining anthocyanin content, a pigment directly related to food freshness. Enzyme activity is influenced by the presence of O_2 presence inside the fruit. As chitosan forma a barrier around the fruit, darkeningis reduced. Furthermore, the positive charges present in the coating can stabilize anthocyanines, helping in maintaining fruit colour (TEZOTTO-ULIANA et al., 2014).

The United States Department of Agriculture (RATKOVICH et al., 2013) implemented a project to develop green nanotechnology for eliminating foodborne pathogens. In this study, the USDA envisaged the development of a nanoparticle wash treatment with the capability of significantly reducing or eliminating pathogenic bacteria associated with fresh or fresh-cut fruits and vegetables, to be used with minimal processing. The specific tasks involve the design, synthesis, and characterization of ultrapotent chitosan nanoparticles coated by antimicrobial peptides, the evaluation of peptide-enhanced nanoparticles as a lysis agent in realistic food processing environments, and the development of a postharvest nanoparticle electric field treatment for decreasing the bacterial load of fresh fruits and vegetables.

2.1.6.5 Food nanotechnology

The versatility of chitosan nanoparticles has generated a wide range of applications in the food industry. The main focus was to develop chitosan-based films to be used as packaging material to act against bacteria and fungi and to improve shelf life by preserving

the foodstuff and maintaining food quality. The use of chitosan nanoparticle- based edible films as a food coating has been reported with respect to a variety of food, including cheese and meat products, such as fermented sausages (WANG, X. et al., 2004). In another study, Sato et al. (2012) (SATO, A. C. K. et al., 2011) demonstrated the possibility of producing food-grade stable nanoparticles with simple processing techniques, using lecithin and sodium caseinate, which could be further used as base systems for the production of nanocapsules.

2.2 CONCLUSIONS

Chitosan is a versatile food biopolymer that has a variety of applications in all areas of food science. Chitosan possesses promising broad spectrum antimicrobial activities, and has, thus, been widely studied as a food preservative to improve food quality and extend the shelf life of perishable food products. All of these intrinsic properties vary with MW and DD, both of which are the most important characteristics of chitosan. Chitosan is, therefore, a versatile and promising biodegradable polymer for food packaging. In addition, it possesses immense potential as an antimicrobial packaging material, due to its antimicrobial activity and non-toxicity.

Inherent antibacterial properties and its film-forming ability make chitosan an ideal choice for use as a biodegradable antimicrobial packaging material that can be used to improve the storability of perishable foods. It has convincingly been proved that chitosan films exhibit good antimicrobial activity, which can help in extending food shelf life. Hence, it is no surprise if a widespread use of chitosan films is witnessed in tomorrow’s food packaging.

Acknowledgments

The authors acknowledge the financial support of Fundação Carlos Chagas Filho de Amparo à Pesquisa do Estado do Rio de Janeiro (FAPERJ, Rio de Janeiro, Brazil), Conselho Nacional de Desenvolvimento Científico e Tecnológico (CNPq, Brasília, Brazil) and Coordenação de Aperfeiçoamento de Pessoal de Nível Superior (CAPES, Brasília, Brazil).

Legends

Figure 1. Molecular structures of (a) chitin and (b) chitosan (SHUKLA, SUDHEESH K. et al., 2013)

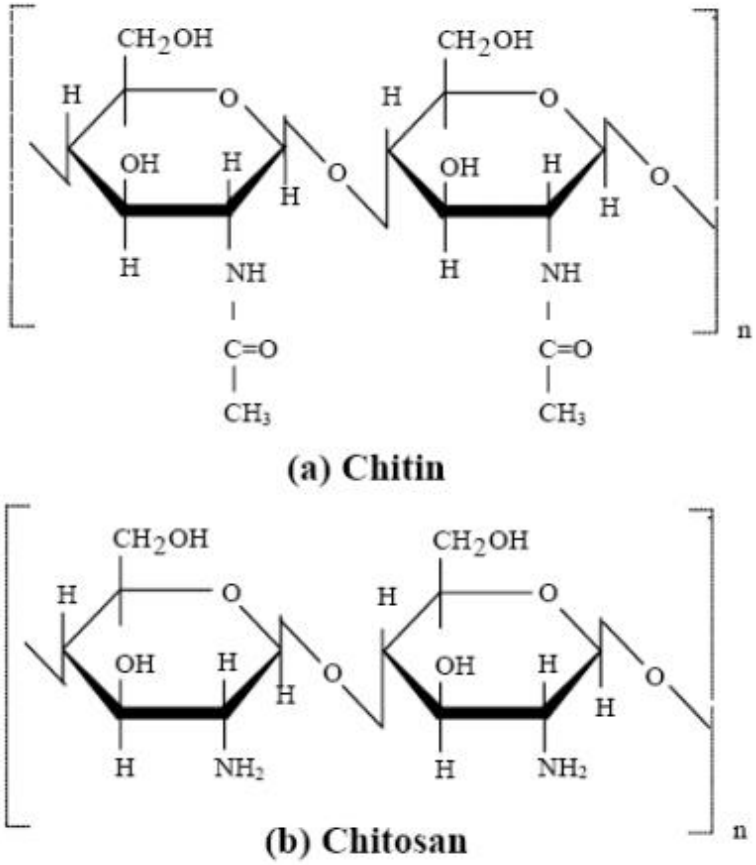

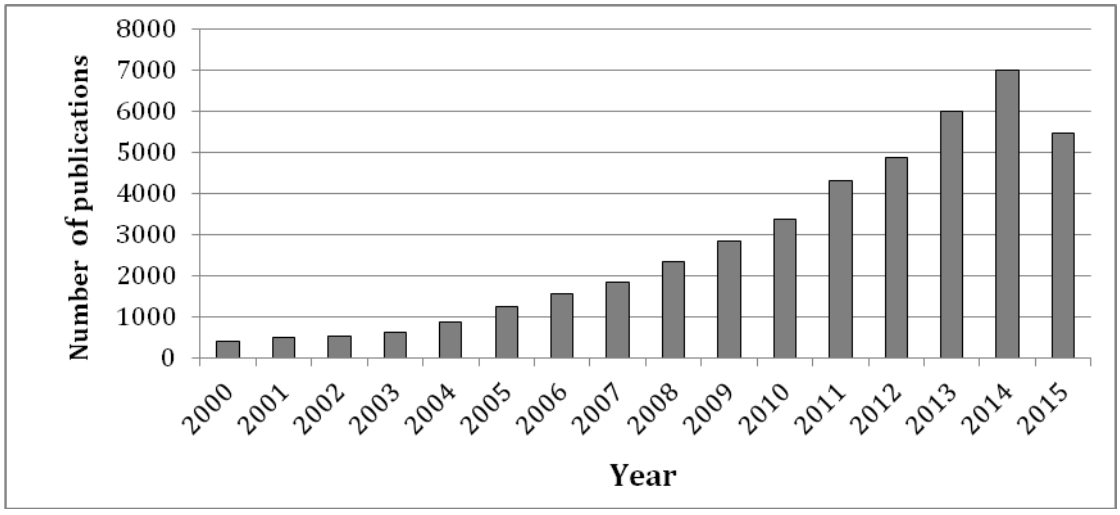

Figure 2 – Data obtained at the site sciencedirect.com – June/2015-21:00 h, search using the following words: "*Chitosan and Application*".

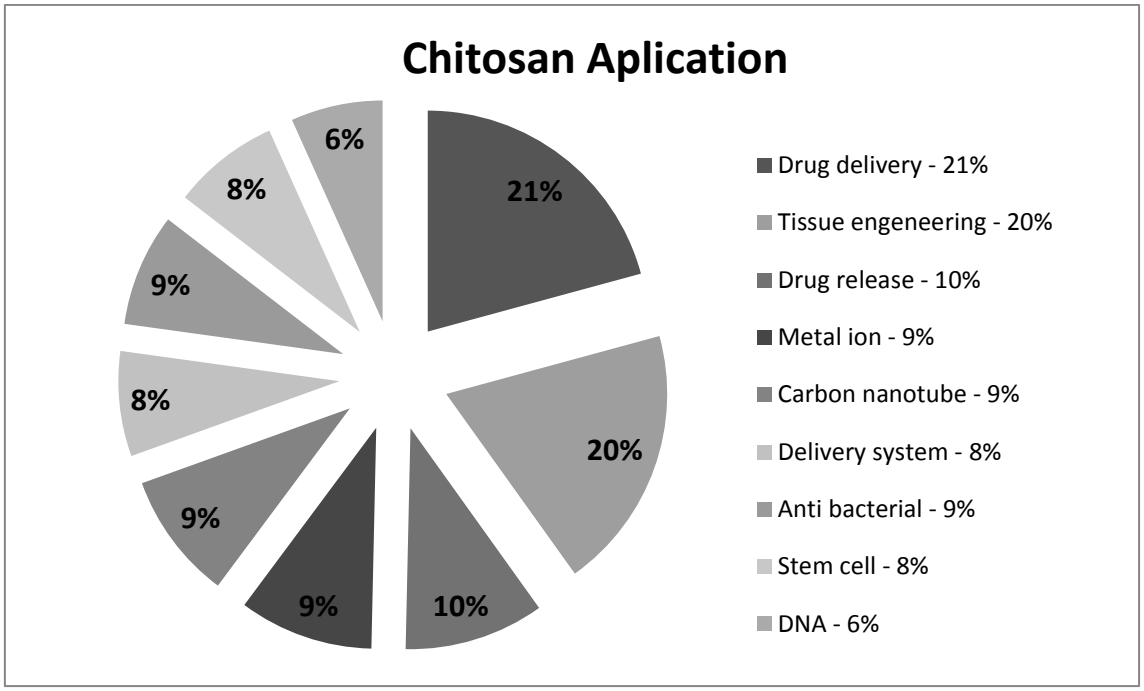

Figure 3 – Major chitosan applications. Source: sciencedirect.com – June/2015-21:00, search using the following words: “Chitosan” and “Application”, between 2000 and 2015.

Table 1. Applications of chitosan and its derivatives in the food industry (GAVHANE et al., 2013).

Use	Example	References
Antimicrobial agent	Bactericidal, fungicidal; measure of mold contamination in agricultural commodities	(MARTÍNEZ-CAMACHO et al., 2010; YANG, T.-C.; CHOU; LI, 2005)
Edible film industry	Controlled moisture transfer between food and the surrounding environment; controlled release of antimicrobial substances, antioxidants, nutrients,; reduction of partial oxygen pressure; controlled rate of respiration, temperature control	(ABUGOCH et al., 2011; AI et al., 2012; DEVLIEGHERE; VERMEULEN; DEBEVERE, 2004; KHUNAWATTANAKUL et al., 2011)
Additives	Clarification and deacification of fruits and beverages, natural flavor extender, texture controlling agent, emulsifying agent, colour stabilization	(ALBERTENGO et al., 2013; G, 2007; RUNGSARDTHONG et al., 2006)
Nutritional quality	Dietary fibre; hypocholesterolemic effect; livestock and fish feed additive, reduction of lipid absorption; production of single cell proteins; antigastritic agent	(CARREAU, 1972; LINDEN et al., 2000; MAEZAKI et al., 1993)
Recovery of solid materials from food processing wastes	Affinity flocculation; Fractionation of agar	(RENAULT et al., 2009; ZENG; WU; KENNEDY, 2008)
Purification of potable water	Recovery of metal ions, pesticides phenols and PCB´s; removal of dyes	(BORGES et al., 2013; BORMAN, 1990).

3 CAPITULO II
PROPRIEDADES MECANICAS DE FILMES E SOLUÇÕES POLIMÉRICAS

3.1 REOLOGIA

As analises reológicas levam em consideração os esforços internos que um dado material é ou não capaz de suportar, e as suas correspondentes deformações durante a aplicação de uma tensão. Portanto pode ser definida como a ciência que estuda como a matéria se deforma ou escoa, quando está submetida a um esforço originado por forças externas, podendo o material estar no estado líquido, gasoso ou sólido. Cada material possui características reológicas especificas, embora existam alguns tipos básicos de comportamento mecânico (elasticidade, plasticidade e viscosidade) que permitem analisar o comportamento reológico de inúmeros materiais, tais como fluidos.

Por definição um fluido pode ser uma substancia que não possui forma própria e assume o formato do recipiente. A resistência de um fluido contra qualquer mudança de posição irreversível de seus elementos é chamado de viscosidade. Para que se mantenha um fluxo em um fluido é necessário aplicação de uma força contínua sobre o mesmo (BRUNETTI, 2008). Os fluidos são gases ou líquidos que apresentam pequenas diferenças entre si. O gás ocupa todo o volume do recipiente, enquanto o líquido apresenta uma superfície livre (JAYAKUMAR et al., 2010). Diferentemente da relação de sólidos e líquidos quanto a respostas quando submetidos a tensões de deformação, gases e líquidos não apresentam nenhuma diferença quanto suas respostas reológicas (SCHRAMM, 1994).

3.3.1 **Classificação dos Fluidos**

Os materiais quando apresentados na forma de fluidos são agrupados em diferentes subclassificações, levando em consideração seu comportamento reológico (figura 1). Esses fluidos são classificados, quanto à relação entre a taxa e a tensão de cisalhamento, comportando-se como fluido Newtoniano (água, ar, mel, etc.) quando possuem proporcionalidade constante entre a taxa de cisalhamento e tensão de cisalhamento, caso não apresente esse comportamento são considerados fluidos não-Newtonianos apresentando uma relação não linear. Havendo ainda uma subdivisão entre os fluidos não-Newtonianos (viscoelásticos, dependentes pelo tempo e independentes do tempo) apresentada na figura 1.

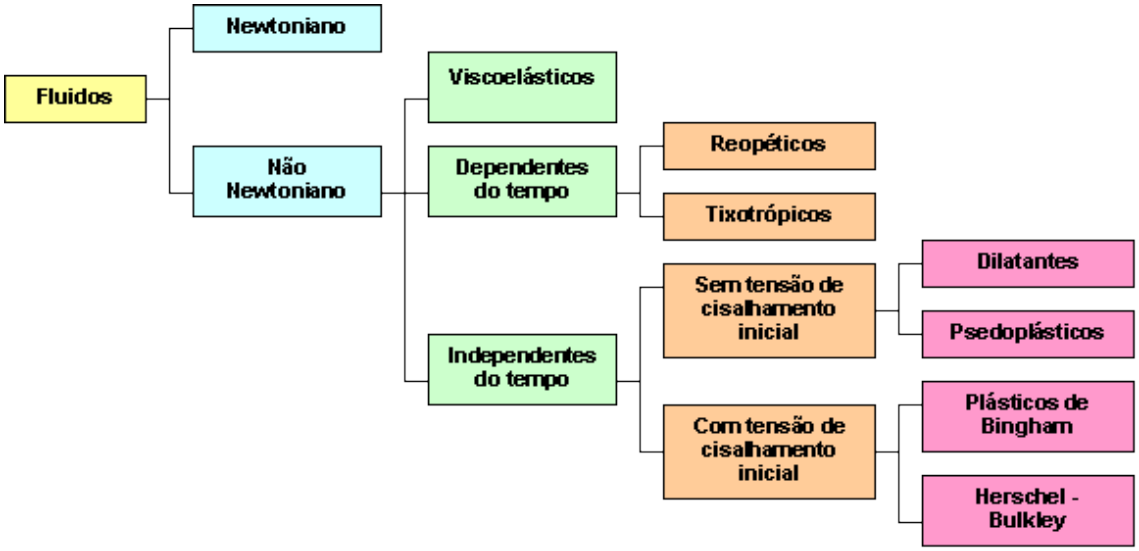

Figura 1. Classificação dos fluidos segundo seus comportamentos reológicos. http://www.setor1.com.br/analises/reologia/cla_ssi.htm

O entendimento e o controle das propriedades reológicas são de fundamental importância na fabricação e no manuseio de uma grande quantidade de materiais (PATEL, M. P.; PATEL; PATEL, 2010) como plástico (CHUNG et al., 2004), alimentos (MOHANRAJ; CHEN, 2007), cosméticos (MEGHA AGARWAL et al., 2015), tintas óleos (AGNIHOTRI; MALLIKARJUNA; AMINABHAVI, 2004), lubrificantes (SOWJANYA et al., 2013) e em processos de bombeamento de líquidos em tubulações e moldagem de plásticos (PITTS et al., 2014).

Os parâmetros reológicos para cada fluido podem ser determinados através de modelos matemáticos particulares para cada fluido, o qual influência diretamente na interpretação dos resultados de respostas do fluido. Os modelos mais comumente utilizados são os de Newton, de Ostwald de Waale (Lei das potências), de Bingham e de Herschel and Bulkley apresentadas na tabela 1. A figura 2 mostra as curvas de fluxo características referente aos modelos matemáticos mencionados acima.

A viscosidade dos fluidos Newtonianos pode ser descrita matematicamente através da experiência realizada por Newton (figura 3), onde o fluido cisalhado entre uma placa móvel e uma placa estacionaria gera a equação (1), a qual descreve o comportamento de fluidos ideais.

$$\tau = \eta\dot{\gamma} \qquad \text{equação 1}$$

Onde τ representa a tensão de cisalhamento, força por unidade de área cisalhante expresso em N/m^2 ou pascal (Pa), η é o valor da viscosidade, expresso em Pa·s e $\dot{\gamma}$ é a variação da deformação (taxa de cisalhamento) em função do tempo.

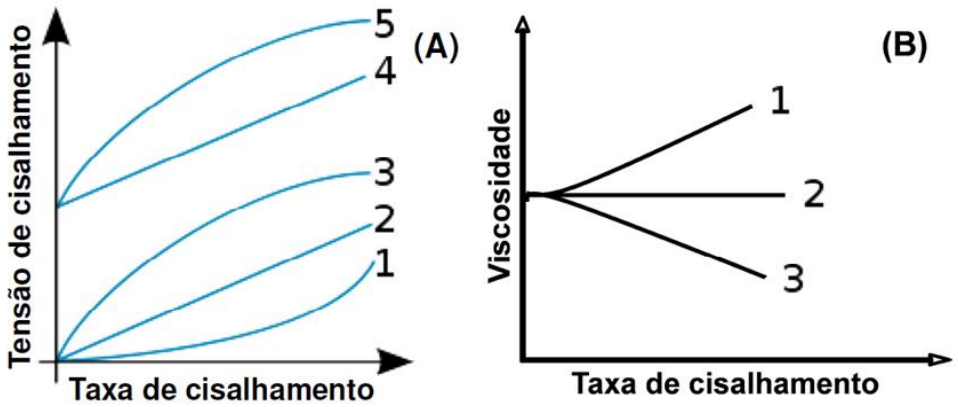

Figura 2. Representação do comportamento do fluido na Lei das Potencias. Curvas de fluxo de fluidos da potencia, (1) fluidos dilatantes, (2) Newtonianos, (3) Pseudoplásticos (Ostwald Waale), (4) Bingham e (5) Plástico (Carsson e Herschel . and Bulkley) (RATKOVICH et al., 2013).

Em geral os polímeros são moléculas que geram fluidos com comportamento não-Newtoniano, devido sua capacidade de formar géis de diferentes resistências ao fluxo, dependendo da estrutura e concentração. Como a lei de Newton não se aplica a esses fluidos existem diferentes modelos empíricos que são propostos para se calcular a viscosidade aparente desses fluidos (tabela 1). A escolha do modelo a ser aplicado depende das características do fluido, sendo a utilização do modelo correto de fundamental importância para a obtenção de resultados que expressem o real comportamento de resposta do fluido.

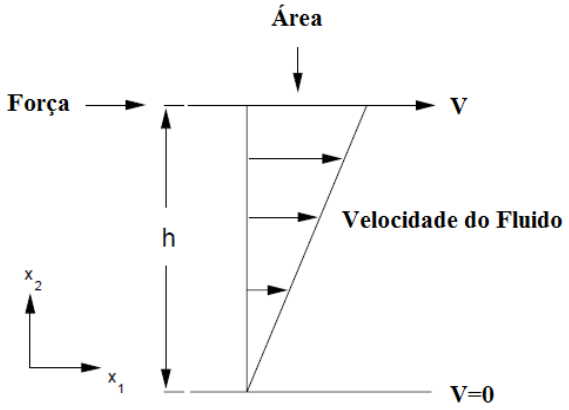

Figura 3. Fluxo entra placas paralelas.

Tabela 1. Modelos matemáticos aplicáveis a fluidos não-Newtonianos (RATKOVICH et al., 2013):

Lei da Potância (Ostwald de Waele)	$\tau = \eta_a \gamma^n$
Bringham	$\tau = \tau_0 + k\dot{\gamma}$
Herschel and Bulkely (0<n< ∞)	$\tau = \tau_0 + k\dot{\gamma}^n$
Casson	$\tau^{0,5} = \tau_0^{0,5} + \mu_\infty^{0,5}\dot{\gamma}^{0,5}$
Sisko	$\mu = \mu_\infty + k\dot{\gamma}^{n-1}$
Cross	$\frac{\mu - \mu_\infty}{\mu_0 - \mu_\infty} = \frac{1}{1 + (\lambda\dot{\gamma})^m}$
Carreau	$\frac{\mu - \mu_\infty}{\mu_0 - \mu_\infty} = (1 + (\lambda\dot{\gamma})^2)^{\frac{n-1}{2}}$

O modelo de Ostwald-de-Waele conhecido como lei da potencia é bastante utilizado para descrever comportamentos de fluidos. Durante experimentos em que visavam examinar o comportamento de fluidos sob escoamento cisalhante, Ostwald verificou que estes apresentavam comportamentos muito divergentes dos previstos por Newton, esses fluidos apresentavam uma relação entre tensão de cisalhamento (τ) por taxa de deformação ($\dot{\gamma}$) não linear. Diante disso ele propôs o modelo matemático descrito na equação 2:

$$\tau = K \ \dot{\gamma}^n \text{.....Equação 2}$$

Onde K representa o índice de consistência, o qual indica o grau de resistência do fluido diante do escoamento e n uma grandeza adimensional que representa o índice da lei das potências do comportamento do fluido, indicando o afastamento físico do modelo Newtoniano, quando $n > 1$ o fluido é considerado dilatante (figura 2, linha 1), encontrado em suspensões concentradas de amido, quando a viscosidade aparente e a taxa de deformação crescem na mesma proporção, n=1 fluido Newtoniano, nesta condição K é convertido para η (figura 2, linha 2) e $n < 1$ fluido pseudoplástico (figura 2, linha 3), em que a viscosidade aparente decresce com a taxa de deformação. A maior parte dos fluidos não-newtonianos apresentam este comportamento (MELO, 2008).

O entendimento do fenômeno reológico é baseado em duas teorias principais: (i) teorias que usam relações macroscópicas tensão-deformação-tempo e (ii) teorias moleculares que fornecem evidências de comportamento viscoelástico da estrutura e conformação molecular. Para polímeros sintéticos, ambas as relações são validas, entretanto para sistemas biológicos o que pode ser considerado uma dispersão heterogênea, exibe uma considerável variabilidade nas propriedades reológicas devido à complexidade inerente da amostra, por isso, a aplicação de modelos reológicos clássicos é limitada para certos tipos de amostra (ZOON et al., 1990).

3.3.2 **Reologia aplicada à quitosana**

A reologia pode ser utilizada para definir, por exemplo, o comportamento do fluxo de polímeros fundidos a fim de caracterizar a sua capacidade de processamento, dando percepções da estrutura molecular, e indicando influências relacionadas com a mistura de polímero ou composição.

A investigação do comportamento reológico das soluções de quitosana vem sendo realizada por meio de estudos que avaliam a influência de diferentes parâmetros: tais como composição química, concentração, força iônica, pH e o efeito do tipo de ácido, além do envolvimento do fenômeno de associação hidrofóbica ligado ao comportamento viscoelástico das soluções de quitosana (HAMDINE; HEUZEY; BÉGIN, 2005) Alguns modelos matemáticos representam de forma mais clara as respostas do material, sendo que para soluções de quitosana os modelos de Cross (CROSS, 1965) e Carreau (CARREAU, 1972) tem representado de forma mais clara seu comportamento.

A quitosana vem sendo amplamente utilizada em estudos que tem com objetivo a formação de filmes e géis através da mistura da mesma a moléculas com potencial reticulante (SCHIFFMAN; SCHAUER, 2007). Em relação à formação de géis quimicamente reticulados por meio de ligações covalente entre as cadeias com quitosana, ARGÜELLES-MONAL et al. (1998) realizaram um estudo sobre a dinâmica oscilatória de sistemas apresentados na forma de géis quitosana-glutaraldeido. Devido às características ligadas a viscoelasticidade, bem como as propriedades mecânicas e a função das ligações cruzadas que formam os géis, os autores sugeriram que a formação de um gel reticulado ocorre, devido ao comportamento das moléculas de glutaraldeido, que forma uma ponte entre as cadeias de quitosana restringindo a mobilidade das mesmas. Sistemas como esse podem apresentar várias formas no processo de relaxação, na qual a água contida nas ligações das moléculas do sistema de gel podem estar envolvidas com o processo de relaxação das ligações de hidrogênio (CHENG et al., 1998).

Estudos demonstraram propriedades reológicas e de inchamento em amostras de quitosana-polietileno, onde foi relatado que essa mistura pode ter sua capacidade de inchamento controlada pela modificação do pH do meio, e que ocorre a formação de uma rede interpenetrante na presença do óxido de etileno o que faz aumentar suas propriedades elásticas (KHALID et al., 1999). Essas propriedades reológicas apresentadas por hidrogéis pseudoplasticos podem ser alteradas dependendo do tipo e teor das substâncias misturadas e das interações que ocasionalmente irão ocorrer entre os polímeros e/ou as substâncias, BODEK (2000) com amostras de quitosana/metilcelulose ligadas a fármacos.

3.3.3 **Comportamento de polímeros em solução**

As propriedades das soluções poliméricas não são apenas dependentes das características físico-químicas dos polímeros, mas estão diretamente dependentes à sua concentração (*C*). Quando em soluções diluídas, as cadeias poliméricas se organizam de forma isolada umas das outras separadas pelo solvente, diminuindo a possibilidade de agregação das mesmas, facilitando assim a determinação, do volume hidrodinâmico e da conformação das moléculas. Estes parâmetros são de grande importância na determinação das propriedades físicas dos polímeros (KASAAI, MOHAMMAD R et al., 2008). No regime concentrado, as macromoléculas estão entrelaçadas e as dimensões das cadeias são independentes da concentração polimérica. O regime diluído e o concentrado são definidos a partir do *overlap concentration* (*C**), que é a concentração de polímero na qual as cadeias começam a se sobrepor e a *entanglement concentration* (C_e), concentração na qual acima dela

as cadeias formam emaranhados e são independentes da concentração do polímero (Figura 4). Resumindo, a solução é considerada diluída quando $C < C^*$ e soluções concentradas quando $C > C_e$ (CHO, J. et al., 2006).

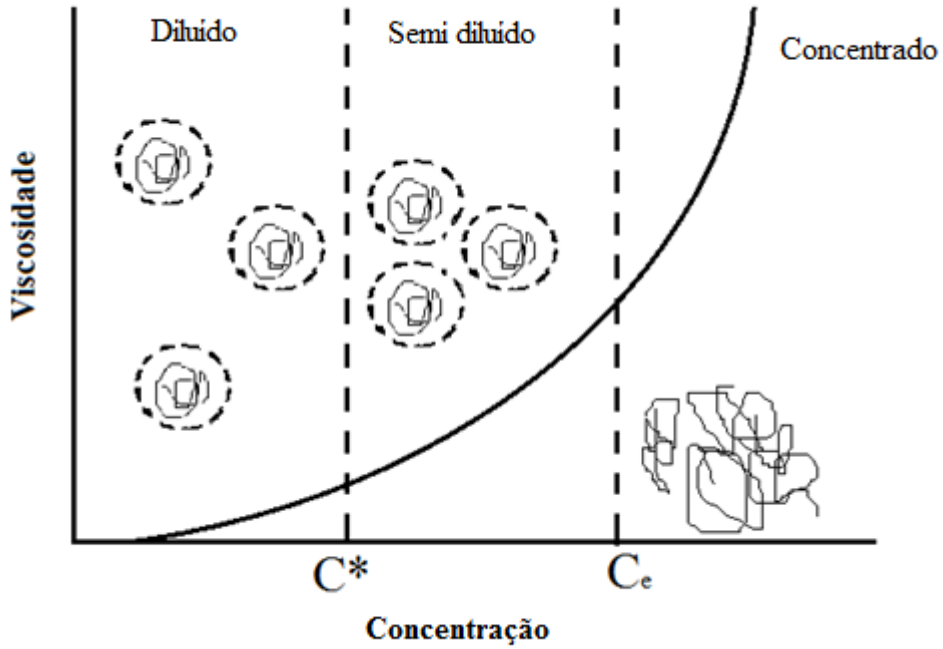

Figura 4. Representação das fases de uma solução polimérica.

Acima de *C**, as propriedades reológicas das soluções poliméricas no estado semidiluído e concentrado tem sido caracterizada em termos da constante cisalhamento simples e da pequena amplitude oscilatória de cisalhamento. A regra de Cox-Merz (COX; MERZ, 1958) vem sendo amplamente usada em polímeros fundidos, concentrados ou semi diluídos para estimar a viscosidade de cisalhamento constante $\eta(\dot{\gamma})$ a partir da viscosidade dinâmica e complexa $|\eta^*(\omega)|$, que pode ser mais facilmente obtido através da equação 3:

$\eta(\dot{\gamma})|_{\gamma \doteq \omega} = |\eta^*(\omega)|$.....equação 3

Essa regra foi aplicada com sucesso em grande número de soluções poliméricas (CARREAU; DE KEE; CHHABRA, 1997; LAUTEN; NYSTRÖM, 2000). Esse princípio pode prever $\eta(\dot{\gamma})$ a partir de medidas oscilatórias, como também pode ser prevista a $|\eta^*(\omega)|$ a partir de dados obtidos da viscosidade estacionária (*steady*) como demonstrado na equação 3. Essa estimativa pode sofre variações quando avaliada em alta frequência.

3.3.4 **Aplicação na formação de filmes**

A indústria de embalagens e de alimentos tem unido esforços para reduzir os custos sobre a produção e sobre a quantidade de embalagens de alimentos descartados no meio ambiente, introduzindo a utilização de materiais biodegradáveis, como alternativa favorável ao meio ambiente, em substituição aos polímeros sintéticos. Muitos dos materiais plásticos tradicionais, como poliestireno e polipropileno, não são biodegradáveis nem recicláveis, gerando aumento de resíduos. De acordo com a *Environmental Protection Agency* (EPA), mais de 13 mil toneladas de resíduos de embalagens plásticas foram gerados nos Estados Unidos em 2010 (KAHHAT; WILLIAMS, 2012).

Como alternativa ao uso de filmes plásticos vem sendo introduzido à utilização de filmes formados por biopolímeros, os quais são oriundos de recursos renováveis e geralmente obtidos a partir de matérias primas brutas como celulose e proteínas; a partir da síntese de monômeros bioderivados como o polilactato, ou ainda, de polímeros naturais produzidos por microrganismos como polihidroxibutirato e polihidroxivalerato (PETERSEN et al., 1999).

Polímeros biodegradáveis podem ser utilizados na forma de filmes e/ou revestimentos comestíveis. Os filmes comestíveis podem ser utilizados individualmente como cobertura de pequenos produtos alimentares, que não são constantemente embalados individualmente, tais como cerejas (YAMAN; BAYOINDIRLI, 2002), pistache (JAVANMARD, 2008) e cogumelos (EISSA, 2007). Outras aplicações de filmes comestíveis também podem ser observadas em embalagens de sopas secas ou em bebidas em pó (KROCHTA; MULDER-JOHNSTON, 1997). O interesse em coberturas comestíveis vem crescendo devido a sua capacidade de reduzir as taxas de respiração e transpiração, e aumentar o período de estocagem e a retenção de firmeza de frutos (VU et al., 2011). Além disso, filmes poliméricos biodegradáveis podem ser usados como agente carreador de diversos tipos de aditivos.

Dentre alguns sistemas de cobertura, a quitosana vem sendo testada com vantagem devido as suas características de atoxicidade, biodegradabilidade e potencial antimicrobiano, incluindo o baixo custo relativo de produção e a aprovação do seu uso como aditivo alimentar foi feito pelo "*United States Food and Drug administration" (USFDA)* (KNORR, 1986). Com isso a aplicação desses materiais pode melhorar a qualidade dos produtos alimentares.

3.3.4.1. Propriedades mecânicas dos filmes

A determinação das propriedades mecânicas dos biofilmes inclui a avaliação da resistência à tração, alongamento, deformação e modulo de elasticidade que são de fundamental importância para que o material tenha a força mecânica necessária para manter a integridade do produto durante o manuseio e armazenamento.

A resistência à tração é definida como a máxima de tensão que o material pode suportar e é considerada como sendo a carga máxima exercida sobre a amostra durante o ensaio. O alongamento é a alteração máxima no comprimento do filme antes da ruptura e é expressa como a percentagem de alteração do comprimento original do material. O modulo de elasticidade (Modulo de Young) é definido como a razão entre a tensão exercida e a deformação sofrida pelo material, representada pela parte linear inicial da curva de tensão (MCHUGH; KROCHTA, 1994). A curva típica de ensaio de tração está representada na figura 5.

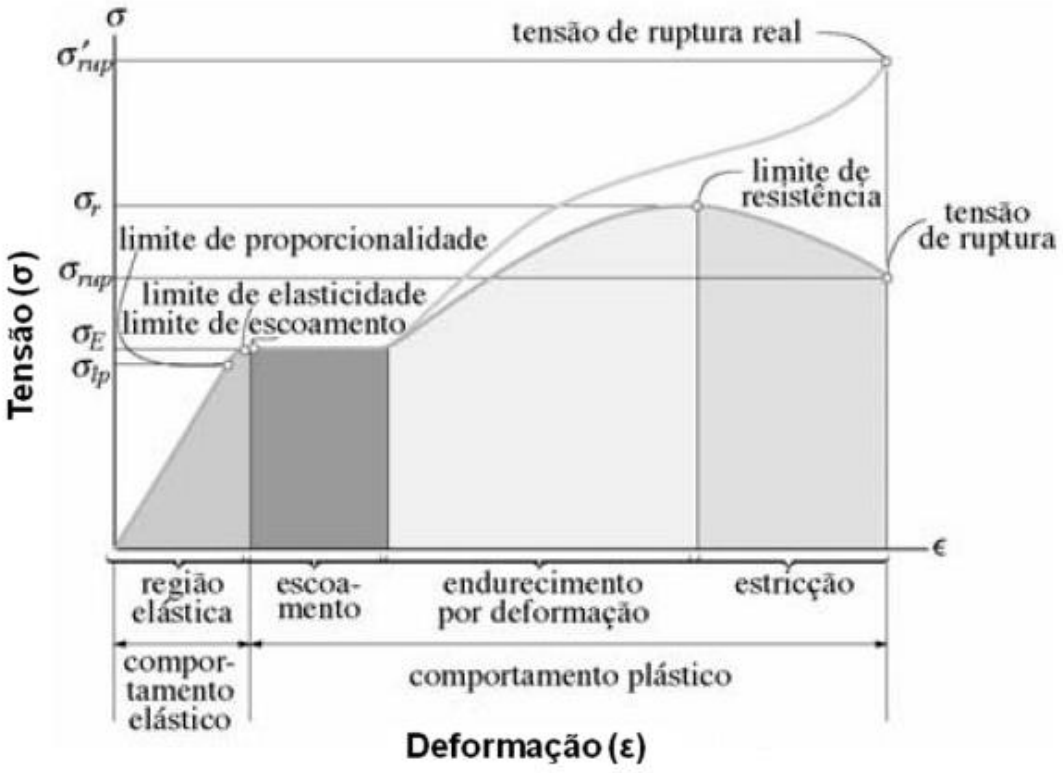

Figura 5. Curva de tensão *vs* deformação, onde a curva de tensão real expressa o comportamento de um filme polimérico (RESIN, 2010).

As propriedades mecânicas dos biofilmes dependem da composição e da condição ambiental. A incorporação de plastificantes aumenta a mobilidade das cadeias poliméricas o que leva ao aumento do alongamento e diminuição da resistência a tração (SOTHORNVIT, R. et al., 2007). Já a incorporação de outros aditivos podem melhorar propriedades do filme. A umidade no ambiente afeta diretamente as propriedades mecânicas dos filmes. Os filmes hidrofílicos absorvem a umidade mais rapidamente, aumentando o efeito da água, que age como plastificante entre as cadeias poliméricas, que por consequência diminui a resistência à tração, aumentando a extensibilidade do filme e expondo o produto armazenado a uma humidade excessiva (CHO, S. Y.; RHEE, 2002).

3.3.4.2 Propriedade de barreira

Uma parte significativa da perda de qualidade dos alimentos está relacionada com fatores ligados à transferência de umidade, gases, aroma e cor, a partir de influências do ambiente. Durante o período de armazenamento, diversas reações químicas e/ou enzimáticas são deteriorantes ao alimento, tais como, oxidação lipídica, reação de Maillard e escurecimento enzimático, bem como o crescimento de microrganismos deteriorantes que ocorre com o aumento da à atividade de água um fator critico no armazenamento de produtos alimentares. Embalagens produzidas por biopolímeros devem ter propriedades de transferência de massa apropriadas, de maneira a manter o produto conservado. A perda de umidade de frutas e legumes durante um longo período de armazenamento pode resultar em perda de massa e encolhimento (OLIVAS; BARBOSA-CÁNOVAS, 2005). Da mesma forma transferências indesejada de gases podem causar problemas, como no caso da oxidação de óleos quando expostos a uma quantidade excessiva de oxigênio devido à difusão indesejada do ambiente para o alimento, causando perda nutricional e deterioração da textura, sabor, cor e aroma, causando eventual desvalorização do produto (MATE; KROCHTA, 1996).

A natureza e composição do biofilme e as condições ambientais (umidade, pressão e temperatura) tem grande influência nas propriedades de barreira nos produtos alimentares. Polímeros com elevada polaridade (filmes a base de amido, quitosana e proteínas) possuem elevada permeabilidade ao vapor d’água, porém baixa permeabilidade a gases (MCHUGH; KROCHTA, 1994).

3.3.5 **Biofilmes de quitosana**

O uso de quitosana como base na formação de filmes, tem a capacidade de diminuir as taxas de respiração e a produção de etileno em framboesas (TEZOTTO-ULIANA et al., 2014). A quitosana apresenta excelente permeabilidade seletiva aos gases respiratórios, atuando como barreira da passagem de O_2 (ELSABEE; ABDOU, 2013).

A redução da perda de massa com o uso da quitosana também foi relacionada com a formação da barreira seletiva em torno da superfície do fruto, reduzindo: a perda de umidade e a respiração, e os principais processos metabólicos que levam a perda de água (HONG et al., 2012; SOTHORNVIT, RUNGSINEE; RHIM; HONG, 2009).

A adição de nanopartículas a matrizes poliméricas com o intuito de formar nanocompósitos a fim de melhorar as características dos filmes poliméricos (propriedades mecânicas, térmicas e propriedade de barreira) vem sendo amplamente explorada. Nanocompósitos são materiais onde um dos seus constituintes apresenta dimensão menor do que 100 nm (ARORA; PADUA, 2010). O TiO_2 e o ZnO na forma de nanopartículas são exemplos de nanopartículas que vem sendo explorados (SOTHORNVIT, RUNGSINEE et al., 2009). A adição desses nanopartículas a uma matriz, a fim de formar um nanocompósito, é capaz de altera significativamente as propriedades mecânicas, diminuir a permeabilidade ao vapor d'água e melhorar o potencial antimicrobiano dos filmes contra patógenos alimentares.

Existe um grande número de estudos que examinam o efeito da quitina/quitosana, caseinato de sódio/quitosana e ácidos orgânicos na utilização em películas para o controle do crescimento de microrganismos, com aplicação na forma de embalagem de alimentos (MOREIRA, MARIA DEL ROSARIO et al., 2011) Entretanto, pouco vem sendo estudado na avaliação das formas nanoparticuladas dessas substâncias com aplicação para o mesmo fim.

O potencial de aplicação para uma dada nanopartícula depende de alguns fatores, incluindo tipo do material (REN et al., 2009), forma da partícula (WANG, R. H. et al., 2005) e concentração usada (KIM, B. et al., 2003). As propriedades intrínsecas das nanopartículas são determinadas predominantemente a partir da forma, tamanho, composição, cristalinidade e morfologia (NADANATHANGAM VIGNESHWARAN et al., 2006). A avaliação da atividade antimicrobiana de quitosanas de baixo e médio peso molecular em comparação com conservantes usuais da indústria alimentícia (ácido benzóico e ácido sórbico), concluiu que as quitosanas apresentaram melhor atividade antimicrobiana são melhores conservantes industriais (CRUZ-ROMERO; KERRY, 2011). As nanopartículas solúveis de quitosana tem grande potencial na utilização como antimicrobiano em embalagens bioativas.

4 **OBJETIVOS**

4.1 OBJETIVO GERAL

Estabelecer uma nova metodologia para a produção de bioplásticos de nanopartículas a partir de quitosana e avaliar as suas propriedades como filme.

Estudar a atividade antimicrobiana das nanopartículas de quitosana contra patógenos alimentares.

4.2 OBJETIVOS ESPECÍFICOS

Produzir nanopartículas de quitosana de forma controlada, pelo processo de ultrassonicação;

Avaliar as características mecânicas e estruturais das soluções, produzidas a partir de diferentes proporções de misturas entre fibras/nanopartículas de quitosana, a partir de diferentes métodos reológicos;

Produzir biofilmes de quitosana a partir de misturas entre fibras/nanopartículas de quitosana;

Avaliar a influência das nanopartículas: na morfologia, nas propriedades mecânicas, na permeabilidade a vapor de água e morfologia dos filmes produzidos;

Avaliar o potencial antimicrobiano das fibras e nanopartículas de quitosana sobre patógenos alimentares;

3 CAPITULO III – ESTUDO ORIGINAL 1

TWEAKING THE MECHANICAL AND STRUCTURAL PROPERTIES OF COLLOIDAL CHITOSANS BY SONICATION (Publicado na **Food Hydrocolloids**)

Laidson P. Gomes,[1,2] Hiléia K. S. Souza,[1] José M. Campiña,[3*] Cristina T. Andrade,[4] Vânia M. Flosi Paschoalin,[2] A. F. Silva,[3] and Maria P. Gonçalves[1]*

[1] REQUIMTE/LAQV**,** Departamento de Engenharia Química. Faculdade de Engenharia. Universidade do Porto. Rua Dr. Roberto Frias, 4200-465, Porto, Portugal.

[2] LAABBM, Instituto de Química, Universidade Federal do Rio de Janeiro, UFRJ, Av. Athos da Silveira Ramos 149, CT, Bl A, sala 545, Ilha do Fundão, CEP 21941-909, Rio de Janeiro Brazil.

[3] Centro de Investigação em Química da Universidade do Porto (CIQ-UP). Departamento de Química e Bioquímica. Faculdade de Ciências. Rua do Campo Alegre, 687, 4169-007, Porto, Portugal.

[4] Programa Ciência de Alimentos, Instituto de Macromoléculas Professora Eloisa Mano, Universidade Federal do Rio de Janeiro, Centro de Tecnologia, Bloco J 21941-598, Rio de Janeiro, RJ, Brazil

Abstract

Compared to the oil-derived plastics typically used in food packaging, biofilms of pure chitosan present serious moisture issues. The physical degradation of the polysaccharide with ultrasound effectively reduces the water vapor permeability in these films but, unfortunately, they also turn more brittle. Blending chitosans of different morphology and molecular mass (*M)* is an unexplored strategy that could bring balance without the need of incorporating toxic or non-biodegradable plasticizers. To this end, we prepared and characterized the mixtures of a high-*M* chitosan with the products of its own ultrasonic fragmentation. Biopolymer degradation was followed by dynamic light scattering (DLS) and the mechanical and structural characteristics of the mixtures were evaluated from different rheological methods and atomic force microscopy (AFM). The results indicate that, through the control of the sonication time and mixture ratio, it is possible to adjust the viscoelasticity and morphological aspect of the mixtures at intermediate levels relative to their individual components. In a more general sense, it is emphasized the importance of design and materials processing for the development of a novel generation of additive-free sustainable but functional bioplastics.

Keywords: Biofabrication, Ultrasound, Colloidal Chitosan, Rheology, AFM

5.1 INTRODUCTION

The growing societal demands on sustainability and environmental protection are expected to trigger a deep transformation of industrial manufacturing. In this sense, the harnessing of abundant biomass resources must pave the way towards a greener bioeconomy. Natural biopolymers are suitable resources for biofabrication because of their good biodegradability, biocompatibility, and abundance. Chitosan (a polysaccharide obtained by N-deacetylation of chitin, its natural precursor) which is usually extracted from insect and marine crustacean shells (DEL AGUILA et al., 2012) is widely used in the food and cosmetic industries due to its good processability as hydrogels, membranes, colloidal microparticles, nanoparticles, and so on (IKEDA et al., 1993; JAYAKUMAR et al., 2010; LAPLANTE; TURGEON; PAQUIN, 2006; LIU, Z. et al., 2012; PAN et al., 2002; PILLAI; PAUL; SHARMA, 2009; SCHRAMM, 1994; SHUKLA, SUDHEESH K. et al., 2013; TOMASIK; ZARANYIKA, 1995). Due to its great versatility, the use of chitosans in a new generation of nanobiomaterials for analysis (BORGES et al., 2013), catalysis, tissue engineering (KIM, I.-Y. et al., 2008), gene-delivery, and other applications (MIZRAHY; PEER, 2012; PAYNE; RAGHAVAN, 2007), is being widely investigated.

Regarding its use in biofabrication, applications have been mainly restricted to thin films for food packaging and dressings for surgical wounds (MADHUMATHI et al., 2010; SEBTI et al., 2007). Although the replacement of non-biodegradable plastics derived from crude oil by materials based on renewable and more sustainable resources, such as natural biopolymers, has been anticipated since the early 90s (BORMAN, 1990; CHIELLINI; SOLARO, 1996; HOSOKAWA et al., 1990), the attempts to reproduce 3D objects of pure chitosan with the good organization (and structural properties) which usually characterize chitin systems in nature, have failed so far. In this respect, a significant step forward has been given very recently thanks to the development of a new manufacturing strategy that yields chitosan items in a variety of colors and shapes and with good mechanical properties for commercial exploitation (FERNANDEZ; INGBER, 2014). In the particular field of food packaging, chitosan films have evidenced poorer mechanical properties and much higher moisture sensitivity than their oil-derived counterparts (MIMA et al., 1983; NADARAJAH, 2005). Unfortunately, the large retention of water turns these films unsuitable for their use in direct contact with foodstuffs (OLABARRIETA et al., 2001). To circumvent these issues, researchers have explored using different solvents (NADARAJAH et al., 2006), chemically-

derivatized chitosans (NIKOLAEV et al., 1987), or blending chitosan with synthetic or natural compounds (referred to as *plasticizers*) (ZIANI et al., 2008).

The compatibility, miscibility, morphology, and spinnability of chitosan blends have been extensively assessed in the literature (AZEVEDO et al., 2013; FERNANDES et al., 2009; HOMAYONI; RAVANDI; VALIZADEH, 2009; KUMAR et al., 2010; RAO; JOHNS, 2008; WRZYSZCZYNSKI et al., 1995). For instance, (FERNANDES et al., 2009) found enhanced mechanical properties in chitosan/bacterial cellulose biofilms. (AZEVEDO et al., 2013) reported a notable improvement of the elasticity in biofilms of chitosan/cellulose blends. In general, the properties of these blends are mainly determined by the compatibility between their components: i.e. whether inter- and intra-molecular interactions between the polysaccharide and the plasticizer lead to an intimate combination and macroscopically uniform physical properties (KUMAR et al., 2010). However, leaving apart the controversial migration of the plasticizer into the packaged food, the brittle nature of these biomaterials remains a challenge to overcome. Ultrasonic irradiation has emerged as a rapid, easy-to-use, and low-cost tool for the degradation of biopolymers such as starch (TOMASIK; ZARANYIKA, 1995), pectins (SESHADRI et al., 2003) etc. Whereas the chosen frequency mostly determines the energy available to trigger a random or a bond-specific chain scission (in chitosan it occurs, preferentially, through the β-(1→4) linkage), the intensity and irradiation time (t_S) control the extension of the process (BAXTER et al., 2005; CZECHOWSKA-BISKUP et al., 2005; KASAAI, MOHAMMAD R et al., 2008).

Engineering films made of pure natural and biodegradable components with improved moisture resistance but still retaining good shear strength and flexibility, remains a challenge to improve the sustainability of the food packaging industry. In a recent paper, we demonstrated that the sonication of a chitosan with high degree of deacetylation (*DD*=90%) and molecular mass (*M*) induces a transition from a material mostly composed of colloidal microfibers (non-sonicated sample) to a morphology dominated by the presence of spherical nanoparticles (NPs) whose size is reduced upon increasing t_S (SOUZA, H. K. S. et al., 2013). In parallel with this transition, the mechanical properties of the corresponding biofilms turned increasingly poorer (with a significant decline of the tensile strength and Young´s modulus). Interestingly, the lowest water permeabilities were exhibited by the films prepared from the most degraded chitosans what suggests that the high surface areas and surface-to-volume ratios characterizing the nanoparticulated systems may provide a physical barrier to water molecules.

Under the light of these results, one may wonder whether using mixtures of fibrous and nanoparticulated chitosans as film precursors would bring some balance by ensuring both reasonable mechanical properties, thanks to the presence of the microfibers, and enhanced moisture resistance potentially provided by the NPs (a graphical representation of the concept is shown in Scheme 1). In this work, we evaluate these prospects by preparing colloidal mixtures of high-*M* (non-sonicated) chitosans and their corresponding low-*M* counterparts (obtained by ultrasonic irradiation) at different ratios. The viscoelastic behavior and morphology of the mixtures have been investigated by means of rheological measurements and atomic force microscopy (AFM).The dynamic light scattering technique (DLS) has been used to estimate the size distributions of chitosan colloids before, *NS*, and after sonication for different times, *S* (t_S).

5.2 EXPERIMENTAL

5.2.1 **Materials and Solutions**

For this investigation, a commercial ChitoClear® chitosan kindly supplied by Primex (Siglufjordur, Iceland) was used. This product is extracted from shrimp shells from the North Atlantic Ocean further de-acetylated to a degree of *DD*=90%. Although the average *M* was declared to fall in the range 250-300 kDa, the viscosity-average molecular mass (M_V) is over 650 kDa as it was determined in a previous work (SOUZA, H. K. S. et al., 2013). Hereinafter, we will refer to this high-*M* chitosan as CHIT90. Glacial acetic acid (Merck, purity: >99%), sodium acetate trihydrate (Merck, suprapur), sodium chloride (NaCl, Sigma-Aldrich, >99.9%), and ethanol (Aga), were all analytical grade and used without further purification. A 0.1 M acetate buffer solution pH 6.0 (ACB) was prepared in ultrapure water (18.2 MΩ s). When required, the pH was adjusted by addition of drops of glacial acetic acid or sodium acetate. CHIT90 was suspended at 3% (w/w) in this buffer and, after gently stirring for 2 h, stored at 4 °C (stock suspension). Before any measurement or ultrasonic treatment, aliquots of this stock were incubated at room temperature (RT) for 60 min. The equilibrated samples were, then, centrifuged for 20 min at 21,000 x g (9 ACC, 20 °C) with a Beckman Coulter centrifuge Alegra 25R to remove the large aggregates. Thereby, a stable colloidal dispersion of CHIT90 was obtained.

5.2.2 **Biopolymer Degradation & DLS Analysis**

After centrifugation, 30 mg aliquots of the CHIT90 dispersion were placed in ice and ultrasonicated for a period of time between 0 and 30 min increased at 2 min per sample (the so called sonication time, t_S). A SONIC ultrasonic probe (model 750 W), equipped with a 1/2" tip, was used to this end (constant duty cycle and 40% amplitude). The ultrasonic degradation of CHIT90 was followed by dynamic light scattering (DLS). For these purposes, aliquots of the sonicated dispersions were diluted 100 times and placed in fluorescence quartz cuvettes (Hellma 111-QS, 10 mm light path). The measurements were acquired at constant temperature (20 ºC) in a high-performance W130i DLS system (Avid Nano, UK) equipped with a 660 nm light source and operated at 90 º. In a previous viscosimetric study (SOUZA, H. K. S. et al., 2013), it was shown that the progressive sonication of CHIT90, under identical conditions to those applied in this work, results in a continuous decrease of the viscosity-average molecular mass (M_V) from a value of 660 kDa (non-sonicated sample) to 540 (t_S=5 min), 327 (15 min), and 291 kDa (30 min).

Although DLS analysis is commonly applied to small spherical particles (BERNE; PECORA, 1976), it also works with more complex samples containing species of different size and morphology (e.g. polymers, native proteins and their various aggregates, etc) (LORBER et al., 2012). In order to minimize uncontrolled external factors and multiple scattering effects (which typically affect the analysis of concentrated or highly polydisperse samples), 5 measurements were consecutively gathered for each sample and the results were analyzed with the software i-Size 2.0. The average values of the diffusion constant (D) and the hydrodynamic radius (R_h) were, thereby, extracted. The polydispersity index (PdI) was also estimated by comparison of the averaged autocorrelation curve with the perfect exponential of a monodisperse reference sample. From R_h and PdI, i-Size calculated the particle size distributions (plotted in respect to R_h). The statistical significance was assessed from the standard deviation of the different measurements collected for each sample. Other relevant parameters, such as the % of intensity scattered by each type of particle (% intensity), were also derived from this analysis (see Table 1).

5.2.3 **Mixture Preparation and Rheological Measurements**

The colloidal mixtures were prepared by adding the proper weight of CHIT90 stock dispersion (the non-sonicated component henceforth referred to as *NS*-CHIT90) to aliquots of the same which were previously sonicated for different times (the sonicated component or *S* (t_S)). Different *NS:S* (t_S) mixing ratios (7:3, 1:1, and 3:7) and sonication times (t_S=5, 15, 30 min) were explored. Small-deformation oscillatory measurements (frequency sweeps between 0.01 and 12 Hz) were performed with an ARG2 rheometer operated at 25 °C (TA Instruments, cone geometry: 2° angle, 40 mm diameter, and 54 μm gap). A 10% shear strain was applied in order to ensure working in the linear viscoelastic region (which was determined in preliminary experiments). Each individual test was completed in about 26 min.

The general flow behavior of the samples was further studied through rotational tests. To this end, steady-shear experiments were performed at intermediate shear rates ($\dot{\gamma}$≈0.1-300 s^{-1}). Logarithmic ramps (which reduce the initial acceleration and instrument inertia) were applied to increase/decrease the applied torque. In all cases, the samples were covered with a thin layer of paraffin oil to prevent from evaporation. Every test was completed in about 1 hour (30 min to vary the applied torque in each sense). Each rheological measurement was performed in triplicate.

5.2.4 **Atomic force microscopy (AFM)**

The morphology of the colloidal mixtures was investigated at the solid-gas interface with a PicoLe 5100 atomic force microscope (Agilent Technologies USA) operated in tapping mode. PPP-NCH-20 n^+-silicon cantilevers from Nanosensors (Switzerland) with the following characteristics were used: high aspect ratio with a tip height of 10-15 μm and radius of curvature <10 nm, low spring constant (10-130 N/m), and high resonance frequency (204-497 kHz). The mixtures were diluted 10^3 times and 100 μL aliquots were subsequently drop-casted onto freshly cleaved discs of mica (Muscovite V-4, 15 mm diameter). The samples were air dried for about 20 min, then, washed with ultrapure water and dried under a nitrogen stream. The resulting substrates were scanned in topography and amplitude with a resolution

of 512 x 512 pixels over representative regions of 5 x 5 μm^2. The raw AFM data was processed using the software Gwyddion 2.25. In order to correct bow/tilt artifacts, the images were flattened line-by-line in the horizontal direction with a quadratic polynomial. Caribbean and green color palettes were added to the topographic and amplitude images, respectively. Gwyddion was also used to extract relevant statistical parameters such as the average root-mean-square surface roughness (R_{MS}) and the average height (H_{AV}).

5.3 RESULTS AND DISCUSSION

5.3.1 **DLS Studies**

The colloidal particle distributions calculated for the sonicated samples are displayed in Figure 1a. For simplicity, only the curves for t_S=4 (red solid line), 8 (green), and 20 min (blue), are shown. The distribution for the non-sonicated sample (t_S= 0; i.e. *NS*-CHIT90) has also been included for comparative purposes (black solid line). For each single peak, the centre values of the R_h and the amplitude of scattered light have been extracted (Table 1). Starting with the analysis of the *NS*-CHIT90 sample, three major bands centered at R_h = 0.02 (peak 1), 0.18 (peak 2), and 19.5 μm (peak 3) can be distinguished. This evidence indicates that this commercial product is characterized by a high degree of polydispersity what: (1) is well supported by the high polydispersity index derived from the mathematical analysis of the data (*PdI*=3), and (2) agrees with the conclusions of a previous investigation on the morphology of this material (SOUZA, H. K. S. et al., 2013). The atomic force microscopy (AFM) data published in the latter work unveiled the presence of low-*M* chitosan, under the form of spherical nanoparticles of about 300 nm in diameter (LMCH-NPs), lying on top of a polymeric matrix with dimensions in the microscale (HMCH-microfibers). The scanning electron microscope (SEM), confirmed the coexistence of HMCH-microfibers and different types of LMCH, mainly: (1) nanofibers of about 150 nm, and (2) much smaller spherical NPs of 10-20 nm (not seen in AFM). Hence, the size distribution derived from the DLS measurements in this study; which supports the coexistence of HMCH-microfibers (peak 3) and LMCH-NPs of medium (peak 2) and small size (peak 1); is in good agreement with the microscopic evidence reported there.

Further analysis of the DLS data also returned the percentages of light intensity scattered by each individual type of colloid (Figure 1b and Table 1). The results show that up to a 48% of the intensity scattered by *NS*-CHIT90, occurred through the HMCH-microfibers (open squares in Fig 1b). In parallel, the LMCH-NPs of medium size were responsible for a similar percentage (46%, open circles). In big contrast, the smallest NPs contributed only to a 5.7% of the scattered intensity (explaining, perhaps, why they were not seen under the AFM in the referred work). In conclusion, the commercial chitosan used in this study can be roughly considered as composed of HMCH-microfibers and LMCH-NPs (of about 200 nm) in a 1:1 ratio. The effect of ultrasonication on this colloidal system can be inferred, in first place, from the evolution in the intensity of the peaks in Fig 1a. By increasing t_S, the intensity of the light scattered by the HMCH-microfibers was dramatically reduced as indicated by the decrease of peak 3. In contrast, the scattering induced by both types of LMCH-NPs was shown to increase (peaks 1 and 2). Nonetheless, while the contribution of the smallest NPs did it in a very slightly way (as indicated by the small changes in peak 1), the intensity scattered by the medium-sized NPs increased significantly. These observations support the continuous degradation of the HMCH-microfibers in favor of a concomitant increase in the population of LMCH-NPs (especially those of medium size).

This fact is not only accounted by the discussed increase of the light scattered by LMCH-NPs with peak R_h (i.e. through the increase of peak intensities) but may also be reflected in an increase of light scattered by NPs with R_h in the vicinity of the peak values (i.e. through peak broadening). Such a behavior was noticed after increasing t_S from 4 to 8 min. In contrast to the expected behavior, the intensity of peak 2 decreased. However, it was significantly widened as well (the integrated area grew from 7.3 to 10.4 nm, see Table 1). This evidence suggests that, for this specific experiment (8 min), sonication produced slightly more polydisperse patterns characterized by larger contents in colloids with R_h surrounding the central peak values (further investigation is still required but experimental issues such as the lack of a full control of the temperature in these experiments, could underlie this behavior). After all, the relevant fact is that the integrated areas shown in Table 1 for both peaks confirm the increased populations of *LMCH-NPs* compared to the *S* (4 min) sample, thus, following the general trend described above.

Obviously, the scission of the HMCH-microfibers to LMCH-NPs can also induce slight shifts in the positions of the peaks as observed in the figure. The average peak values calculated in the range 0-30 min are: 28 ± 10 (peak 1), 220 ± 50 (peak 2), and 18000 ± 3000

nm (peak 3). The evolution in the contribution of each type of colloid to the scattering of light was studied as function of t_S. Figure 1b shows the percentage of intensity scattered by HMCH-microfibers (open squares) and LMCH-NPs of medium (open circles) and small size (open triangles) in the samples irradiated for different times. Despite the complexity of the samples, correlation factors as high as R^2>0.97 were obtained from the linear regression of the data registered for the two major colloids (i.e. the microfibers and the medium-sized NPs).

According to these results, the contribution of the microfibers to the scattering of light drops linearly when t_S is increased. Concomitantly, a linear increase in the % intensity of medium-sized NPs is also noticed. It is noteworthy that the slopes were nearly identical in both cases (in absolute value, 1.57 vs 1.64 min^{-1}, respectively). This evidence seems to confirm that the degradation of HMCH by sonication feeds the increase in the populations of the LMCH-NPs. As it was suggested from the little changes detected in peak 1 (Fig 1a), the modest increase in the % intensity of the smallest NPs seems to confirm that the degradation of HMCH-microfibers in *NS* CHIT90 mostly yields LMCH-NPs of medium size. The general conclusions are: (1) sonication degrades HMCH-microfibers in CHIT90 at an apparent constant rate, (2) degradation seems complete for t_S<25 min (beyond this value, % intensity is almost negligible), (3) the degradation of the HMCH-microfibers mainly produces, at nearly identical rate, LMCH- NPs with average size of 220 ± 50 nm, (4) the smallest NPs (28 ± 10 nm) appear to be a minor product of sonication under the studied conditions.

5.3.2 **Mechanical Tests under Dynamic Shear**

Mechanical spectra were recorded for the mixtures (colored symbols in Figure 2) prepared with 7:3 (up triangles), 1:1 (down triangles), and 3:7 ratio (stars) by sweeping the angular frequency of the shear (ω). The *S* components were previously sonicated for t_S=5 (panel a), 15 (panel b), and 30 min (panel c). The storage (G´) and loss (G´´) moduli are represented in Figure 2 by filled and open symbols, respectively. The measurements performed for the individual *NS* and *S* (t_S) components (black squares and circles, respectively) have been also included in each panel for comparison purposes. As seen in the figure, G´´ exhibited higher values than G´ in every case. Only in the case of the *NS* sample, both curves showed to converge at high ω (with a hypothetical crossover beyond the upper

limit of ω =100 rad s^{-1}). According to Steffe et al. (1996) (HANAOR et al., 2012), this behavior is typical of viscoelastic fluids. In contrast, as stated by Rao et al. (2010) (TANG, H. et al., 2010), the energy required for deforming liquids with G´´ >> G´ is dissipated viscously what induces a liquid-like behavior. The data collected for the isolated *S* (t_S) components illustrates well how by increasing t_S: (1) the magnitude of both moduli decreased in the whole frequency range, and (2) the (log G´´- log G´) differential followed a clear increase.

These effects were already unveiled in our previous work and were attributed to a continuous decrease in the viscoelasticity of the solutions occurring in parallel to the increase in the irradiation time (SOUZA, H. K. S. et al., 2013). This behavior indicated a continuous decline of the entanglement as the degradation progresses. As the sonication of chitosan does not change significantly the *DD*, then, the reduction in the entanglement of the biopolymer has to be primarily ascribed to the decrease in the average molecular mass and the corresponding effects in the size and morphology of the colloids (which were investigated above with the DLS technique). It is noteworthy that the continuous decrease of the molecular mass under sonication was demonstrated in the referred work from viscosimetric measurements (SOUZA, H. K. S. et al., 2013). These conclusions become more evident after analysis of the *tan* δ *vs.* ω curves in Figure 3. This parameter, which was calculated from the data in Fig 2 as *tan* $\delta = G''/G'$, reflects the overall elasticity of the samples and is expected to decrease as the elastic modulus of the studied material increases. As shown in Figure 3a for the isolated components (filled symbols), the lowest values were registered for the *NS*-CHIT90 (black squares) what confirms the greater elasticity of this sample. By increasing t_S from 0 (black squares) to 30 min (blue diamonds), *tan* δ increased progressively reflecting the reduction in elasticity (increased liquid-like behavior) of the sonicated samples.

The data calculated for different mixtures are presented in Figure 3b (colored open symbols). Regardless of the applied t_S, reducing the amount of *NS*-CHIT90 in the mixtures resulted in a progressive decrease of the elasticity (increased values of *tan* δ) in the whole frequency range. The poorest viscoelastic properties were always found for the 3:7 mixtures (open stars) which contain the larger fraction of sonicated components. Moreover, the lowest moduli and the highest *tan* δ values (compared to the pure *NS*), were found for the mixtures prepared with *S* (30) (blue open symbols). As discussed in section 3.1, this component seems to be the richest in LMCH-NPs and the poorest in HMCH-microparticles. Hence, depending on the applied t_S and the *NS:S* (t_S) ratio, mixtures can be obtained exhibiting different

viscoelastic properties (as clearly inferred from Figs 2 and 3) but always within the limits defined by the response of their individual components. Indeed, from all the investigated mixtures, only those prepared with *S* (15) and S (30) in 7:3 ratio, exhibited a similar mechanical response. All this is indicating that, through the proper selection of these parameters, the response of the colloidal mixtures to a dynamic shear can be fine-tuned to a desired degree not achievable by their single isolated components.

In this sense, whereas the mixtures prepared with *S* (5) showed to behave more closely to the *NS*-CHIT90 (see Figs 2a and 3b), the ones prepared with *S* (15) and *S* (30) presented viscoelastic properties closer to the ones of their pure *S* components (Figs 2b, 2c, 3a and 3b). In summary, the viscoelastic properties of the commercial chitosan investigated in this work can be tweaked via its mixing with the products of its own sonication. In this respect, the elasticity of the resulting mixtures can be effectively reduced by: (A) increasing the fraction of the sonicated components, and/or (B) increasing the time of exposure of CHIT90 to the ultrasounds.

5.3.3 **Steady Shear Measurements**

Further rheological characterization was performed through the implementation of steady-shear methods. Flow curves (apparent viscosity, η_A, *vs* shear rate, $\dot{\gamma}$) were recorded by using a steady state flow ramp in the 0.1-300 s^{-1} range of shear rate (Figure 4). From the perfect match found in all cases for the increasing (filled symbols) and decreasing (open symbols) flow curves, it is evidenced a time independent flow behavior which is typical of non-thixotropic fluids. In line with the behavior expected from the dynamic data presented in the previous section, the highest values of η_A in the whole range of shear rate were exhibited by the *NS* component (black squares in all panels). In the case of the *S* (t_S) components, η_A showed to decrease (from the high levels of *NS*) with increasing t_S (black circles in all panels). The curves registered for the *NS* and *S* (5) samples exhibited two distinct regions (black squares and circles in Fig 4a): (A) in the low $\dot{\gamma}$ range, η_A is nearly shear-independent what indicates a Newtonian-like behavior; and (B) for higher $\dot{\gamma}$, η_A decreases following a power law which evidences a typical shear-thinning flow behavior.

In the first zone, the disruption of intermolecular entanglements by the action of shear force is well balanced by the formation of new ones so that no net change occurs and the zero-shear viscosity is maintained. However, by increasing $\dot{\gamma}$, entanglement disruption turns predominant over formation and the molecules tend to align in the direction of flow what results in a decrease of the viscosity. Increasing t_S, not only resulted in a shift of this transition to higher values of $\dot{\gamma}$ but also reduced progressively the contribution of the shear-thinning. This is well illustrated by the almost pure Newtonian response registered for the *S* (30) sample (black circles in Fig 4c). Agreeing with previous interpretations, this behavior must be due to a significant decrease in the size of the chitosan colloids (CHUNG et al., 2004; COTTER et al., 2005). Regarding the behavior of the mixtures, the viscosity clearly dropped with decreasing the mixing ratio whatever was the *S* (t_S) component studied. In fact, the lowest viscosities were consistently found for the 3:7 mixtures.

Whereas the magnitude of all these changes was relatively small in the mixtures containing *S* (5) (which exhibited η_A values very close to those of the *NS* CHIT90 at any mixing ratio), much larger variations occurred in the mixtures of *S* (15) and *S* (30). In fact, agreeing with that found in the dynamic tests, the lowest viscosities were consistently found for the richest mixtures in these components (see Figs 4b and 4c). Shear-thinning was also shown to decrease in these mixtures by decreasing the mixing ratio. In particular, while the mixtures of *S* (5) and *S* (15) still exhibited some sort of power law decay, the richest mixture in *S* (30) showed an almost negligible shear-thinning. In general, these results are fully compatible with the conclusions drawn in the previous section. Polymeric fluids undergoing transitions from Newtonian to shear-thinning behavior are usually modeled with the Cross and Carreau equations, respectively (BASTOS et al., 2010; CARREAU, 1972; SOUSA et al., 2013; TOMASIK; ZARANYIKA, 1995):

$$\eta_A = \eta_\infty + [(\eta_0-\eta_\infty)/1+(\tau\cdot\dot{\gamma})^M] \quad (1)$$

$$\eta_A = \eta_\infty + [(\eta_0-\eta_\infty)/(1+(\lambda\cdot\dot{\gamma})^2)^N] \quad (2)$$

where η_A, η_0, and η_∞, are the apparent, the zero-shear rate, and the infinite-shear rate viscosities, respectively, in units of Pa·s; τ and λ are time constants given in s; and *M* and *N* are dimensionless constants related to the power law exponent *n* (*M*=1−*n* and *N*=(1−*n*)/2, with $0 \leq N < 0.5$ for $\eta_\infty << \eta_A << \eta_0$). Assuming that $\eta_0 >> \eta_\infty$ (in this study η_A was never close to η_∞), equations 1 and 2 can be simplified to:

$$\eta_A = \eta_\infty + [\eta_0/A] \quad (3)$$

with $A=1+(\tau\cdot\dot{\gamma})^M$ (Cross) or $A=(1+(\lambda\cdot\dot{\gamma})^2)^N$ (Carreau).

The data collected during the increasing shear rate excursion (filled symbols in Fig 4) were fitted to the simplified Cross (grey straight lines) and Carreau (violet dashed curves) models. Table 2 summarizes the fitting data and includes the residual sum of squares (RSS) and the mean relative deviation (MRD) to assess the quality of the correlations. In general, as it is indicated by the low values obtained for these parameters, the steady shear data gathered for the isolated components and their mixtures fitted reasonably well to both models. The slightly lower values returned from the fittings to the Cross model indicate a slightly better suitability of the latter to describe the studied systems. Newtonian fluids are typically characterized by negligible values of *M* and *N*. Therefore, the non-negligible values derived from these fittings must be taken as an indicator of the degree of departure from a purely Newtonian behavior. In this regard, the decreasing relevance of shear-thinning upon increasing t_S matches perfectly with the concomitant decrease of these constants in the *S* (t_S) series. In the case of the mixtures, and irrespective of the applied t_S, the constants decreased in parallel to the increase in the fraction of the sonicated components.

On the other hand, τ and λ can be regarded as relaxation constants that indicate the onset for shear-thinning. Their drastic reduction in the sonicated components (in respect to the maximum values recorded for *NS* sample), confirms the great effect of the ultrasonic treatment on the viscoelastic response of the colloidal suspensions of the biopolymer. In the case of the mixtures, the magnitude of the returned constants fell always within the range of values delimited by those for their *NS* and *S* components. Nonetheless, while the relaxation times for *S* (5) mixtures were only slightly lower than those found for *NS*, in the case of *S*(15) and S (30), the reduction fell closer to the values registered for the pure sonicated components. Interestingly, these parameters exhibited very little dependence on the mixing ratio.

5.3.4 **Cox-Merz Rule and Temperature Effect**

Despite there is no theoretical link between the data coming from the mechanical tests under steady and dynamic shear conditions, Cox and Merz found a very good empirical correlation between them in certain systems (COX and MERZ,1958). If the rule applies, any of both datasets can be predicted from each other. More specifically, a good correlation was found between the magnitudes of the apparent viscosity in steady shear (η) and the complex viscosity in oscillatory shear ($|\eta^*|$), compared at equal values of shear rate and frequency, for solutions of random-coil polysaccharides and of some synthetic polymers (TANG, H. et al., 2010). Nevertheless, even in these cases, the rule is not followed at higher frequencies where significant departures between both parameters are usually found. Deeper exploration unveiled that the rule generally fails in systems like Boger fluids, dilute solutions, cross-linked or gelled systems, and particulate/aggregated dispersions (RICHARDSON; ROSS-MURPHY, 1987). In order to study its applicability to the investigated systems the apparent (η_A), complex ($|\eta^*|$), and dynamic (η') viscosities for samples *NS*, *S* (t_S), and their 1:1 mixtures, are plotted in Figure 5. The data gathered for samples *NS*, *S* (5), and its 1:1 mixture (red data), illustrate how η_A departed significantly from both η' and $|\eta^*|$ in the whole ω / $\dot{\gamma}$ range.

The deviation of η_A has been attributed to structure decay due to the effect of the strain deformation applied to the system or to different types of molecular rearrangement occurring in the flow patterns over the applied shear (RICHARDSON; ROSS-MURPHY, 1987). In the latter case, the behavior may be interpreted in terms of specific interpolymer chain interactions occurring in addition to entanglements. These results indicate that, according to the evidence discussed above, the Cox-Merz rule may be not followed by those mixtures characterized by a high elasticity and a high content in HMCH-microfibers (and their aggregates). Hence, these results would agree with the failure of the rule found in other particulate/aggregated systems and, more specifically, in the case of biopolymer dispersions with hyper-entanglement (i.e. high density of entanglements) (CHAMBERLAIN; RAO, 1999). Interestingly, the differences between the viscosities under steady and oscillatory shear were clearly mitigated when t_S was increased. Accordingly, a good correlation was found for *S* (15) and S (30) and their corresponding mixtures within the range 0.1-10 s^{-1}.

Some discrepancies can be found in the literature regarding the applicability of the rule in chitosan-based systems. For instance, Calero et al reported good correlation in chitosan solutions at a temperature of T=25 ºC but a rule failure whenever it was decreased to T<20 ºC (TOMASIK; ZARANYIKA, 1995). On the other hand, Cho et al found the rule´s applicability to depend upon the changes in the ionic strength (I) of the system (CHO, J. et al., 2006). These results are compatible with the behavior shown in Fig 5: i.e. chitosan solutions/dispersions with strong Newtonian character seem to follow the Cox-Merz rule better than those which exhibit enhanced viscoelastic properties. Although in our case these differences seem mainly determined by the changes in M induced by sonication, there is no contradiction with literature data in the sense that other experimental conditions (T, I, etc) and chitosan properties (concentration, DD, etc) can also influence the flow behavior of aqueous polysaccharide solutions/dispersions and, thus, the applicability of the rule.

5.3.5 **AFM Studies**

The atomic force microscope was used to investigate the morphological characteristics of *NS:S* (t_S) mixtures. For this purpose, freshly cleaved mica substrates were modified with a thin colloidal film of each mixture by drop casting. Figure 6 shows the topographic (panel A) and the equivalent amplitude images (panel B) obtained for the prepared films. A quick glance at panel A reveals clear differences in the topography of the different samples. Although a more detailed discussion is given below, these variations appear to be correlated with the changes made in the mixing ratio and sonication time. Starting with the mixtures of *S* (5), the topography of the 7:3 mixture (Fig 6AA) does not look anything like the typical image of a bare mica surface (see supplementary information). The presence of a densely packed film of chitosan (which, indeed, looks like scraped at different locations) is strongly suggested. Its thickness has been estimated in 2 nm from the extracted height profiles. Above this layer, non-branched fiber-like structures with length ranging between 0.5 and more than 1 μm, height around 4 nm, and width about 40 nm, can be distinguished. Apparently, these can form thicker bundles of about 100 nm which organize in local networks (as can be distinguished in the top-left part of the image).

The high packing density of the background layer and the observation of individual fibers on top, are consistent with the AFM and SEM evidence reported for pure films of *NS* CHIT90 and other biopolymers, e.g. agars (SOUZA, H. K. S. et al., 2013), when prepared from relative dilute solutions (<30 $\mu g \cdot mL^{-1}$). Two other types of features can be found in the outermost layer: (1) small particles with diameter and height of about 50 and 6 nm, respectively (tagged as #1 in Fig 6AA), and (2) larger odd-shaped bodies with size larger than 150 nm and height about 10 nm (tagged as #2). Based only on the topographic evidence, it is hard to ascertain whether these particles correspond to LMCH-NPs, fibril aggregates, or protuberances from the underneath layer. It is worth remembering that the DLS data in section 3.1 unveiled the presence of a high % of LMCH-NPs of about 200 nm in the *NS* CHIT90 sample and the consistent increase in its population under sonication. Hence, their observation under the AFM would make sense. Comparing the height of the individual fibers and the underlying film, it is hypothesized that the latter may consist of a monolayer of self-assembled HMCH-microfibers or microfiber-NP conjugates (this mixture contains up to 70% of the fibrous *NS* CHIT90 component).

The analysis of the amplitude scan (Fig 6BA) sheds more light into some of these issues. For instance, the individual fibers appeared much better defined in terms of shape, thus, dispelling any doubt about their morphology. Nevertheless, in great contrast with the topographic evidence, a relatively flat and unscratched underlayer is shown. This is in line with the relatively low surface roughness derived from the statistical analysis of Fig 6AA (R_{MS}=0.50 nm, see other statistical parameters in Table 3). Hence, the crack-like features found in that image should be alternatively interpreted as edge-overshoot artifacts in the z axis; i.e. an exaggeration of the edges along stepped profiles as a consequence of the piezo hysteresis (one of the most common issues in AFM). As for the origin of the spherical features, although the evidence in Fig 6BA is still not conclusive, actually, it seems to support the hypotheses of the aggregated and/or protruding fibrils. Nonetheless, even if these features were undoubtedly attributed to LMCH-NPs (originally present in the NS CHIT90 or coming from its ultrasonic fragmentation), the truly relevant fact is that their relevance in the colloidal films prepared from this mixture is relatively residual.

As it can be seen in the images, significant changes were triggered by increasing the amount of *S* (5) in the mixture (panels B and C in Figs 6A and 6B). In fact, two clear trends are derived from the simple eye inspection of the images:

(1) While the amount of fibers falls sharply (only one of these features is found in Figs 6AB and 6BB), the presence of spherical NPs increases notably in the outermost layer.

(2) The packing density at the underlayer follows a significant decrease.

In spite of the increasingly nanoparticulate texture exhibited by the outermost layer, especially in the case of the 3:7 mixture (Figs 6AC and 6BC), the microfibers are still distinguished as part of the underlayer. In fact, in this specific mixture, the fibers can be traced by following the NPs deposited in the upper layer along their 1D length (as better clarified in the amplitude image). The described transitions are well supported by the statistical data (Table 3). Accordingly, the overall change in the surface texture is perfectly matched by the increase of R_{MS} and H_{AV} , which reached values of 0.79 and 3.05 nm in the case of the 3:7 mixture. It could be argued whether the data for the 1:1 system (which showed a slight decrease in R_{MS}, and a barely unchanged H_{AV}) are against this trend. Nevertheless, it has to be pointed out that the presence of NPs on surface was only predominant for the 3:7 mixture. In fact, compared to the 7:3, the images of the 1:1 film do not only show a negligible amount of fibers but also a similar amount of NPs, which explains the small changes in R_{MS} and H_{AV}. From this analysis, it is postulated that the increase in the fraction of LMCH-NPs (with respect to the HMCH microfibers) induced upon the increase in the mixing ratio is responsible for the changes observed in the morphology. This would be backed by the DLS data presented above which demonstrated that the sonicated samples contain an increased population of NPs coming from the fragmentation of the microfibers.

Hence, the increasing fraction of low-*M* forms of the biopolymer in the mixtures not only explains the lower amount of fibers imaged on surface (and, conversely, the higher amount of NPs) but also the decrease in the packing density of the underneath layer. This seems determined by two main factors: (a) the lower availability of fibers in the mixtures for self-assembly, and (b) the intercalation of the fibers, and/or their bundles, by NPs (an example is indicated by the red arrows in Figs 6AC and 6BC). The role of t_S on the morphological aspect of the mixtures can be derived by comparison of the images in the central and right columns (15 and 30 min) with those placed at their left (5 min). But before proceeding with the statistical analysis of the images, let us emphasize that increasing t_S over 5 min resulted in a virtual demise of the microfibers from the outermost layer (although they seem to be still part of the underlayer). Regarding the effect of t_S in the *NS*-rich samples, i.e. the 7:3 mixtures, there was a clear transition from a landscape dominated by the presence of fiber-like features

at t_S=5 min, to different scenarios for t_S= 15 (Figs 6AD and 6BD) and 30 min (Figs 6AG and 6BG) characterized by an increasing predominance of spherical NPs.

In great contrast to that expected from the DLS results and the previous research on sonicated CHIT90 (SOUZA, H. K. S. et al., 2013), the size of the largest particles increased from 130 nm in image D to about 250 nm in E (as measured from the amplitude image) and the height (extracted from the leveled topographic images) raised from 12 to 40 nm. Such an increase can only be interpreted in terms of an enhancement of aggregation phenomena in the drop casted films. These processes can occur in solution (prior to casting) or through a dewetting-driven effect which involves the formation of microdroplets (KRISHNAN, 2001; SOUZA, H. K. S. et al., 2013). Any of these processes would be likely boosted upon an increase in the fraction of LMCH-NPs as a consequence of prolonged sonication. Hence, because of the reinforcement of colloidal aggregation phenomena, the AFM images would exhibit increasingly larger particles just as verified in Fig 6. This hypothesis also explains the lower amount of small NPs (20-40 nm) found in the images of *S* (30) compared to *S* (15) (images G and D in Figs 6A and 6B). The analysis of images E-H and F-I can provide us with a good perspective on the effects of increasing t_S in the mixtures with larger fractions of the *S* components. To this end, amplitude images are more appropriate as their topographic counterparts are slightly affected by horizontal artifacts from the polynomial leveling. Starting with the 1:1 system, it was observed that the size and height of the largest particles observed in the image for *S* (30) (panel H), which fell at about 150 and 12 nm, respectively; were smaller than those in image G. Comparison with image E is complicated because, in this case, a highly homogeneous composite (where the individual fibers and NPs are difficult to distinguish from each other) was apparently formed.

In the case of the 3:7 mixtures, no apparent differences in size and height were inferred for the NPs displayed in images F and I (which fall, in both cases, within the range of 20-40 and 1-2 nm, respectively). Furthermore, these are much smaller than the largest particles found in G and H. These results suggest that the effect of t_S in the enhancement of aggregation processes was considerably reduced for the 1:1 mixture and almost completely lost for the 3:7 system. The correlation between the relevance of aggregation phenomena observed for the different mixtures of *S* (30) and their content in *NS* CHIT90, indicates a potential involvement of the HMCH-microfibers in the formation of aggregates. Hence, the large particles must be ascribed not only to LMCH-NPs self-aggregation but also to a possible formation of HMCH-LMCH conjugates. In summary, a morphological transition, from a starting material which

seems quite rich in microscopic fibers to others with an aspect increasingly more nanoparticulated, is triggered by increasing t_S or through the variation in the *NS:S* (t_S) mixing ratio. The variety of intermediate morphologies identified in these experiments turns these systems into very promising precursors for the fabrication of chitosan biofilms with tunable properties. Within this context, the 1:1 mixture prepared with *S* (15) (central image in both panels) exhibited a relatively homogenous structure.

5.4. CONCLUSIONS

This work proposes the preparation of blends of colloidal chitosans with different morphology and molecular mass (*M*), as alternative precursors for the fabrication of food packaging films with fine-adjusted properties. Specifically, a commercial chitosan characterized by a high average molecular mass (*M*≈300 kDa) and *DD*=90% was mixed in aqueous solution with the products of its own molecular fragmentation. In this respect, the ultrasounds technique has played a central role in our strategy as an affordable tool to execute the degradation of the biopolymer, and the simultaneous shaping of the resulting colloids, under controlled conditions. The results herein presented demonstrate that through the control of the sonication time and the mixing ratio between sonicated and non-sonicated components, it is possible to adjust the viscoelasticity and the morphological aspect of the mixtures at a variety of levels intermediate between the limits defined by: (a) the shear-thinning flow behavior previously reported for non-sonicated CHIT90 (with a characteristic structure rich in microscopic fibers); and (b) the almost pure Newtonian response of the highly sonicated samples.

Although further experimentation and testing of the corresponding biofilms is required to confirm these claims, the research presented in this paper strongly suggests the validity of the proposed concept. Through the appropriate selection of t_s and mixing ratio, the colloidal mixtures can be prepared with intermediate properties so that a better balance between the mechanical properties and the moisture sensitivity could be met in their corresponding films. Hence, their use as precursors for the fabrication of packaging films to work in direct contact with foodstuffs may be more advantageous. In this respect, the 1:1 mixture prepared with a chitosan sonicated for 15 min emerges from this study as the most promising system to be

tested in future work (due to its significant viscoelasticity and homogeneous morphology). In a more general vein, these results evoke the fundamental role of smart design and processing for the realization of a new generation of additive-free sustainable and fully functional bioplastics.

Acknowledgements

This work was supported by the European Union (FEDER) and National funds from the National Strategic Reference Framework Portugal 2007-2013 (QREN) allocated through the Operational Competitiveness Programme (COMPETE) and the North Portugal Regional Operational Programme (ON.2) (FCOMP-01-0124-FEDER-37285, FCOMP-01-0124-FEDER-041438, NORTE-07-0124-FEDER-000069) to REQUIMTE and CIQ through the Portuguese Foundation for Science and Technology (FCT) (projects: Pest-C/EQB/LA0006/2013, Pest-C/QUI/UI0081/2013, and EXPL/QEQ-QFI/0368/2013). J.M.C.P. is also grateful to the FCT for granting him with a post-doctoral fellowship (SFRH/BPD/75259/2010). L.P.G. acknowledges CAPES (Programa Institucional de Bolsas de Doutorado Sanduíche no Exterior, PDSE; Proc nº 18935/12-5), FAPERJ, and CNPq for the concession of a PhD fellowship.

Author Contributions

C.T.A., V.M.F.P., and M.P.G, conceived the project. L.P.G., J.M.C., and H.K.S.S. designed and performed the rheological, DLS, and AFM experiments. C.T.A., V.M.F.P., M.P.G., H.K.S.S., J.M.C., and A.F.S., analyzed and interpreted the corresponding results. H.K.S.S. and J.M.C. wrote the paper.

Corresponding Authors

Hiléia K. S. Souza (PhD), Tel.: + 351 225 081 884, E-mail: hsouza@fe.up.pt; José M. Campiña (PhD), Tel.: +351 220 402 643, E-mail: jpina@fc.up.pt

Graphical Abstract (for review)

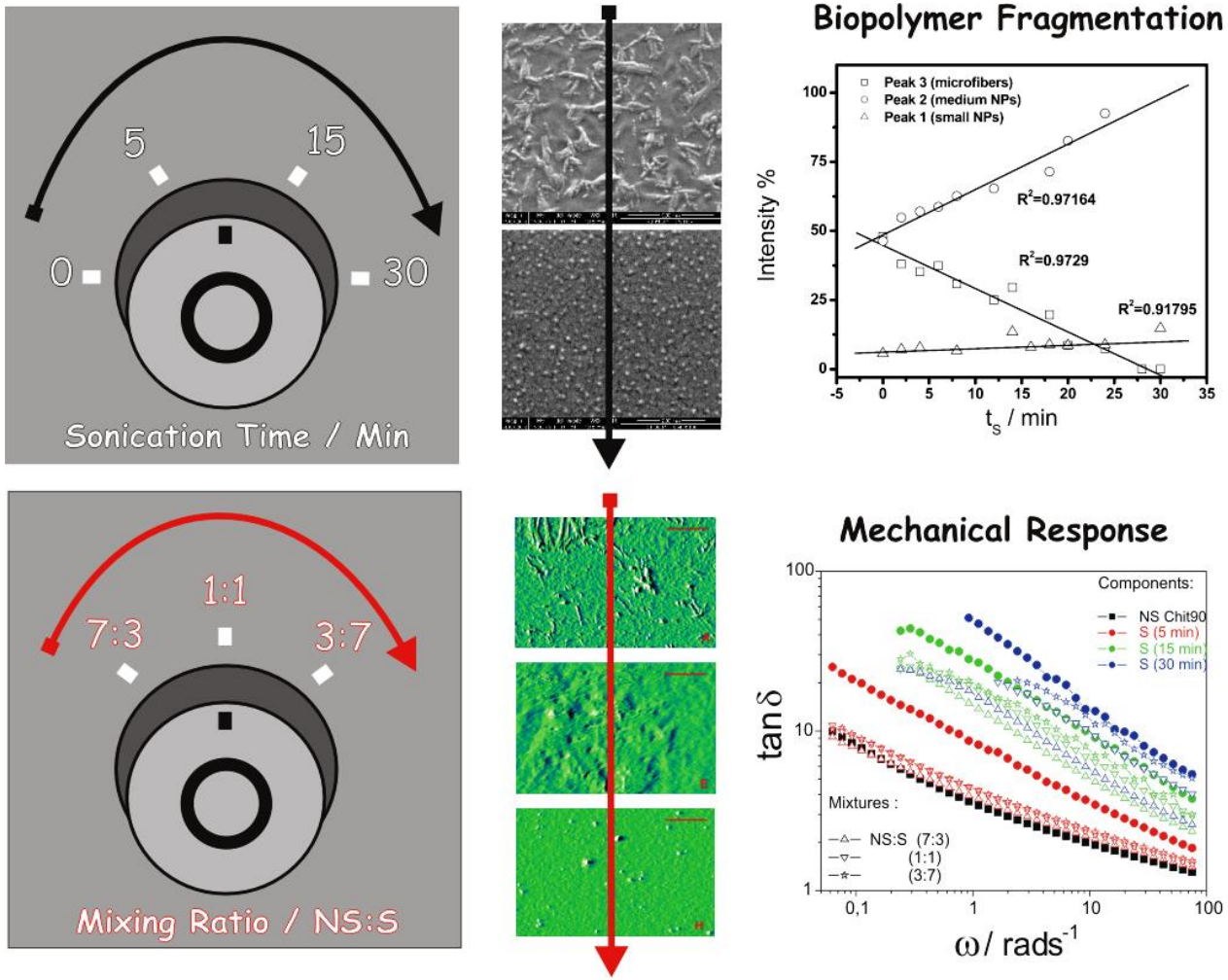

Highlights (for review)

Highlights

- The fragmentation of a fibrous chitosan by ultrasonication was followed with DLS
- Colloidal mixtures of the sonicated samples and the original biopolymer were prepared
- The viscoelasticity and structure of the mixtures were studied by rheology and AFM
- Properties can be tuned through the selection of mixing ratio and sonication time
- Excellent perspectives as precursors of fully biodegradable films for food packaging

Scheme 1. Artwork depicting the main concepts explored in this investigation. The graphical representation of the morphologies characterizing the CHIT90 samples, non-sonicated (blue frame) and after sonication for 60 min (green frame), as well as the properties of their precursor solutions and corresponding transparent films, have been summarized from the results reported in Ref. (SOUZA, H. K. S. et al., 2013). A hypothetical morphology (red frame) and the main questions to answer about the properties of their mixtures are also presented.

Figure 1. **a)** The distributions of the amplitude of the scattered light as a function of the particle hydrodynamic diameter for CHIT90 irradiated with ultrasounds for: 0 (non-sonicated, black solid line), 4 (red), 8 (green), and 20 min (blue). **b)** Evolution of the intensity of light scattered at each of the peaks displayed in **(a)** upon the gradual increase of the sonication time (t_S). The correlation factors obtained from the linear fittings of the data (black solid lines) are also included. The 3% (w/w) CHIT90 dispersions were diluted 10_3 times in all cases before measurements.

Figure 2. Mechanical spectra gathered for the pure Chit90 solutions of *NS* (black squares, all panels) and *S* (black circles, all panels) sonicated for t_S=5 (panel A), 15 (panel B), and 30 min (panel C). The mixtures of these components are represented by the different colored symbols: t_S=5 (red symbols in panel A), 15 (green symbols in panel B), and 30 min (blue symbols in panel C). For each system the following *NS/S* ratios were studied: 7:3 (up triangles), 1:1 (down triangles), and 3:7 (stars); are also presented. The storage (G') and loss (G'') moduli are represented by the filled and open symbols, respectively.

Figure 3. **(a)** Evolution of *tan* δ as a function of the oscillation frequency (ω) for the isolated samples of *NS* (black filled squares) and *S* treated with t_S=5 (red filled circles), 15 (green filled up triangles), and 30 min (blue filled diamonds). **(b)** Analogous data obtained for the mixtures prepared with the following *NS/S* ratios: 7:3 (open squares), 1:1 (open hexagons), and 3:7 (open stars). Despite all the mixtures prepared from a given *S* component are colored in accordance to **(a)**, arrows and legends have been added for better clarity. *tan* δ was calculated as G''/G' from the data in Figure 2.

Figure 4. Steady shear curves obtained for the pure NS (black squares) and *S* (t_S) components (black circles) treated with t_S= 5 **(a)**, 15 **(b)**, and 30 min **(c)**. Filled symbols represent the increasing shear rate excursion and their open counterparts the decreasing one. The grey straight line and the violet dashed curve represent the fitting of the filled data to the Cross and Carreau models, respectively. The behavior registered for the mixtures of these components are represented by the different colored symbols: t_S=5 (red symbols, panel a), 15 (green

symbols, panel b), and 30 min (blue symbols, panel c). For each system the following *NS:S* (t_S) mixture ratios were studied: 7:3 (up triangles), 1:1 (down triangles), and 3:7 (stars)

Figure 5. Comparison between η_A (solid lines, left scale), $|\eta^*|$ (dashed lines, right scale), and η' (dash dot dotted lines, right scale) measured at 25ºC for *NS* and *S* (t_S) chitosans prepared with t_S= 5, 15, and 30 min (black curves) and their corresponding 1:1 mixtures (red, green, and blue curves, respectively).

Figure 6. AFM images taken in tapping mode for freshly cleaved mica substrates decorated with thin films of the different *NS:S* (t_S) colloidal mixtures. The mica discs (drop-casted with the different colloidal suspensions) were simultaneously scanned in topography **(A)** and amplitude **(B)** over regions of 5 x 5 μm^2. The red scale bars are 1 μm.

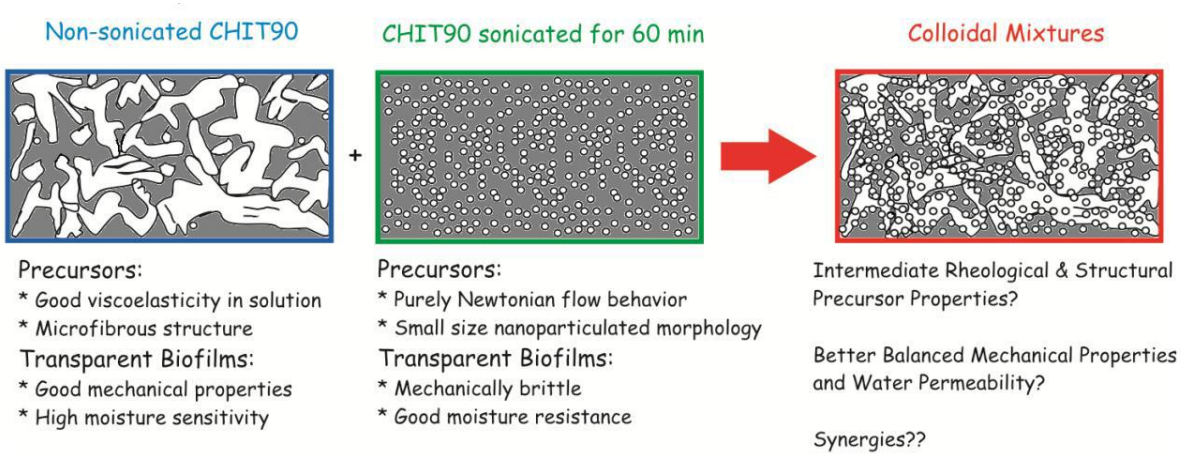

Figure 1

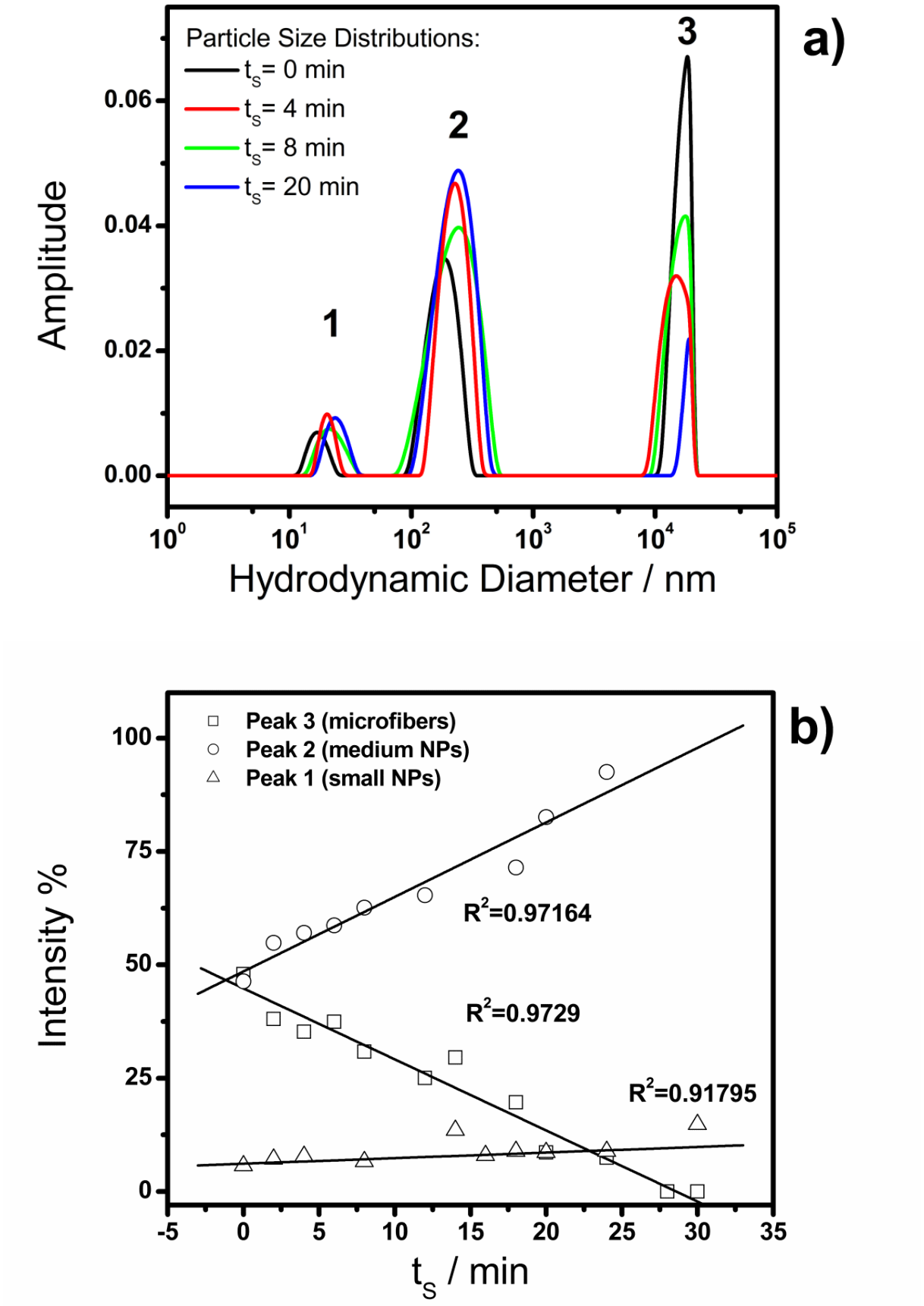
a)
Particle Size Distributions:
t_s= 0 min
t_s= 4 min
t_s= 8 min
t_s= 20 min
1
2
3
Amplitude
0.00
0.02
0.04
0.06
10^0
10^1
10^2
10^3
10^4
10^5
Hydrodynamic Diameter / nm
b)
Peak 3 (microfibers)
Peak 2 (medium NPs)
Peak 1 (small NPs)
R^2=0.97164
R^2=0.9729
R^2=0.91795
Intensity %
0
25
50
75
100
-5
0
5
10
15
20
25
30
35
t_S / min

Figure 2

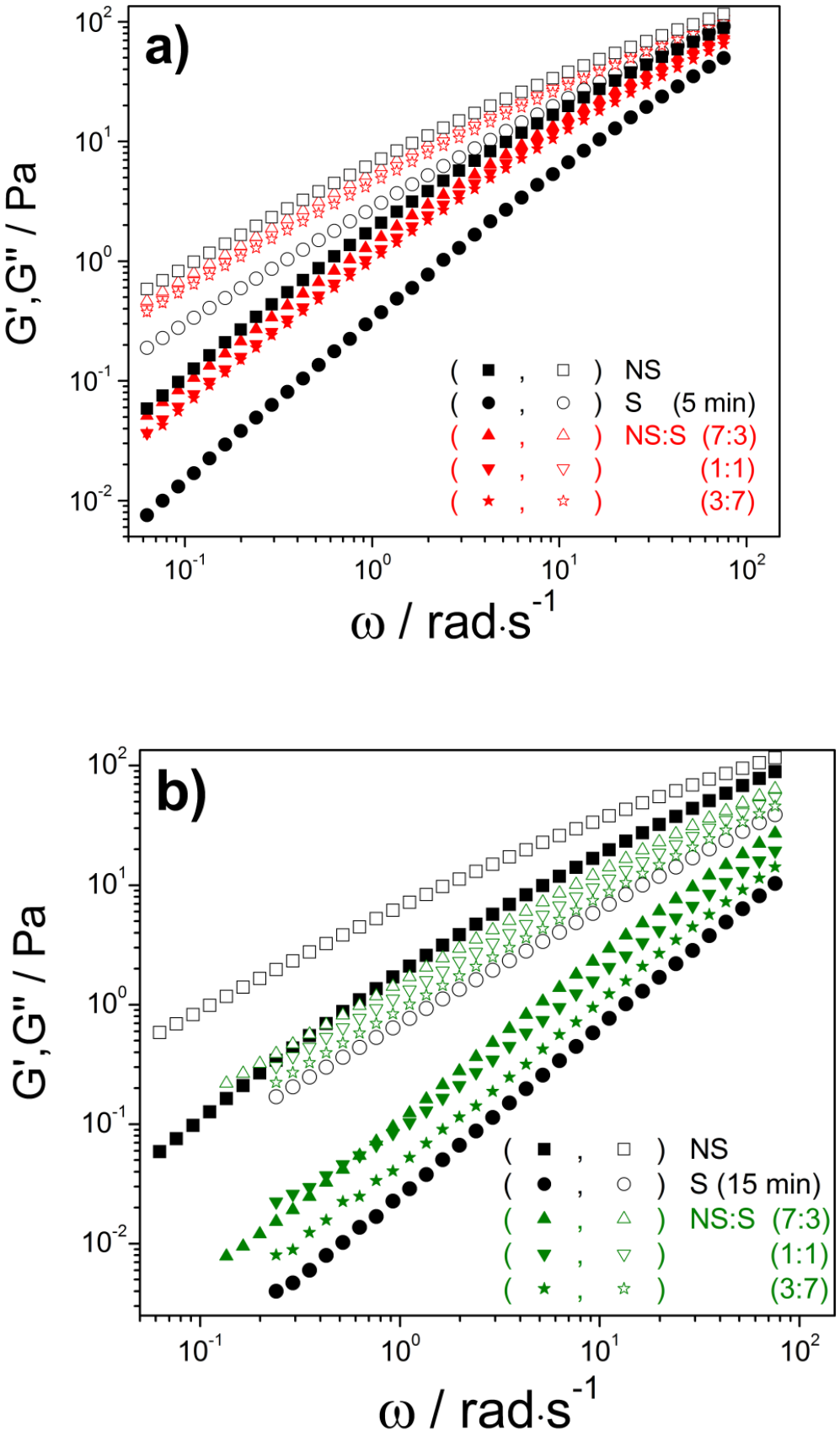
a)
G',G'' / Pa
ω / rad·s-1
(,) NS
(,) S (5 min)
(,) NS:S (7:3)
(1:1)
(3:7)
b)
G',G'' / Pa
ω / rad·s-1
(,) NS
(,) S (15 min)
(,) NS:S (7:3)
(1:1)
(3:7)

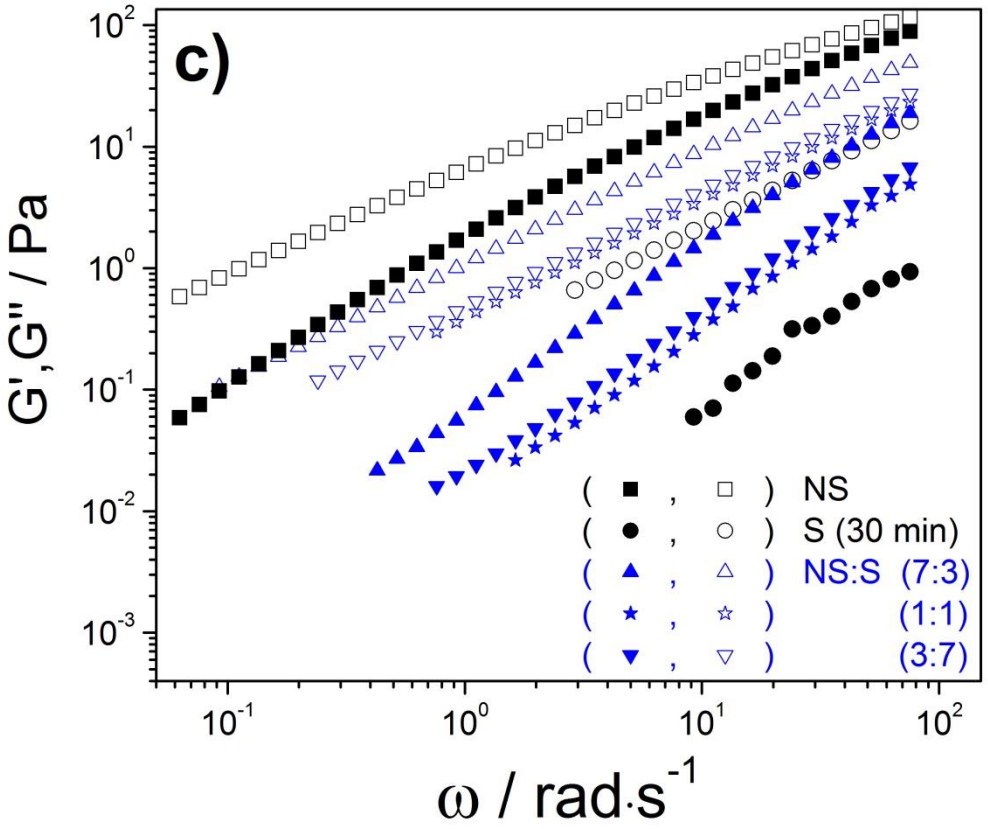
c)
G',G'' / Pa
ω / rad·s-1
(,) NS
(,) S (30 min)
(,) NS:S (7:3)
(,) (1:1)
(,) (3:7)

Figure 3

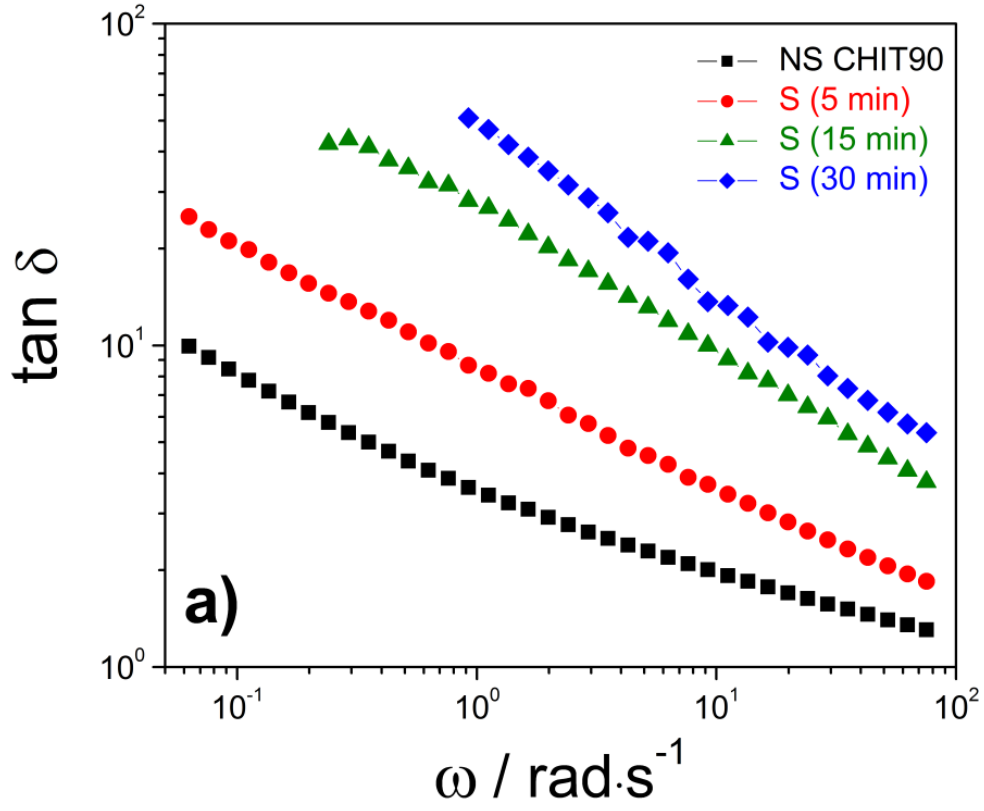
NS CHIT90
S (5 min)
S (15 min)
S (30 min)
a)
tan δ
ω / rad·s-1

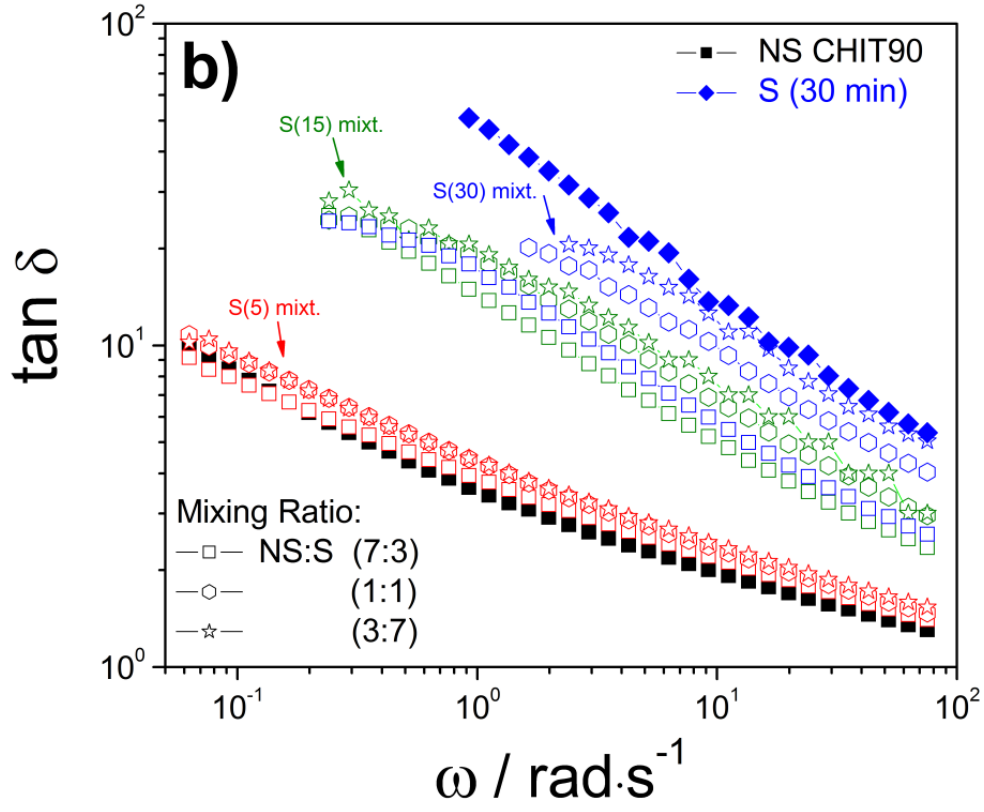
b)
NS CHIT90
S (30 min)
S(15) mixt.
S(30) mixt.
S(5) mixt.
Mixing Ratio:
NS:S (7:3)
(1:1)
(3:7)
tan δ
ω / rad·s-1

Figure 4

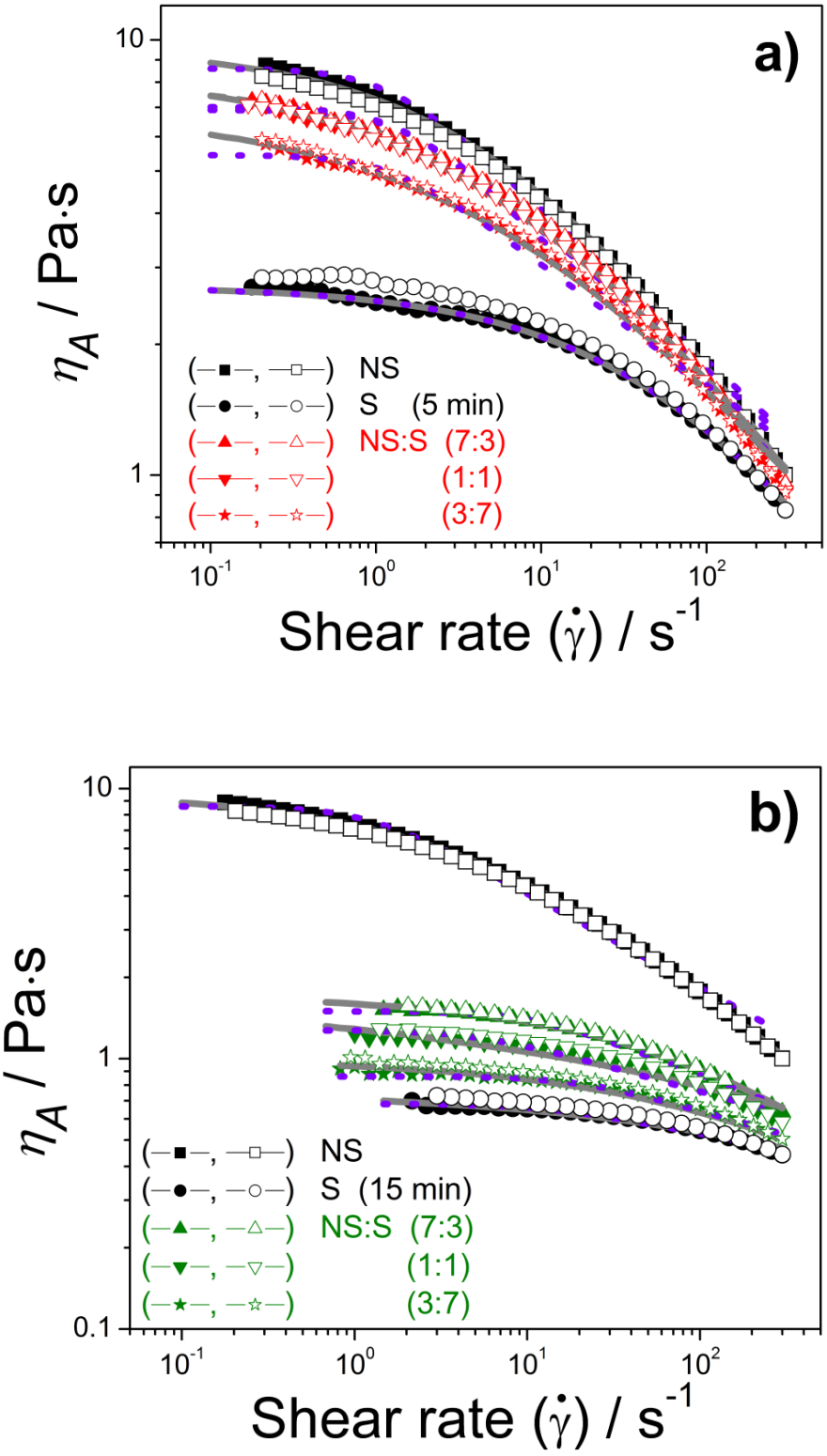
a)
10
1
η_A / Pa·s
(—■—, —□—) NS
(—●—, —○—) S (5 min)
(—▲—, —△—) NS:S (7:3)
(—▼—, —▽—) (1:1)
(—★—, —☆—) (3:7)
10^{-1}
10^{0}
10^{1}
10^{2}
Shear rate ($\dot{\gamma}$) / s^{-1}
b)
10
1
0.1
η_A / Pa·s
(—■—, —□—) NS
(—●—, —○—) S (15 min)
(—▲—, —△—) NS:S (7:3)
(—▼—, —▽—) (1:1)
(—★—, —☆—) (3:7)
10^{-1}
10^{0}
10^{1}
10^{2}
Shear rate ($\dot{\gamma}$) / s^{-1}

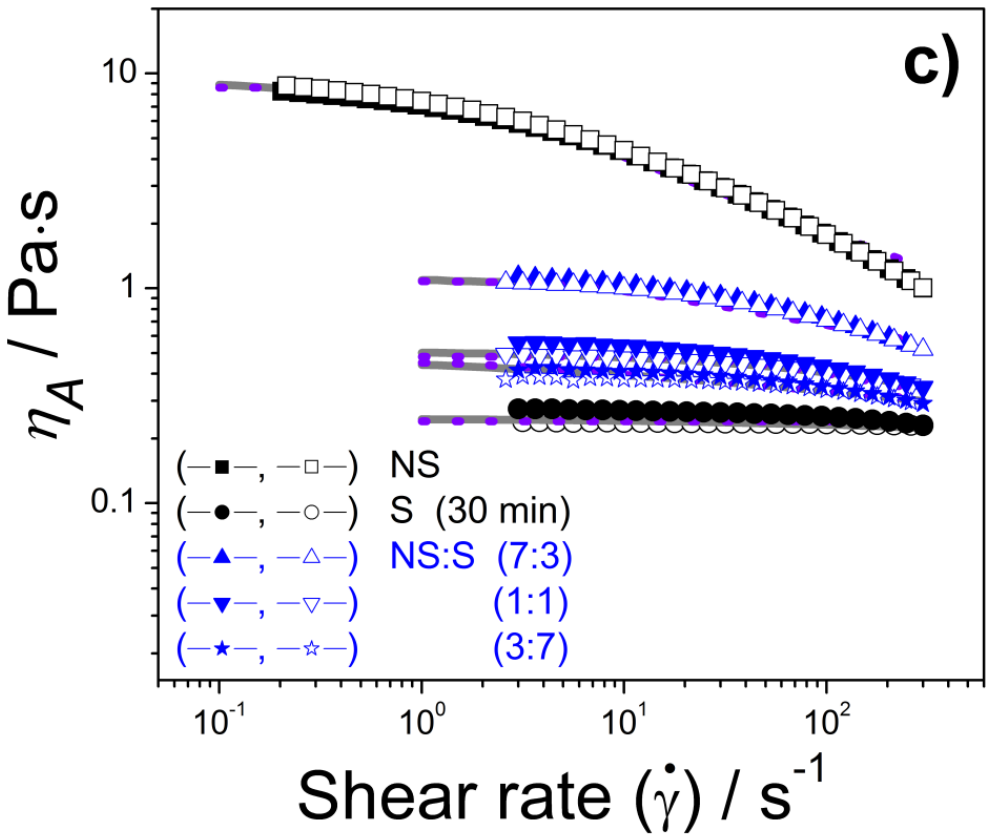
c)
10
1
0.1
η_A / Pa·s
(—■—, —□—) NS
(—●—, —○—) S (30 min)
(—▲—, —△—) NS:S (7:3)
(—▼—, —▽—) (1:1)
(—★—, —☆—) (3:7)
10^{-1}
10^{0}
10^{1}
10^{2}
Shear rate ($\dot{\gamma}$) / s^{-1}

Figure 5

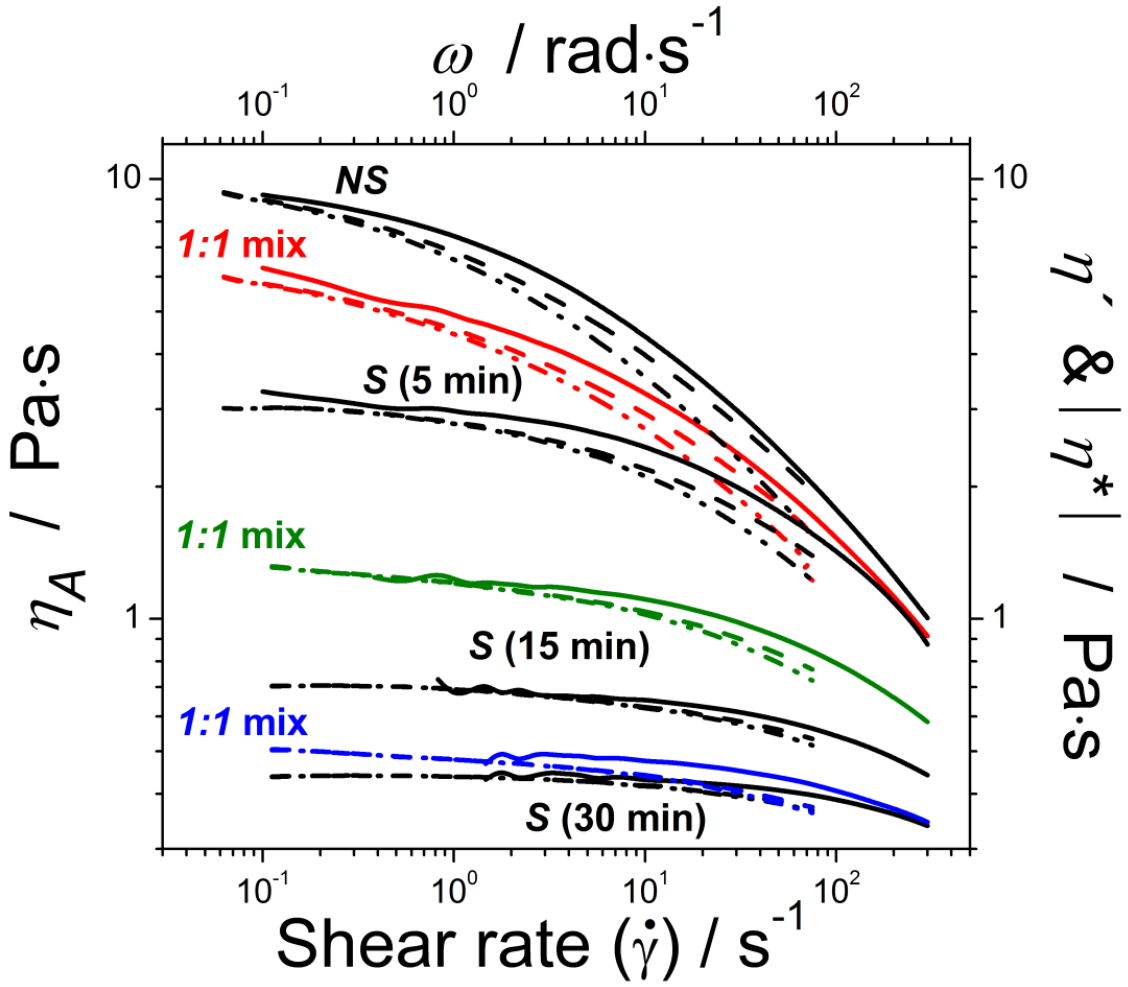
ω / rad·s-1
10-1
100
101
102
10
1
NS
1:1 mix
S (5 min)
1:1 mix
S (15 min)
1:1 mix
S (30 min)
ηA / Pa·s
η', & |η*| / Pa·s
Shear rate (γ̇) / s-1

Figure 6

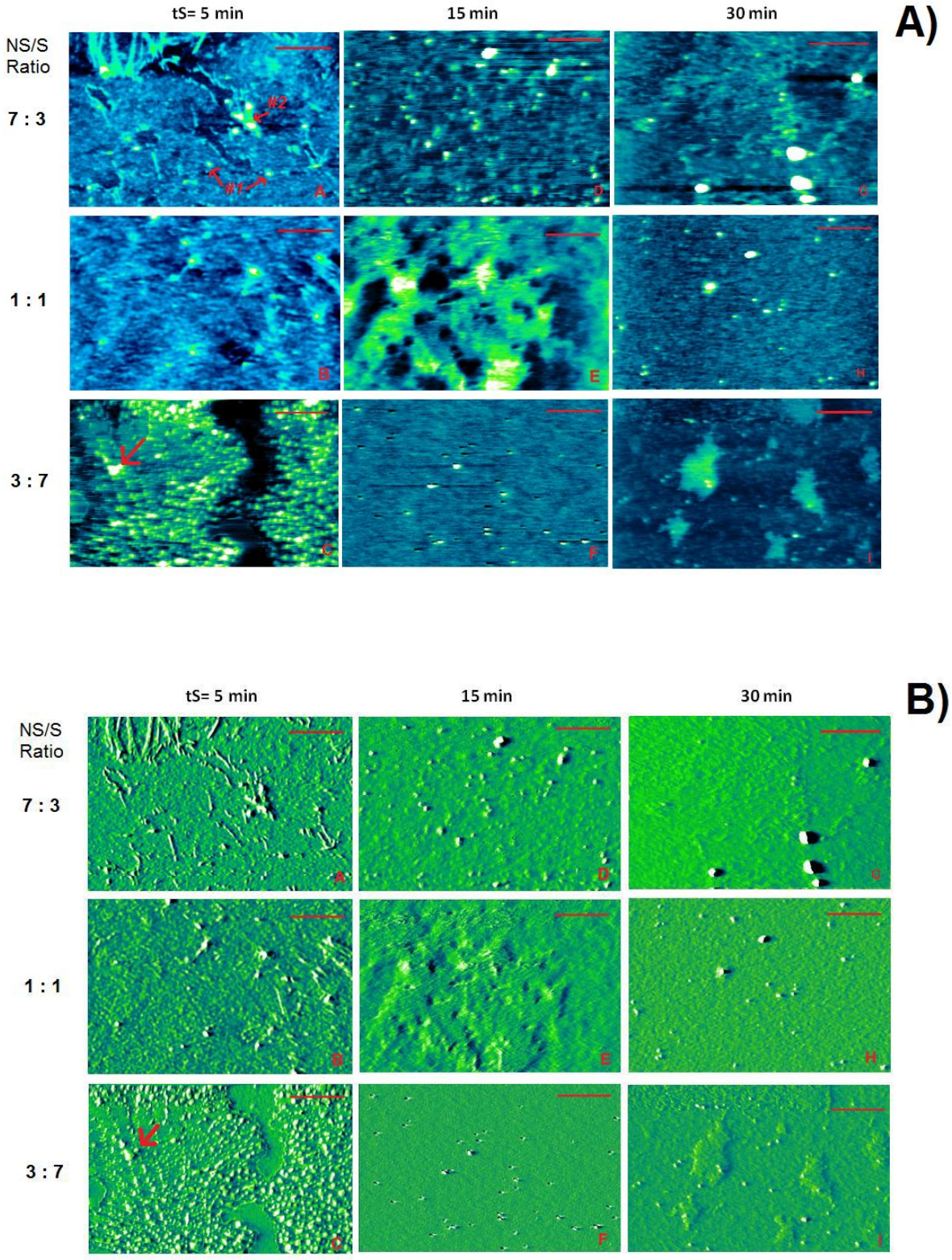
A)
tS= 5 min
15 min
30 min
NS/S Ratio
7 : 3
1 : 1
3 : 7
#1
#2
A
B
C
D
E
F
G
H
I
B)
tS= 5 min
15 min
30 min
NS/S Ratio
7 : 3
1 : 1
3 : 7
A
B
C
D
E
F
G
H
I

Table 1. Peak data, hydrodynamic radius (Rh) and Amplitude, derived from the curves in Figure 1a. Other peak parameters as the percentage of intensity scattered at each peak (Intensity %) and the integrated peak areas (Area) were calculated with i-Size 2.0 and Origin 7.0 software, respectively. The errors for the peak amplitudes were calculated as the standard deviation of the consecutive measurements taken for each sample.

NS-CHIT90	R_h / *µm*	***Amplitude***	***Intensity %***	***Area / nm***
Peak 3	19.5	0.069 ± 0.005	48.0	437.5
Peak 2	0.18	0.035 ± 0.004	46.4	4.746
Peak 1	0.02	0.007 ± 0.003	5.67	0.055
***S* (4 min)**				
Peak 3	15.3	0.032 ± 0.002	35.2	297.8
Peak 2	0.23	0.047 ± 0.008	57.0	7.328
Peak 1	0.02	0.010 ± 0.001	6.25	0.072
***S* (8 min)**				
Peak 3	17.9	0.042 ± 0.004	0.56	334.9
Peak 2	0.26	0.040 ± 0.007	0.54	10.42
Peak 1	0.02	0.008 ± 0.002	6.57	0.104
***S* (20 min)**				
Peak 3	19.5	0.026 ± 0.002	8.61	83.78
Peak 2	0.23	0.049 ± 0.003	82.6	10.45
Peak 1	0.02	0.009 ± 0.001	8.61	0.116

Table 2 Parameters returned upon fitting the data in Figure 4 to the Cross and Carreau simplified models.

		Cross					Carreau				
Chit 90		η_o *(Pa·s)*	τ *(s)*	*M*	*RSS*	*MRD x* 10^{-3}	η_o *(Pa·s)*	λ *(s)*	*N*	*RSS*	$MRD_3 \times 10^{-}$
NS		9.60	0.13400	0.60	0.123	8.4	8.60	0.84	0.18	1.0028	20.1
NS / S (5 min) Mixing Ratio	7 : 3	8.14	0.12970	0.54	0.142	2.7	7.20	0.70	0.17	2.8240	8.4
	1 : 1	8.02	0.12660	0.53	0.537	5.7	7.02	0.67	0.17	3.9040	9.9
	3 : 7	6.81	0.12287	0.48	0.311	4.9	5.62	0.64	0.15	1.7296	8.5
S (5 min)		2.71	0.01287	0.58	0.058	2.6	2.56	0.23	0.11	0.3198	7.6
NS / S (15 min) Mixing Ratio	7 : 3	1.71	0.00780	0.55	0.067	3.9	1.50	0.09	0.12	0.2314	7.5
	1 : 1	1.58	0.01200	0.35	0.211	8.7	1.20	0.08	0.11	0.0800	5.7
	3 : 7	1.01	0.00300	0.41	0.114	8.2	0.86	0.05	0.09	0.1602	9.1
S (15 min)		0.75	0.00160	0.52	0.113	10.4	0.67	0.05	0.07	0.0253	5.5
NS / S (30 min) Mixing Ratio	7 : 3	1.12	0.00400	0.56	0.070	5.8	1.05	0.08	0.08	0.0329	6.2
	1 : 1	0.51	0.00084	0.54	0.057	12.1	0.49	0.06	0.06	0.0449	9.0
	3 : 7	0.52	0.00100	0.45	0.145	17.4	0.39	0.05	0.05	0.1240	15.0
S (30 min)		0.25	0.00001	0.38	0.003	4.7	0.24	0.02	0.02	0.0004	2.1

Table 3 Surface roughness (R_{MS}) and average size (H_{AV}) extracted from the analysis of the images in Fig 6A using the freeware Gwyddion 2.25

t_S / min	***NS:S Mixing Ratio***	***R_{MS} / nm***	***H_{AV} / nm***
	7:3	0.5	1.8
5	1:1	0.4	1.8
	3:7	0.8	3.0
	7:3	1.0	18.3
15	1:1	0.9	5.3
	3:7	0.1	1.0
	7:3	2.0	6.5
30	1:1	0.4	18.4
	3:7	0.3	1.4

Supplemental Materials on:

Tweaking the Mechanical and Structural Properties of Colloidal Chitosans by Sonication

Laidson P. Gomes,[1,2] Hiléia K. S. Souza,[1*] José M. Campiña,[3*] Cristina T. Andrade, [4] Vânia M. Flosi Paschoalin,[2] A. F. Silva,[3] and Maria P. Gonçalves[1]

[1] REQUIMTE/LAQV**,** Departamento de Engenharia Química. Faculdade de Engenharia. Universidade do Porto. Rua Dr. Roberto Frias, 4200-465, Porto, Portugal.

[2] LAABBM, Instituto de Química, Universidade Federal do Rio de Janeiro, UFRJ, Av. Athos da Silveira Ramos 149, CT, Bl A, sala 545, Ilha do Fundão, CEP 21941-909, Rio de Janeiro Brazil.

[3] Centro de Investigação em Química da Universidade do Porto (CIQ-UP). Departamento de Química e Bioquímica. Faculdade de Ciências. Rua do Campo Alegre, 687, 4169-007, Porto, Portugal.

[4] Programa Ciência de Alimentos, Instituto de Macromoléculas Professora Eloisa Mano, Universidade Federal do Rio de Janeiro, Centro de Tecnologia, Bloco J 21941-598, Rio de Janeiro, RJ, Brazil

[*] Corresponding author information: *Hiléia K. S. Souza (PhD), E-mail: hsouza@fe.up.pt, Tel.: + 351 225 081 884; José M. Campiña (PhD), Email: jpina@fc.up.pt , Tel: +351 220 402 643*

1. Additional Material: AFM of bare Muscovite Mica:

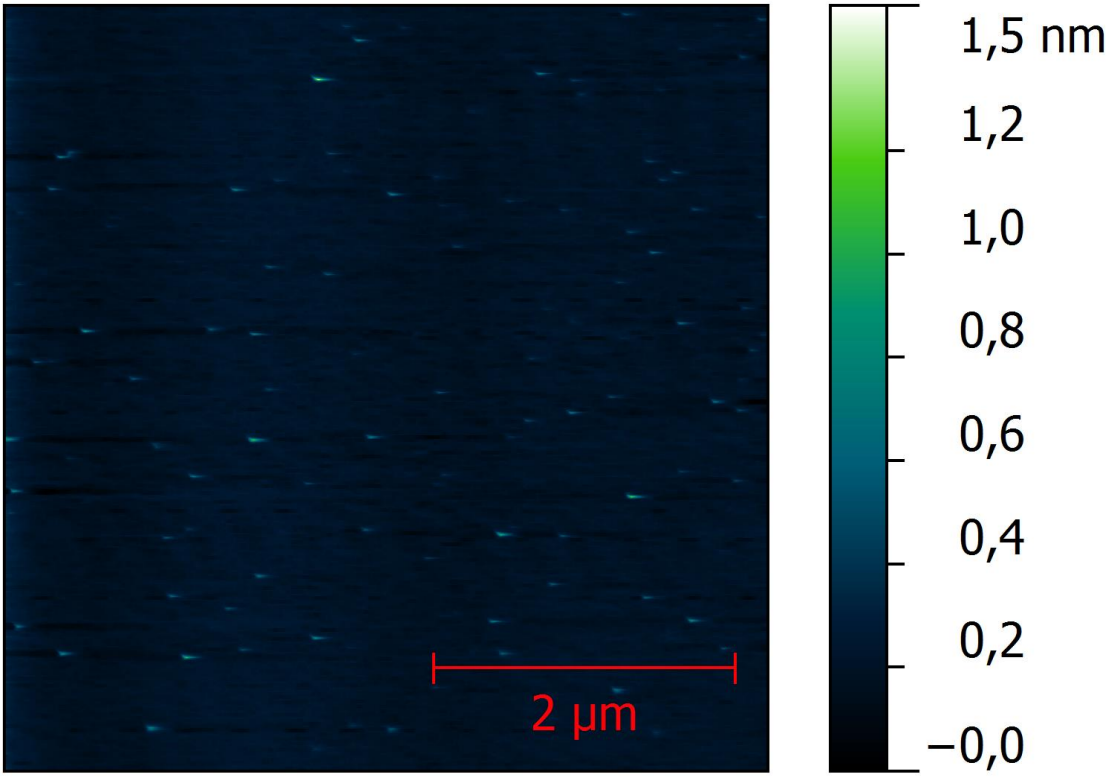

Figure S1. AFM image of a freshly cleaved mica disc (Muscovite V-4, 15 mm diameter) taken in tapping mode. The topography of the bare surface was scanned over a representative sample area of 5 x 5 μm^2.

2. Discussion

Figure S1 shows the image of a representative region of a freshly cleaved mica disc surface. Agreeing with other images previously reported for this substrate (Z. Shao and D. M. Czajkowsky, *Journal of Microscopy,* **2003**, 211,1-7; G. B. Webber et al, *Faraday Discussions,* **2005**, 128, 193-209), the surface seems completely flat and mostly featureless. A series of ultra-small dots (with a "tail" in the direction of sample scanning) can be distinguished from the flat background. The tails indicate that this a type of tip-related artifact. It is well-known that fast scanning hydrophilic surfaces, like muscovite mica, at regions covered with ultrathin layers of water can result in tip-sticking issues as it appears to be reflected in the image. After all, the impact of these artifacts on the image was small so that the general characteristics of the substrates are clearly inferred from the image.

6 CAPITULO IV – ESTUDO ORIGINAL 2

FABRICATION AND CHARACTERIZATION OF FIBERS CHITOSAN-BASED FILMS REINFORCED WITH CHITOSAN NANOPARTICLES

Laidson P. Gomes[1,2], Hiléia K. S. Souza*[2], José M. Campiña*[3], A. Fernando Silva[3], Cristina T. de Andrade[4], Maria P. Gonçalves[2] and Vânia M. F. Paschoalin[1]

1- LAABBM, Universidade Federal do Rio de Janeiro – Instituto de Química – Avenida Athos da Silveira Ramos 149 – 21949-909, Rio de Janeiro, Brazil

2- REQUIMTE, Departamento Engenharia Química, Faculdade de Engenharia, Universidade do Porto, Rua Dr. Roberto Frias, 4200-465, Porto, Portugal

3- Centro de Investigação em Química (CIQ-L4), Departamento de Química, Faculdade de Ciências, Universidade do Porto, Rua do Campo Alegre 687, 4169-007, Cidade do Porto, Portugal

4- Universidade Federal do Rio de Janeiro – Instituto de Macromoléculas Professora Eloisa Mano, Universidade Federal do Rio de Janeiro, Centro de Tecnologia, Bloco J 21941-598, Rio de Janeiro, RJ, Brazil.

*Corresponding author:

Abstract

Blend films composed of chitosan-fibers (CHIT90) and sonicated chitosan (S) were prepared by the knife coating method. The sonicated chitosan were obtained from CHIT90 (NS) (DD = 90%) fragmented by ultrasound. Chitosan nanoparticles obtained in variable extensions (*ts* = 5, 15 and 30 minutes) were used as reinforcing agents in chitosan fibers films. To improve the mechanical properties of biofilms chitosan were reinforced with nanoparticles The biofilms were produced by a homogeneous series of mixtures between NS/S(*ts*) at different ratios (3:7, 1:1 and 7:.3) with the same distribution of degrees of polymerization and without the incorporation of additives or plasticizers. The influence of nanoparticles contents on the microstructure, on mechanical and barrier properties, moisture sensitivity, transparency and color of the blend biofilms were analyzed. The biofilms were investigated by scanning

electron microscopy (SEM), which showed a homogeneous morphology. The mechanical strength and stiffness of transparent biofilms were positively affected when stress tests were applied. The addition of nanoparticles improved the mechanical properties of films. The produced biofilms presented superior elongation at break. Sensitivity to moisture was significantly decreased through water vapor permeability measurements and water sorption isothermal data with the decreasing of molecular mass from biofilms constituents. These findings may be useful for the future design of bioplastics with improved properties, as well as for the development of biocompatible nanoparticles with tunable size and molecular mass. Addition of nanoparticles improved the mechanical properties of films.

Keywords: Chitosan, Biofilms, Nanoparticles, Mechanical proprieties, Water vapor permeability, Scanning electronic microscopy.

6.1 INTRODUCTION

There is a worldwide interest in replacing the use of oil-based synthetic plastics with biodegradable, nontoxic and edible materials in packages. The development of new package products can benefit various industrial activities, particularly the production, distribution and commercialization of food (DAVIDOVICH-PINHAS et al., 2014). Chitosan (CH), a polysaccharide derived from chitin, is a promising biopolymer since chitin is the second most abundant polysaccharide in nature and can be obtained as a reject of the seafood industry in coastal regions, inland or even associated to shrimp aquaculture production. Besides the environmental benefits related to the removal of seafood residues and the replacement of petroleum-based-packages (CHANTARASATAPORN et al., 2013), chitosan can be considered an active package material, since its physicochemical properties, such as molecular weight and degree of deacetylation, can confer special activities to chitosan, including antimicrobial activity, which can be very useful in food packing (COOKSEY, 2005). The polycationic nature of these polymers also allows the association with natural antibiotics or antioxidants, reinforcing the applicability of these polymers in food preservation (FAN et al., 2014). Chitosan biofilms can be used in multi-layer packaging and provide opportunities for new product development (DEBEAUFORT et al., 1998).

In fact, the fabrication of transparent CH bioplastics for food packaging, and other applications has been widely studied (SOUZA, H. K. S. et al., 2013). Unfortunately, pure CH biofilms suffer from poorer mechanical properties and enhanced moisture sensitivity than their oil-derived counterparts (PENG; LI, 2014). The use of certain plasticizers (ethylene glycol, for example) has solved some of these limitations (SRINIVASA; RAMESH; THARANATHAN, 2007). However, possible transfer to food poses a health threat. Recently, irradiation of high molar mass CHs by ultrasonication has been shown to transform fibrous structures in the range of microns (CFBs) to tiny spherical nanoparticles (CNPs) (LU et al., 2013b) CHs treated with increasingly longer sonication times yield biofilms with improved moisture resistance but degraded mechanical properties (ANTONIOU et al., 2015).

With the purpose of reducing moisture sensitivity and still retaining significant strength and flexibility (with no aid of plasticizers), an approach based on the use of fiber blends and nanoparticles is presented. The focus of our study was to improve the fiber mechanical properties without affecting their biocompatibility. In the proposed treatments, we sought to reduce fiber diameters to produce a compact structure and improve their strength properties. To this end, CH was submitted to controlled fragmentation to CNPs by ultrasonication at different time intervals (*ts* = 5, 10 and 30 min). The resulting solutions were mixed with unmodified CHIT90 (NS) at different ratios (NS/S(*ts*): 3:7, 1:1, 7:3) and their biofilms prepared through the knife-coating method. The physical, functional and barrier properties of the blend films were correlated with the amount of each component of the mixture. Mechanical properties were assessed by tensile tests and moisture sensitivity was evaluated by contact angle measurements of water vapor permeability and water sorption isothermal measurements. Morphology was also studied by scanning electron microscopy (SEM). The results evidenced enhanced moisture resistance and improved mechanical properties compared to biofilms prepared from their individual precursor species. It was showed that reduction in fiber diameters was due to the formation of a crystalline structure and was translated into improvement in fiber strength.

6.2 MATERIAL AND METHODS

6.2.1 **Material and solutions**

Chitosans 150-200 kDa with *DD* 90% (CHIT90) were purchased from Primex (Siglufjordur, Iceland). Chitosan 3 % (w/w) were solved in 0.1 M acetate buffer pH 6.0

prepared with distilled water and the pH was adjusted by the addition of drops of glacial acetic acid or sodium acetate. After stirring for 2 h, the solutions were stored at 4 ºC. Before measurements, Chito90 stock solutions were incubated at room temperature for 60 min and subsequently centrifuged at 21,000 x g (9 ACC, 25 ºC) for 30 min using a Beckman Coulter centrifuge (Model Alegra 25R).

6.2.2 **Ultrasonic rupture of chitosan fibers**

Thirty mL of the Chito90 stock solutions were submitted to ultrasonic irradiation (S) on ice for defined period of time (*ts*= 0, 5, 15 and 30 min) using an ultrasonic probe (Sonic, model 750 watts) equipped with a 1/2" microtip (constant duty cycle and 40% amplitude) with intervals of 1/1s. Measurements were performed in triplicate.

6.2.3 **Mixing solutions**

The filming-forming solutions of low molar mass chitosan (LMm chitosan-nanoparticles) prepared by sonication at different sonication times (S (*ts*)) were mixed with the stock solution of CHIT90 (NS). Biofilms were prepared using blends among Chito90 and nanoparticles using the nanoparticles with the same distribution of degrees of polymerization but at different NS/S(*ts*) ratios: 3:7, 1:1, and 7:3. The 09 different mixtures were magnetically stirred for 5 min and subsequently individually used for the biofilm fabrication.

6.2.4 **Bioplastic film fabrication**

Chitosan biofilms were prepared by the knife coating method (SOUZA, H. K. S. et al., 2013). For these purposes, 30 mL of a 3 % (w/w) solution were spread at 0.3 $m \cdot s^{-1}$ onto an acrylic plate using a film applicator (Sheen, model 1132N, UK). The plates were put in an environmental test chamber (T= 40ºC and RH= 60 %, relative humidity) and dried for 18 h. Subsequently, they were peeled off from their supports, rinsed with distilled water, and stored

for 18 h in environmental test chamber. Smooth and homogeneous films were obtained. The film thicknesses were measured with 1 μm resolution using an Absolute Digimatic Indicator (ID-F150, Mitutoyo Co., Japan) and three independent measurements were averaged for each case.

6.2.5 **Color and Opacity**

Color and opacity parameters were determined by a Minolta colorimeter CR300 series (Tokyo, Japan). The color of the films was determined using the CIELab color parameters, while lightness (L*) and chromaticity parameters a* (red - green) and b* (yellow – blue) were also measured. The color of the films was expressed as the difference of color (ΔE*) according to Eq.(1). The variables L_s^*, a_s^* and b_s^* are CIELab standards for the white standard used as the film background (PENG; LI, 2014).

$$\Delta E^* = \sqrt{(L^* - L_s^*)^2 + (a^* - a_s^*)^2 + (b^* - b_s^*)^2} \qquad (1)$$

Film opacity was determined according to the Minolta-lab method in reflectance mode (THAKHIEW; DEVAHASTIN; SOPONRONNARIT, 2013). Opacity (*Y*) was calculated from the relationship between the opacity of the film superposed on the black standard (Y_{black}) and on the white standard (Y_{white}), according to the following equation:

$$Y = \frac{Y_{\text{black}}}{Y_{\text{white}}} 100 \qquad (2)$$

For each biofilm condition, five readings were performed.

6.2.6 **Scanning Electron Microscopy (SEM)**

The SEM images were acquired in the secondary electron mode using an FEI Quanta 400 FEG microscope located at CEMUP (Centro de Materiais da Universidade do Porto). Samples were previously cryo-fractured using liquid N_2 and mounted on aluminum stubs covered with double-coated carbon conductive adhesive tabs. Afterwards, the samples were coated with a thin film of Au/Pb and imaged in the high-vacuum/secondary electron imaging mode scanning electron microscope using an accelerating voltage of 10 kV and the working distances oscillated between 10.4 to 13.8 mm.

Blend film features: mechanical resistance, water vapor permeability and water sorption

6.2.7 **Mechanical characteristics**

Measurements were performed on a texture analyzer (TA.XT2, Stable Micro Systems, Surrey, UK) equipped with tensile test attachments. The test specimens consisted of strips of uniform width and length (25 × 100 mm) conditioned for 07 days in a climatic chamber (T= 25 ºC, RH= 53 %). Experiments were run immediately after removing the specimens from the climatic chamber to minimize water adsorption/desorption.

The distance between the grips was 60 mm and the applied test speed was 0.1 mm s^{-1}, while force (N) and deformation (% strain) were recorded. Parameters such as elongation at break (%), tensile strength (MPa), and Young's modulus (MPa), were determined. Typical errors in the latter parameters were ~1 MPa. Five replicates were performed in each condition.

6.2.8 **Water Vapor Permeability (WVP)**

Permeability tests were conducted according to the American Society of Testing and Materials Standard Method 96 (ASTMD882-9 1996). Transparent films, cut in 80 mm diameter discs, were equilibrated for 7 days in the environmental chamber (T= 25ºC, RH = 53%). The films were tightly sealed in a permeation cell containing anhydrous calcium chloride (RH = 2%) and stored at room temperature in a container filled with distilled water (RH = 100%). Air convection was used to facilitate water diffusion. The cell was periodically weighed and the permeability to water, given as the water vapor transfer rate (*WVTR*) in $g \cdot m^{-1} \cdot s^{-1} \cdot Pa^{-1}$, was calculated according to Equation (3)

$$WVTR = (\Delta m\ x) / (A\ \Delta t\ \Delta p) \qquad (3)$$

where Δm is the weight gain (g), x is the film thickness (m), and A is the area (0.003 m^2) exposed for a certain period Δt (s) to a partial water vapor pressure Δp (Pa).

6.2.9 **Water Sorption Isotherms**

The films were cut into 25 x 25 mm^2 pieces and dried under vacuum at 60 ºC for 40 h. Then, they were placed at 25 ºC into hermetic containers with equilibrium water activities (a_W) ranging between 0.1 and 0.9. The samples were periodically weighed until achieving a constant value (2-7 days). The water sorption isotherm was determined for each sample by the correlation of a_W with the moisture content on a dry basis, X_e. The Guggenheim-Anderson-de Boer (GAB) equation:

$$X^e = (C \cdot k \cdot X^0 \cdot a^W) / ([1-k \cdot a^W] \cdot [1-k \cdot a^W + C \cdot k \cdot a^W]) \qquad (4)$$

is a typical model for fitting sigmoid-shaped equilibrium moisture isotherms in foodstuffs (AL-MUHTASEB; MCMINN; MAGEE, 2004; ROSA; MORAES; PINTO, 2010). X_0

represents the monolayer moisture content, also on dry basis, and *C* is a constant, which depends on the difference between the heats of sorption of the monomolecular and multimolecular layers. *k* is another constant reflecting the difference between the heat of sorption of the multilayer and the heat of water vapor condensation.

6.2.10 **Statistical analysis**

Data were analyzed by an ANOVA with Bonferroni's post-test using the software package GraphPad Prism San Diego, California, USA, version 5.00 for Windows www.graphpad.com. The statistical significance was assessed from the standard derivation of different measurements collected from each sample, with a significance leveled at $p < 0.05$.

6.3 RESULTS AND DISCUSSION

6.3.1 **Mechanical properties**

The determination of the mechanical properties of the chitosan biofilms, obtained by fibres (non-sonicated (NS) sample), nanoparticles (sonicated (S) sample) and NS/S(*ts*) CHIT90 blends, is essential for the adequate design of biopolymer films for packaging with a certain degree of resistance.

Using knife coating technique, homogeneous, transparent, and flexible films (without use of plasticizer) were obtained from NS CHIT90 mixed with various amount of chitosan nanoparticles ranging from 6-15nm (obtained after ultrasonication of CHIT90 at 5,15 and 30 min). The influence of the nature and content of the NS, S(*ts)* and the NS/S(*ts*) mixture on the large strain behavior of chitosan based films (conditioned at 25ºC and 53% relative humidity) was studied up to its failure by typical tensile experiments. The mean values of tensile strength (*TS*), Young's modulus (*Y*) and elongation break (*E*) measured determined from the corresponding stress–strain plots as well as the values of thickness (*d*), are displayed in Table 1.

Remarkably, the thickness of the film made up of non-sonicated CHIT90 (NS) was higher to those of sonicated and NS/S(*ts*) blend films. The films produced by sonicated (S) samples were more fine than the NS/S(*ts*) mixture. The NS (CHIT90) films presented similar values of *TS, E* and Y (82.8±2.7 MPa, 2.9±0.1% and 35.2±0.9 MPa respectively. Again, times of sonication changed the physical characteristics of the films decreasing its mechanical properties.

Incorporation of nanoparticles into the fiber solutions leads to interesting results. In general, films prepared with NS/S(*ts*) showed enhanced mechanical resistance when compared with its sonicated precursors. Different TS behaviour was observed depending on the films mixture preparation. In this sense an increase in TS was observed for NS/S(5 and 15 min) mixing ratio, showing a gain of resistance for the NS/S(5) 3:7 and NS/S(15) 7:3and 1:1 mixture, respectively, however a decrease in TS values was observed for other mixtures. The NS/S(5) showed a resistance gain with the decreasing of the mixing ratio, exhibiting a better performance when the 3:7 NS/S(5) mixing ratio was used. Regarding the film formulation NS/S(30) mixing ratio, no variation was observed in the maximum film stress of films (Table 1).

The film ability to stretch (E) also varied for the different film formulations (Table 1). When compared the S(5) films, an improvement of the E values was verified at the different mixtures, if they are compared with its sonicated precursors. As it can be observed, an increment in nanoparticles in the mixture leads to an increase in E properties for NS/S(5) mixing ratio. Nevertheless, the increasing in nanoparticles ratios seems not to influence the E values for the remaining film formulations NS/S(15 and 30) mixing ratios. ,the different behavior observed for the blended NS/S(ts) films may be ascribed to some balance of the mechanical properties, thanks to the presence of the microfibers, provided by the NPs.

The film that presented the highest TS and E was those prepared with 7:3 (95.9±3.5 and 5.3±3.0) respectively and 1:1 (96.1±3.1 and 6.9±0.9 respectively) ratio, having a higher value than NS CHIT90 film and two times greater than the precursors S(15). From these results, it is possible to infer that the better performance of these films seems to be due to the size of the nanoparticles obtained after 15 min sonication. Those blends contain larger and adequate number of β→1,4 glycoside bonds and a high number of active sites at the end of polymer chains (GOCHO et al., 2000) than that S(5), which enables a higher interaction between the molecules, making them very strong. Additionally, the polymers chains in the

blended film are tightly bounded, with a decrease in the degree of flexibility for NS films and an increase for the nanoparticled ones.

On the other hand, the NS/S(5) mixing ratio, 1:1 film showed a remarkable improvement of the percentage of elongation (E%), fourfold higher than NS sample, and six times higher than nanoparticle pioneers S(5) film. The nanoparticles used to make this film has a larger size than those produced by the ultrasound treatments for 15 and 30 min (Capítulo III), allowing for a large number of crosslinks that increase the elongation at break feature. It seems that the polymer chains of the blended film, although covalently bounded, preserved a certain degree of chain flexibility.

Regarding the elastic modulus (Y), three groups with distinct properties were observed: (i) films prepared with the NS/S(5) mixture presented lower values of Y than their NS and S precursors; (ii) an opposite behavior was observed for films prepared with NS/S(15) and (iii) NS/S(30) films presented values of Y lower than NS films and threefold higher than the S(30) films. However, within each group, an increase of nanoparticles in the blend formulation does not cause differences in Y.

The nanoparticles generated by ultrasound treatments produced new interactions by crosslinking through the chitosan amino group that would normally be involved in the hydrogen binding between the chitosan fibers (CHIT90) and the nanoparticles (ALBANNA et al., 2013; OSTROWSKA-CZUBENKO; GIERSZEWSKA-DRUŻYŃSKA, 2009) In films made up of chitosan and alginate, it was demonstrated that a three-dimensional network was formed by chemical or physical crosslinking of the hydrophilic polymer chains (OSTROWSKA-CZUBENKO; GIERSZEWSKA-DRUŻYŃSKA, 2009). In chemical gels, polymer chains are connected by covalent bonds, but in physical gels they are held together by molecular entanglements, not covalently bonds, such as Van der Waals interactions, ionic interactions, hydrogen bonding, hydrophobic interactions, traces of crystallinity and multiple helices.

Mechanical testing results confirmed the proposed hypothesis that mixing fiber and chitosan nanoparticles results in an improvement film in improved TS, E and Y films properties. In this sense, in the NS/S(*ts*) chitosan films presented here, the nanoparticles seem to have major contact with the surfaces due to their smaller size, increasing the number of chemical crosslinks with the biofilm matrix (CHIT90), thus being able to make more connections and, consequently, improving the mechanical properties of these films.

Usually, all mixtures used produced fiber/nanoparticle films with improved strength and stiffness and decreased fiber elasticity to different extents when compared with NS. Without use of any plasticizer, that could be transfered to the packaged food, these improvements in fiber/nanoparticles film properties should broaden the utility to fabrication of biofilms to be regularly used in agro-resources and in biotechnology as a substitute of bio-fuel plastic.

Table 1. Film thickness (*d*), tensile properties (tensile strength, TS; elongation at break, E; and Young´s modulus, *Y*) and water vapor permeability (WVP) for solid chitosan films prepared from Chito90 and nanoparticle mixtures.

CHIT90	Mixing ratio	*d* / mm	TS / MPa	E / %	Y / MPa	WVP·10^{-11}/ g.$m^{-1}s^{-1}Pa^{-1}$
NS	0	0.01±0.007[a]	82.8±2.7[a,b]	2.9±0.1[a,b]	35.2±0.9[a,b,c]	14.2±1.1
NS/S(5 min)	7:3	0.023±0.004[b,c]	67.3±3.7[b,c]	5.1±0.4[c]	16.1±4.3[d,h,i]	7.89±0.1[1]
	1:1	0.025±0.005[b]	64.3±7.6[b,c]	12.9±0.8	16.2±1.0[d,h]	9.46 ±4.5
	3:7	0.019±0.002[b,c]	100.6±10.5[a,e]	9.58±0.6	17.6±2.3[d,e,g]	5.92 ±0.7[2]
S(5 min)		0.008±0.006[a]	56.0±9.5[c,d]	2.67±0.7[a,b]	18.0±0.8[d,e,f]	13.6±4.4
NS/S(15 min)	7:3	0.019±0.001[b,d]	95.9±3.5[e]	5.3±3.0[c,d,e]	40.7±1.5[b,k]	13.2 ±3.2[3]
	1:1	0.017±0.003[c,d,g]	96.1±3.1[e]	6.94±0.9[e]	50.0±9.4[k]	12.1 ±0.15
	3:7	0.022±0.005[b,d,e,f]	68.9±3.2[c]	6.86±1.4[e]	37.9±5.4[a]	9.08 ±0.7
S(15 min)		0.008±0.001[a]	61.1±20.0[c,f]	3.5±0.1[d]	29.5±5.0[a,b,c,e,j]	7.8±2.0
NS/S(30 min)	7:3	0.027±0.01[f]	34.1±8.4[h,i]	1.51±0.3[b]	24.6±11.2[f,g,i,j]	8.70 ±5.3
	1:1	0.018±0.003[c,e]	49.7±3.0[d,f,i]	1.86±0.16[a,b]	38.9±7.9[a,k]	6.27 ±3.9[1,2,4]
	3:7	0.011±0.001[a,g]	41.0±1.1[d,g,h]	3.0±1.0[a,b]	29.2±3.3[c,f]	3. 93 ±0.4[1,2,4]
S(30 min)		0.009±0.003[a]	26.5±7.9[g]	2.72±.0.9[b,a]	9.1±1.3[g,h]	7.9±0.7

Values are given as means ± standard deviations. Same subscript letters within the same column indicate non-significant differences ($p > 0.05$, Bonferroni test). For WVP parameter, the samples with the same number showed significant differences, number 1 represent difference for sample NS; number 1 represent difference for sample NS; number 2 represent difference for sample S(5 min); number 3 represent difference for sample NS(5)3:7; number 4 represent difference for sample NS(15)7:3, ($p < 0.05$, Bonferroni test).

6.3.2 **Water vapor permeability (WVP) and moisture sorption isotherm**

The water permeability and water absorption properties of films are involved with the diffusion of molecules through the film matrix, representing the equilibrium relationship between its moisture content and the water activity (aw), which are necessary to predict the properties of films in different environments.

In line with this discussion, the water vapour permeability measures of the NS, S and NS/S(*ts*) of the films are displayed in Table 1. Films produced with sonicated chitosan seem to decrease water vapor permeability (WVP), while maintaining other desirable mechanical properties. In other words, when compared with NS WVP values, the blends obtained with sonicated nanoparticles NS/S(*ts*), showed decreased: water permeating per area unit area (WVP) and time to through the packing material. The WVP values ranged between 3.9 – 14.2 x 10^{-11}/g.m^{-1}.s^{-1}.Pa^{-1} (Table 1).

The chitosan film reinforced with S (15 min) chitosan nanoparticles had the highest WVP, ranging from 13.2 – 9.08.x 10^{-11}/g.m^{-1}.s^{-1}.Pa^{-1}. This was because chitosan nanoparticle obtained after 15 min sonication decreased the compactness of the films. The blend films made with S(30) showed the smallest WVP values, which decreased as the proportion of nanoparticles was enhanced. Values varied between 3.9 – 8.7 x 10^{-11}/g.m^{-1}.s^{-1}.Pa^{-1} a decrease is WVP was observed in the 3:7 mixing (table 1). The behaviour could be explained since the lower diffusion rates for water or gas molecules result from transport obstruction through the molecular network packing. (RAMOS et al., 2013). In general, the WVP values of NS chitosan films are similar to that found for chitosan films prepared without plasticizers (HWANG et al., 2003; SOUZA, H. K. S. et al., 2013) . However these values are lower when compared with those made up by chitosan DD 92% solution diluted in acetic acid (KIM, K. M. et al., 2006) and by other biopolymers, such as protein and cellulose (PARK; CHINNAN, 1995).

In a recent study (SOUZA, H. K. S. et al., 2013), it was demonstrated that films prepared from the most ruptured degraded CHIT90 exhibited the lowest water permeability. Small and spherical low molecular mass chitosan particles contain larger spherulytic crystallite and more crystalline domains, which enhances the resistance to solvent penetration (SOUZA, B. W. S. et al., 2010).

The WVP results found here are in agreement with this hypothesis. Since, the 3:7 ratio NS/S(30) films exhibited lowest WVP values, it can hypothesize that an increase in S(30) nanoparticle proportion result in WVP decreases, confirming that these samples filled the voids shaped by the fibril matrix and consequently result in films where the permeation of water molecules is more difficult. However, when chitosan nanoparticles were obtained after 15 min sonication, it seems that the nanoparticles would tend to form aggregates, which could not contribute to preventing water molecule diffusion; thus, the WVP is increased.

Additional increment of chitosan nanoparticles induced a reduction in WVP for others systems. For instance, chitosan nanoparticles increased the barrier effect for banana films (FABER et al., 2004), in poly(caprolactone), composite films (FABER et al., 2005) and was successfully used as reinforcement material in methylcelluose based film (DE MOURA et al., 2009). Since these features are involved in the physicochemical and microbiological deterioration of food (JANJARASSKUL; KROCHTA, 2010), the NS/S blends obtained herein show desirable characteristic for biofilms to be applied on fruit and seed coating.

Moistures of the sorption isotherms are important to evaluate the effect of temperature and relative humidity on film properties (LAI; PADUA, 1998). Addition or removal of water may cause phase transitions in the macromolecular structure (TORRES, 1994). The GAB was used to fit the water adsorption data of the NS, S and NS/S(*ts*) films. A goodness of the fit was acquired and the fitting parameters are displayed in Table 2.

The change in the moisture sorption isotherms of NS, S(*ts*) and NS/S(*ts*) showed the equilibrium moisture content of all of these films was dramatically increased in values above aw = 0.6 for precursor (NS and S(*ts*)) films and aw = 0.3 for the blends (NS/S(*ts*)), was observed the presence of nanoparticles affected the moisture sorption isotherms of the NS/S(*ts*) films (figures 1).

The equilibrium moisture content of the NS/S(*ts*) films decreased as nanoparticles is submitted to different time period of sonication (*ts*= 5, 15 or 30 min). The NS/S(30) presents the lowest moisture content at a given aw. It seems that the smallest nanoparticles provide less active sites to bind water molecules hydroxyl groups.

The isothermal results of NS and S(*ts*) films showed good agreement with those previously described (SOUZA, H. K. S. et al., 2013). The *k* values are in accordance with the recommended values ($0.6<k<1.0$) (GARCíA-OLMEDO et al., 2001). The amount of water

involved in the adsorption of one monolayer is quantitatively described (on a dry basis) by X_0 (SOUZA, H. K. S. et al., 2013). In the present study, the blend films showed different behaviour, according to the qualitative analysis of the curves, an increase of X_0 values is observed for NS/S 15 and 30 min mixtures when compared with sonicated precursors. X_0 also was higher for these mixtures, indicating that these films present the highest number of sorption sites that adsorbed in a monolayer of dry films. No significant differences in X_0 were observed at distinct NS/S mixing ratios.

Table 2. GAB parameters obtained from fitting the data in the GAB model. Values are displayed as mean ± standard deviations.

Chit 90	**Mix ratio**	**C**	**k**	**Xo**	**R^2**
NS	0	0,017	0,9	0,12	0,9908
NS/S (5 min)	7:3	2.84	1.0	0,0045	0,9813
	1:1	1.6	1.0	0.01	0.991
	3:7	1,0	1.0	0,01	0,9818
S (5 min)		2.0	0.90	0.01	0.997
NS/S (15 min)	7:3	5.5	0.99	0.1	0.995
	1:1	3,5	0.88	0,008	0.995
	3:7	2.2	0.95	0.1	0.999
S (15 min)		3.1	1.05	0.003	0.997
NS/S (30 min) Mixing ratio	7:3	0,0023	1,0	0,1	0,99289
	1:1	0,0023	1,0	0.1	0,98445
	3:7	0,0136	0,9	0.1	0,97354
S (30 min)		11.6	1.0	0.002	0.998

Chitosan has three predominant adsorption sites: the hydroxyl group, the amino group and the polymer chain ends. The decrease in molecular weight increases the number of polymer chain ends per unit weight. Thereby, the adsorption sites are newly produced from increasing degradation process, due to the decrease in the molecular weight of chitosan (GOCHO et al., 2000). This observation is in agreement with mechanical properties results because of the highest young modulus values that was found in NS/S(15 and 30) mixtures. Instead to the data observed for the set of blend films containing S(5 min) showed a decrease in water activity (a_w) in one monolayer adsorption, where it was observed lower values of Xo,

representing low number of sorption sites in a monolayer of dry films. The values of Xo for these samples are similar considering all ratios used.

Accompanied by k values approaching to 1, a very high value of C was found for NS/S(15) in the blend, 7:3. This kind of GAB parameter combinations is related to the multilayer molecules of the film, which have properties comparable with those of bulk liquid molecules. In other words, high C values in the blend film could be associated with the sorption of water by NS/S(15) 7:3 ratio, that is apparently characterized by a monolayer of molecules. The following molecules are a little structured (or not) in a multilayer, nevertheless its characteristics are comparable with the molecules in bulk liquid.

In contrast the NS/S(30) showed decreased C values. The water molecules are less strongly bounded to the material since they are organized in monolayer. These materials are also organized in multilayers where upon the water molecules differ significantly from bulk liquid molecules. Considering also that the smallest nanoparticles (30 min) provide a petty number of adsorption sites, and present high water adsorption (X_0), one can conclude that high and strong interactions could occur between fibres and nanoparticles. These results are in line with the WVP measures. As discussed above the, blend prepared with 3:7 NS/S(30) presented the lowest WVP values and, on the contrary, the NS/S(15) blend was considered the most permeable.

Additionally, X_0 and C values was lower when compared with NS/S(5) and NS/S(15) blends. This behaviour indicates that NS/S(5) adsorbed less water than the NS/S(15). However, NS/S(5) blends presented C values higher than NS/S(30), showing more adsorption of water for these samples. Again these results corroborate with WVP measures where WVP values for NS/S(5) samples fluctuated between NS/S(15 and 30) levels.

Sorption results are also in accordance with mechanical properties results. Since nanoparticles provided after 15 min of sonication are larger than those obtained after 30 min. The former samples presented more β→1,4 linked. When mixed with NS samples generated films with a superior resistance (stronger bonds, see Table 1). However they present high C and WVP values due to the not homogeneous filling of fibre holes. Regarding NS/S(30), the sample presented the lowest TS (less β→1,4 linkage and smaller macromolecules) and C values. In this case, nanoparticles (S) are more cohesively structured with the fibres (NS) resulting in homogeneous filling (closing the holes that exist in fibre structures) not leaving

spaces for water molecules which make these films less permeable and more compacted (figure 3).

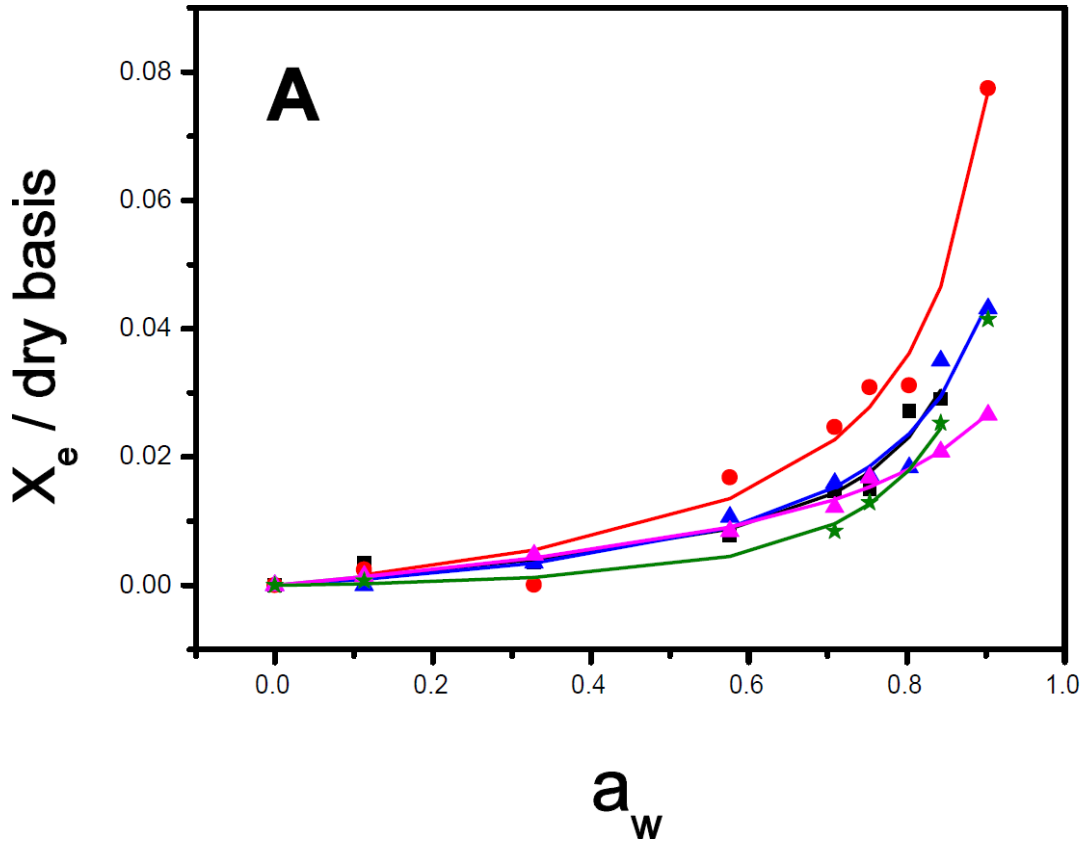

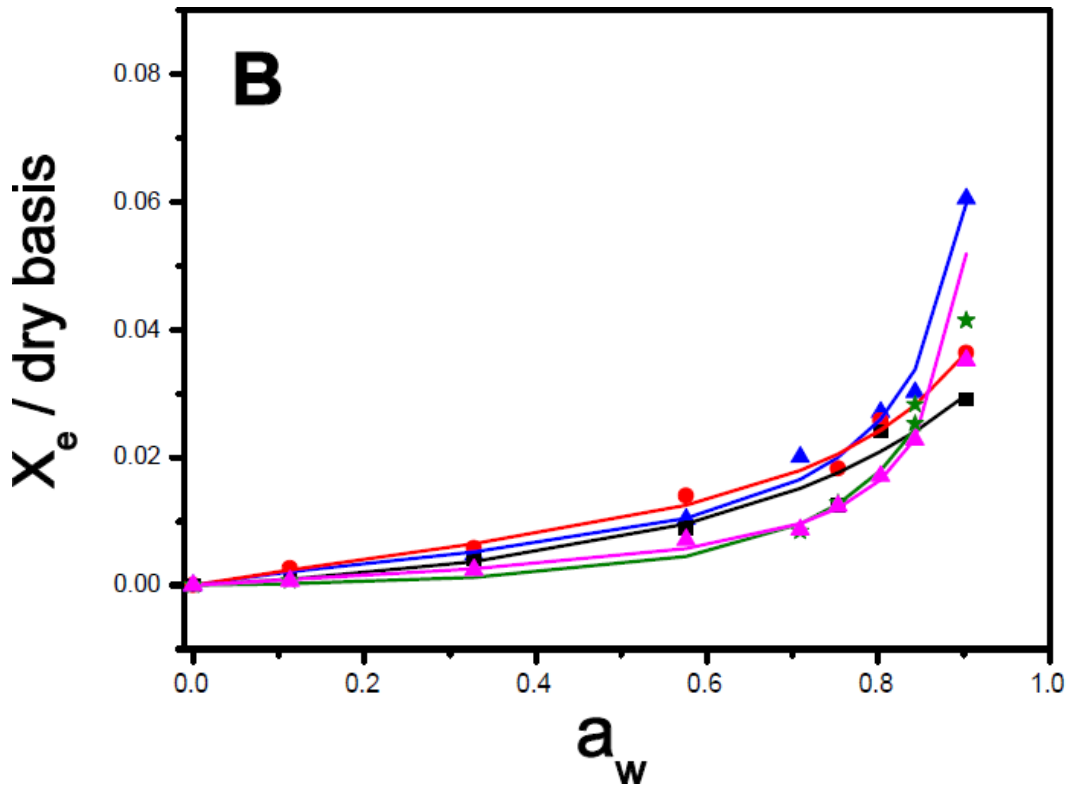

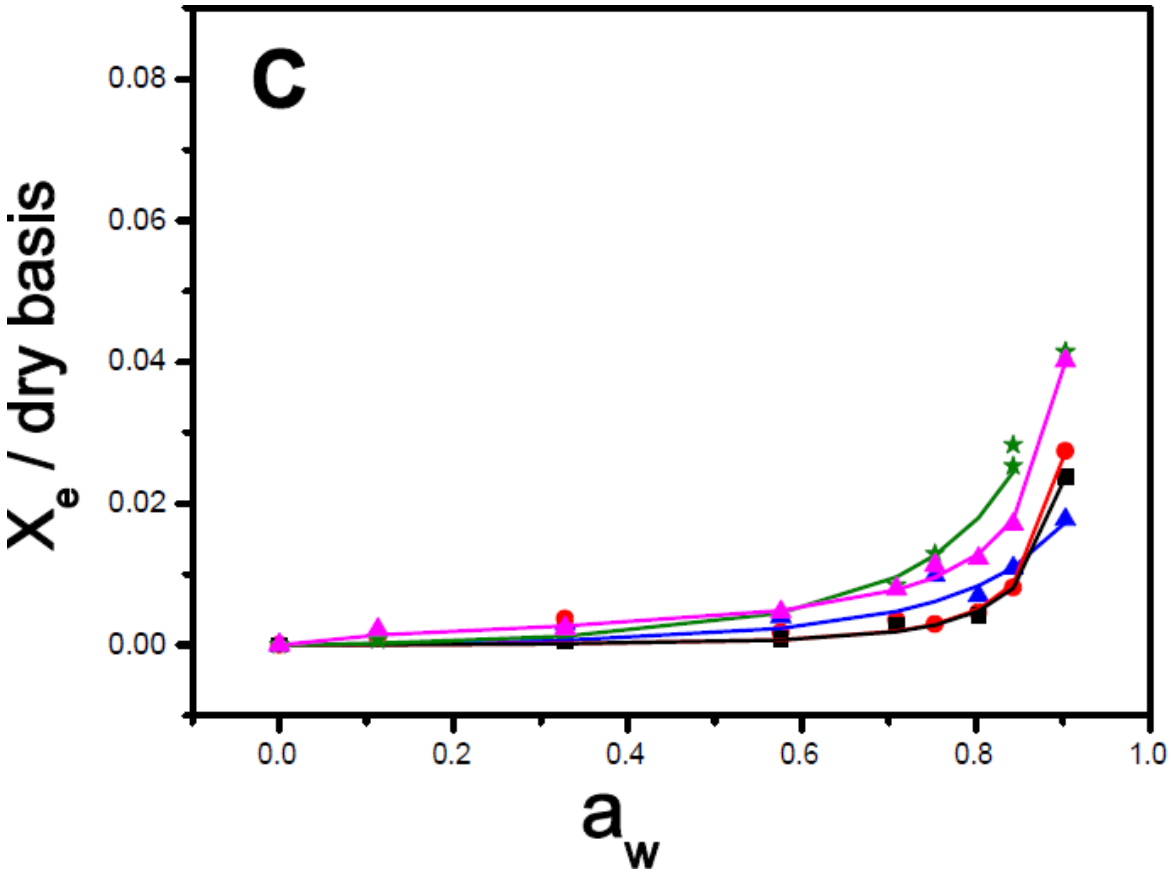

Figure 1. Effect of different NS/S(*ts*) mixing ratio concentrations on the equilibrium moisture content of the films, fitted with GAB model. The GAB fitting (solid lines, for each sample), NS (green stars, all panels) and S (pink triangles, all panels)., For each system the following NS/S ratios were studied: 7:3 (black squares), 1:1 (red circles), and 3:7 (blue triangles) in all panels;. Sonicated for *ts* =5 (panel A), 15 (panel B), and 30 min (panel C).

6.3.3 **Morphology of the chitosan blend films**

Cross sections of the cryo-fractured NS (CHIT90) and S (5 min) are showed in Fig 2A and B, and 1:1 blends to NS/S (5, 15 and 30) are presented in Figs 2. In line with the previous results NS and S(5) present large fibers and spherical nanoparticles, respectively.

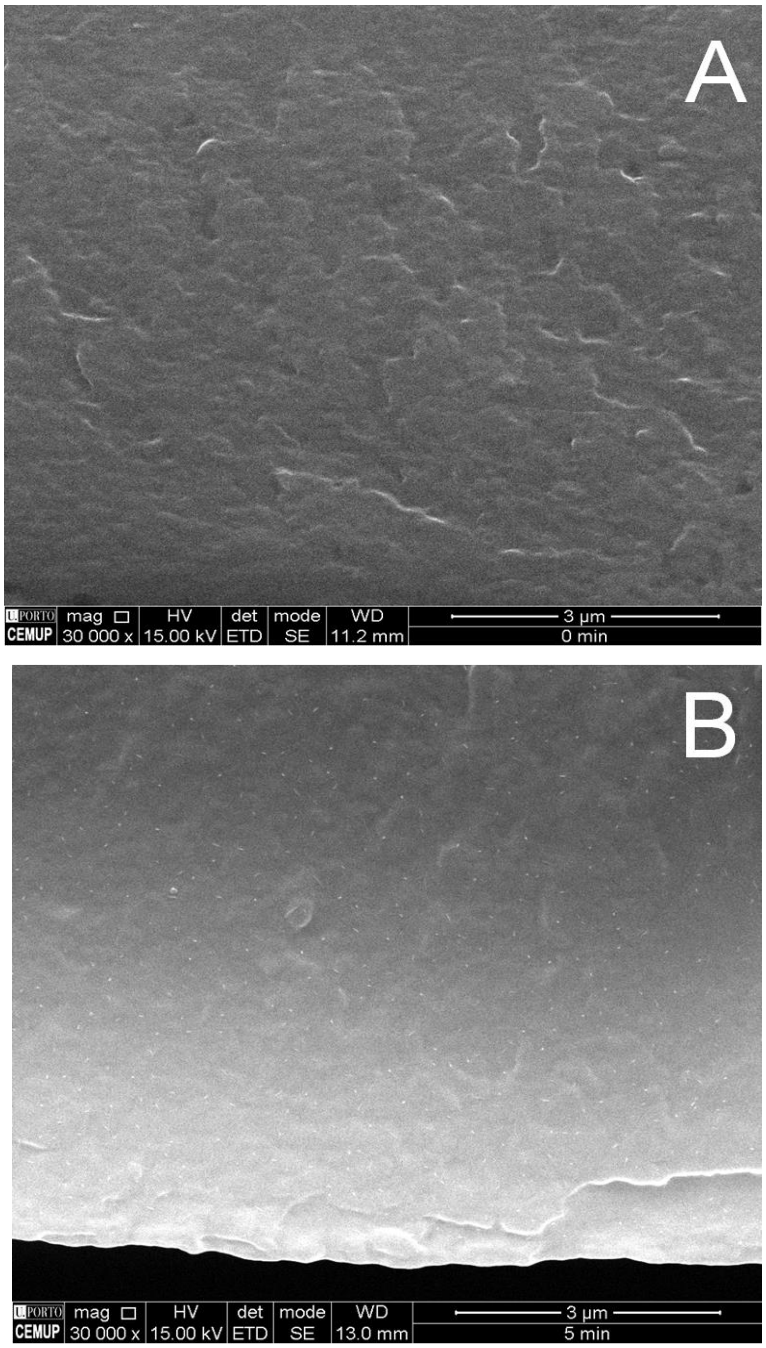

Figure 2. Representative SEM pictures of the cross-sections of cryo-fractured films at 30,000x magnification (A — NS CHIT90 and B — S(5).

The SEM micrographs of the fractured surface of NS/S (5, 15 and 30 min) of 1:1 blends films are illustrated in Figure 3. It was observed, a distinct superficial arrangement after the incorporation of nanoparticles into the fiber film matrixes resulting in films with a large number of small discrete nanoparticles within fibres as exhibited in the Fig 3, and more clearly showed in the Fig 3A.

As observed in a previous study (Capítulo II) the size of nanoparticles are dependent of sonication time sonication. For instance, image of blends prepared at 1:1 ratio with S(15 and 30) (Figure 3B and 3C) showed a cross-section more homogeneous and smooth. This observation shows that after adding the nanoparticles sonicated by 15 and 30 min the interfacial interaction between fibers from NS chitosan and S were improved.

These results are in accordance with mechanical and WVP evaluations. As discussed above, a very good improvement of mechanical properties (TS, E and Y) was observed for NS/S(15) 1:1 when compared with their precursors. Nevertheless blends prepared with NS/S (1:1) 30 min presented also an improvement of mechanical properties (when compared with their sonicated precursors), showing the lowest WVP values.

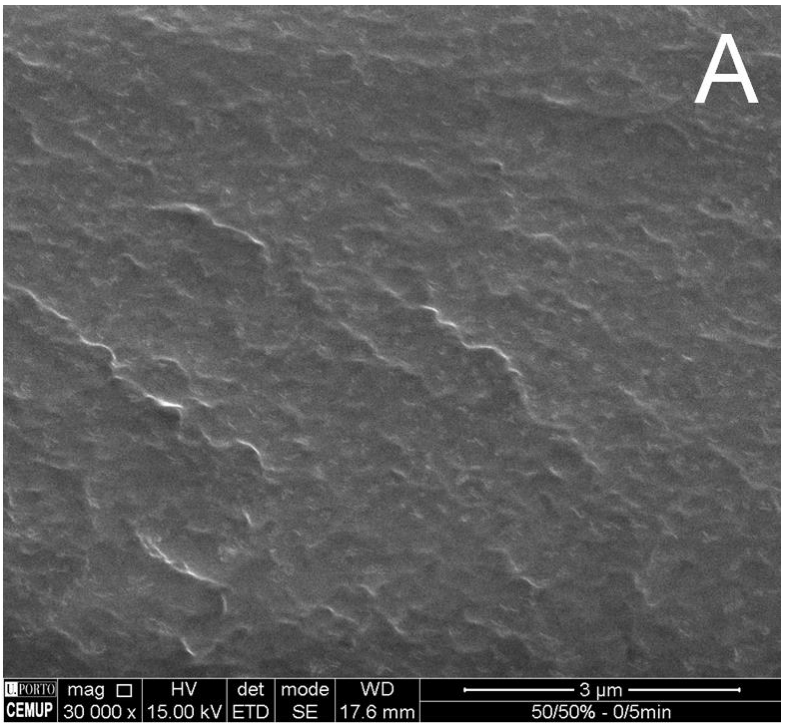

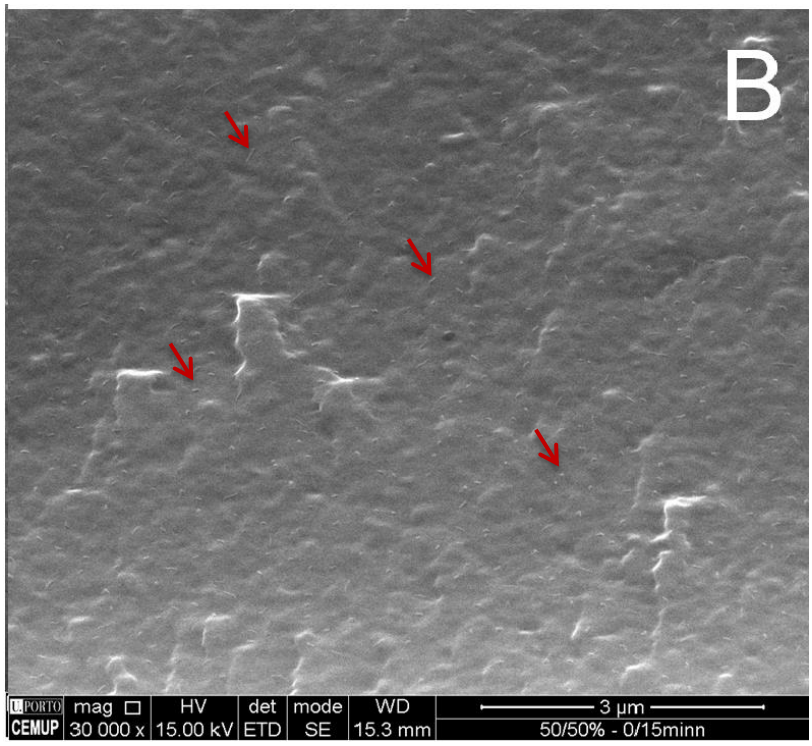

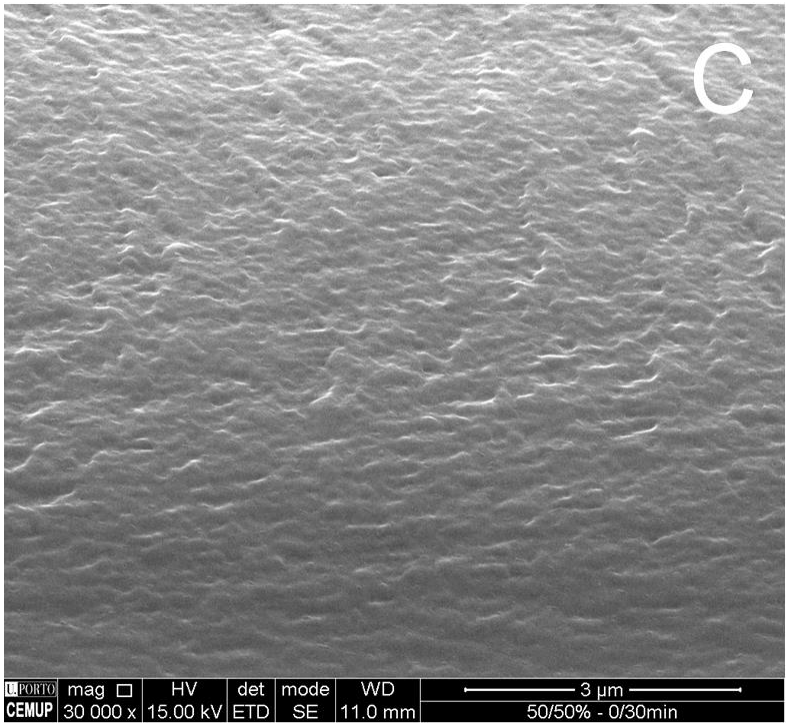

Figure 3. Representative SEM pictures of the cross-sections of cryo-fractured NS/S(*ts)* 1:1 ratio films at 30,000x magnification A — NS/S(5), B — NS/S(15) and C— NS/S(30).Red arrows indicated the preference of small fibrils and spherical nanoparticles, apparently distributed within the film.

6.3.4 **Color properties**

Color is an important object measurement for image understanding and object description, used for conferring quality evaluation and inspection of food products. Color measurements can be performed by visual (human) inspection, traditional instruments such as colorimeters, or computer vision (WU; SUN, 2013). The parameter ΔE provides a good measure of color difference, since it takes in consideration the following three parameters: lightness (L), red – green (a) and yellow – blue (b) components.

The total color difference and opacity of the films produced are summarized in Table 3. All blends of chitosan films were very transparent, with L coordinate ≥ 91. When color parameters of blend films were compared to those CHIT90 films, significant differences were observed when 15 and 30 min-sonicated particles were used. Addition of nanoparticles into the fibers affected the a* (red-green) and the b* (yellow-blue) measurements. Great values of b* were observed for NS/S (15 min).

Table 3. Color parameters

CHIT90	Mixing ratio	L*	a*	b*	ΔE*	Opacity
NS	**0**	95.67±0.2[a]	-0.302±0.04[a]	3.26±0.2[a]	2.1±0.3[a]	10.4±0.2[a]
NS/S(5 min)	**7:3**	97.22±0.2[c]	-0.21±0.1[a]	3.05±0.8[a,b,d]	1.3±0.8[a]	-
	1:1	95.38±0.1[a]	-0.27±0.06[a]	3.4±0.2[c,d]	2.4±0.2[a]	12.2±1.9[a,b]
	3:7	96.88±0.8[b,c]	-0.33±0.3[a]	3.9±1.7[a,c]	2.3±1.8[a]	-
S(5 min)		96.17±0.5[a,b]	0.002±0.008[a]	2.6±0.1[a,b]	1.3±0.4[a]	12.3±0.8[b]
NS/S(15 min)	**7:3**	91.30±0.8[e]	-0.53±0.06[a]	5.52±0.2[e]	7.0±0.7[c]	13.4±0.6[c]
	1:1	92.65±0.8[d]	-0.52±0.07[a]	5.05±0.2[e]	5.6±0.7[b]	13.2±0.4[c]
	3:7	95.24±1.0[a]	-0.26±0.04[a]	3.72±0.2[a]	2.8±0.8[a]	10.4±1.5[a]
S(15 min)		96.25±0.4[a]	0.07±0.04[a]	2.57±0.3[e]	1.8±0.5[a]	12.3±0.7[c]
NS/S(30 min)	**7:3**	95.01±0.6[i]	-0.11±0.1[a]	3.39±0.4[a,g]	2.6±0.8[a,e]	10.7±0.9[a,e]
	1:1	95.86±0.7[a,h]	-0.18±0.08[a]	3.42±0.2[a,g]	2.1±0.5[a,e]	12.2±1.1[d,e]
	3:7	94.63±0.7[g]	-0.32±0.04[a]	3.90±0.3[g]	3.3±0.7[e]	12.0±1,1[a,d,e]
S(30 min)		93.34±0.6[f]	-0.56±0.06[a]	5.2±0.3[f]	5.1±0.7[d]	12.6±0.6[d]

CIELab standards were used as the white standard with the film background: Ls*(97.10), as*(0.05) and bs*(1.76). Mean values ± standard deviations. Superscripts in the same column with different letters indicate significant differences ($p < 0.05$).

Sonication time periods lead to a significant effect on the total color differences when compared withNS blend films. The S(30) films presented the highest value of ΔE (5.1 ±0.7). Regarding mixture films, incorporation of nanoparticles (S:15 and 30 min) had a significant increased effect on the ΔE, that is, the high S(15), the highest ΔE for those blend films in the films 7:3 and 1:1 ratio. Additionally, the results indicated that the addition of S(5) to the blend does not lead to statistically significant changes ($p > 0.05$) in ΔE values . The highest values of opacity was founded in NS/S(15) 7:3 and 1:1 ratios.

The total color difference (ΔE) observed between all samples was discrete in comparison with other films, mainly those produced from soybean protein concentrate with plasticizer (CIANNAMEA; STEFANI; RUSECKAITE, 2014). Indeed, it has considered that the incorporation of plasticizers can promote more transparency, since these molecules interact between protein chains, decreasing the absorbance in the visible region (SOTHORNVIT, R. et al., 2007).

Even in the chitosan films, the addition of plasticizers such as glycerol and Tween 20 showed L value that indicates film lightness and yellowness decreases (ZIANI et al., 2008) as reported previously (LOPEZ et al., 2014).

An increment of nanoparticles in the blend led to an increase in the films' opacity comparatively with NS film (table 4). The blend films containing S 15 min showed the highest opacity. The nanoparticles may be embedded in the interspaces of chitosan film, which prevented light transmittance and leading to higher opacity.

Table 4 shows that, in general, with the addition of nanoparticles, the opacity value of the NS/S(*ts*) films increase when compared with NS film , suggesting that the chitosan fiber film was more transparent than the NS/S films. Highest values of opacity was found in NS/S(15) 7:3 and 1:1 ratio.

6.4 CONCLUSION

In this study it was produced fine films by knife-coating technic, from blends of non-sonicated (CHIT90) and colloidal chitosans, NS/S(*ts*) (3:7, 1:1 and 7:3). The colloidal solutions produced by ultrassonication (for different times *ts*= 5, 15 and 30min), present various morphologies and molecular weights. The results herein showed that it was produced films with different mechanical, water moister proprieties and WVP adjusted though the controlling of mixing ratios of NS/S(*ts*) it is able to being able to produce flexible films with good transparency and homogeneous morphology (without use of plasticizer).

The film produced with proportion NS/S(5) 3:7and NS/S (15) 7:3 e 1:1,showed better tense average. The increment in nanoparticles leads to an increase in E properties for NS/S(5 and 15 min) mixing ratios. Chitosan film reinforced with S(*ts*) showed an improvement at the WVP. Additional increment of chitosan nanoparticles induced a reduction of WVP for others systems, the blends made with S(30) showed the smallest WVP values. The equilibrium

moisture content of all films dramatically increased above aw = 0.6 for precursors films and aw = 0.3 for the blends. Films reinforced with nanoparticles showed little change in the color proprieties without compromised the film transparencies.

7 CAPITULO V – ESTUDO ORIGINAL 3

ANTIMICROBIAL ACTIVITY OF CHITOSAN NANOPARTICLES OBTAINED BY ULTRASOUND IRRADIATION (Manuscrito em preparação)

Abstract

Chitosan is a natural polysaccharide prepared by the N-deacetylation of chitin. In this study, the physical- chemical and inhibitory characteristics of chitosan nanoparticles produced by ultrasound irradiation were evaluated. The physicochemical properties of the nanoparticles were determined by dynamic light scattering and zeta potential analysis. The antibacterial activity of chitosan nanoparticles against *E. coli* was evaluated by calculation of minimum inhibitory concentration (MIC) and minimum bactericidal concentration (MBC). Results showed that chitosan nanoparticles could inhibit the growth of the bacteria tested. The MIC values were inferior to 0.5mg/mL, and the MBC values of nanoparticles were similar or higher than MIC. DNA release measurements revealed that the exposure of *E. coli* to the chitosan nanoparticles led to the disruption of cell membranes and the leakage of cytoplasm and nucleus contents.

7.1 INTRODUCTION

During the last decades, the number of studies on the use of engineered nanoparticles (NPs) and nanomaterials (NMs) has increased in many research areas, with important applications in water purification, drug delivery, antimicrobial treatments, tissue engineering, biosensors, detection of analyses related to magnetic diagnostics and detection: pathogen, toxins, drug residues and vitamins (THATAI et al., 2014). Several methods have been developed for the production of NPs, such as ionotropic gelation, spray drying, emulsification, coacervation and, more recently, ultrassonication (SINHA et al., 2004) One of the applications of high intensity ultrasound (US) is the effective polymer degradation, breaking up aggregates and reducing NP size and polydispersity. Ultrassonication leads to the decrease in the mean diameter and polydispersity of particle size when the duration time or amplitude of the irradiation is increased (GOMES, LAIDSON P. et al., 2016; TANG, E. S. K. et al., 2003). The application of studies regarding nano-based composites and the physical stability of NPs are directly linked to material characteristics, such as chemical composition, size, shape, surface charge density, hydrophobicity (NEL et al., 2006), polydispersity and the presence or absence of functional groups or other chemicals (MAGREZ et al., 2006). These important characteristics define the potential applications for NPs.

Biodegradable NPs have being attracted great attention, due to their ability not only to protect proteins and peptides from degradation but also due to their desirable release profiles.

Among these macromolecules, chitosan (CS) has been studied during the last two decades. CS is produced by the removal of acetyl groups by alkali or enzymatic (GOMES, LAIDSON P. et al., 2014) treatment of the chitin chain leaving behind a reactive amino group (NH_2), responsible for chitosan versatility (WANG, W. et al., 2008). As a natural polysaccharide and potential biological compatibility with chemically versatile NH_3^+ groups, the amino groups, at pH lower than 6.5 the amines are protonated and CS acquires polycationic behavior, showed a polyelectrolyte behavior (NAGPAL; SINGH; MISHRA, 2010).

Chitosan possesses a wide range of useful properties, specifically; biocompatible, biodegradability and antibacterial activity. CS applications include water treatment, chromatography, cosmetic additives, coatings for food conservation, as fruits and sliced sausages, seed preservation against microbial spoilage, production of biodegradable films and microcapsule implants for drug and vaccine delivery (Capítulo I) (XIA et al., 2011). The inhibition activity described for chitosan has been observed that depends on its molecular wight (MW), degree acetylation (DA), pH and, of course, the target organism (HERNÁNDEZ-LAUZARDO et al., 2008; TSAI; SU, 1999). Chitosan shows several advantages over other types of disinfectants, since it possesses high-antimicrobial activity, a broad activity spectrum and low toxicity to mammalian cells (LIU, X. D. et al., 2001).

Nanoscale chitosan and its derivatives have also been considered as antimicrobial agent against bacteria, viruses and fungi (QI et al., 2004) The nano-CS may present several molecular weights and show known antimicrobial activity, some studies demonstrated low toxicity, being safe for human applications (MUZZARELLI; A, 2011).

The investigation of chitosan antimicrobial properties has been a long journey of scientific exploration and technological development. The distinct physical states and MWs of chitosan and its derivatives render distinctive antibacterial action mechanisms. Chitosan can inhibit and suppress microbial activities through electrostatic charge interaction between the positive charges on polycationic chitosan macromolecules (amino groups) with the negative charges on the microbial surface (AZIZ et al., 2012). This interaction causes disruption on the microbial cells, which then change their metabolism and lead to cell death (EL-SHARIF; HUSSAIN, 2011; LECETA et al., 2013). On the other hand, low molecular weight water-soluble chitosan and ultrafine nanoparticles can penetrate bacterial cell walls and combine with bacterial DNA, inhibiting mRNA synthesis and DNA transcription (SUDARSHAN, N. R. et al., 1992). HMW water-soluble chitosan and solid chitosan, including larger sized nanoparticles, interact with the cell surface instead, altering cell permeability (CHOI et al.,

2001; EATON et al., 2008; LEUBA; STOSSEL, 1986), resulting in membrane degradation or forming an impermeable layer around the cell, at blocks the transport of essential solutes into the cell .

Although, there are few studies on NPs forms of CS concerning to antimicrobial activity, the small size of chitosan nanoparticles renders them unique physicochemical properties, such as large surface area (providing more cationic sites) and high reactivity, which could, thus, potentially enhance the charge interaction on the microbial surface and lead to superior antimicrobial effects (ZHANG, L. et al., 2010).

The objective of this study is to evaluate the physical- chemical characteristics of chitosan NPs produced by green process chemistry and its antimicrobial activity against food pathogens as *Escherichia coli* and *Staphylococcus aureus* process evaluate from antimicrobial activity.

7.2 MATERIALS AND METHODS

7.2.1 **Polymer degradation**

Nanoparticles (NPs) were produced from two commercial chitosan, of medium (CS-MMW) and low molecular weight (CS-LMW) with degree acetylation >75% (Sigma-Aldrich® Saint-Louis, MO - USA). Samples (2%) were solubilized in 0.1 M sodium acetate pH 4.0, in ice bath and irradiated with ultrasonic probe SONIC model 750 W, equipped with a 1/2" microtip at 4ºC for 30 min. The irradiation was performed under constant duty cycle and 40% amplitude with 1/1s intervals.

7.2.2**. Dynamic light scattering (DLS) measurements**

The measurements of hydrodynamic radius (*Rh*) and polydispersity index (PdI) of, pre (CS-MMW and CS-LMW) and post (CS-MMW30 and CS-LMW30) irradiation, were performed using a DynaPro NanoStar (Wyatt Technology Corporation, Santa Barbara, USA).

7.2.3 **Zeta potential (ζ-potential)**

Zeta potential measurements were performed by applying an electric field across the samples and the value of the zeta potential was obtained by measuring the velocity of the electrophoretic mobility of the particles using the laser Doppler anemometry technique. The measurements were performed five times for each sample at 25 °C using a NanoBrook 90Plus PALS (Brookhaven Instruments Corporation, New York, USA).

7.2.4 **Antimicrobial activity**

7.2.4.1 Determination of minimum inhibitory concentration (MIC)

Escherichia coli DH5α strain (INCQS-Fiocruz) was grown in Luria-Bertani (LB) medium (BD, Sparks Glencoe, EUA), in an orbital shaker at 200 rpm, 37°C, for 24 h. One milliliter of the culture was centrifuged at 5000 x g for 2 min and the supernatant was discarded. The cellular density was adjusted in saline solution (0.85% NaCl) to the turbidity equivalent to McFarland 0.5 standard ($1.5x10^8$ CFU/ml) (SHUKLA, SUDHEESH K et al., 2013) and it was used as an inoculum. The antimicrobial activity of the produced chitosan samples (CS-MMW, CS-LMW, CS-MMW30 and CS-LMW30) were evaluated on batch cultures containing chitosan derivatives 0.5 and1.0 mg/ml in suspension against 10^7 CFU/ml. One hundred microliters of the each mixture was withdrawn and added to 96 wells microplate (Cellstar, Greiner bio). The microplates were incubated at the same conditions above for 24 h and the optical densities were determined at 620 nm by VitorX4 (PerkinElmer, USA). The inhibitory percentage was calculated using the method described by MADUREIRA et al. (2015).

7.2.4.2 Determination of the minimal bacterial concentration (MBC)

The MBC concentration that allows the initial viable cells to be reduced at least 99.9% was evaluated by adding 20 µl aliquots of negative wells (no growth), plated on LB and incubated at 37 °C for 48 h.

7.2.4.3 *In vitro* growth inhibition of chitosan

Antibacterial activity of chitosan against *E. coli* DH5α was evaluated by inoculating 100 µL overnight bacterial culture at 37 °C with 220 rpm into chitosan solutions of 0.5 and 1.0 mg/mL, . In addition, the effect of the incubation time was evaluated by inoculating 100µL of the overnight bacteria culture into chitosan solution and incubating the mixture for 1, 2, 4 and 6 h at 37°C. Bacteria enumeration was determined by counting of colonies on LB plate after overnight at 37 °C.. The experiments were performed in triplicate.

7.2.5 **Integrity of cell membrane**

Cell membrane integrity of *E. coli* was as reported in the literature (SUDARSHAN, N.; HOOVER, D.; KNORR, D., 1992). In brief, the cultured bacteria were harvested in the different intervals of time (1, 2, 4, 6 h), washed twice, and suspended in sterile 0.85% NaCl solution. The bacterial suspension was adjusted to 0.6 at OD_{630nm} and the absorbance at 260 nm was accompanied by spectrophotometry (Beckman DU 640 spectrophotometer, USA).Chitosan stock was inoculated into bacterial suspension to give a final concentration of chitosan at 0.5 and 1mg/mL, respectively, during a same period of time of incubations described above.

7.3 RESULTS AND DISCUSSION

7.3.1 DLS and ζ-potential

The particle size distributions were calculated by DLS and ζ-potential measures before (CS-MMW and CS-LMW) and after (CS-MMW30 and CS-LMW30) the ultrassonication for 30 min. The chitosan fragmentation process by ultrasound and its capacity to produce nanoparticles is already known (Capítulo III), was show in Table 1. The irradiation process increased the % intensity of smaller macromolecules obtained from the degradation of commercial chitosan. The high range of the polydispersity index, 2- 4% (PdI), is an indicative of the existence of group of particles with different sizes (ARORA; PADUA, 2010).

The radius mean values of measured at 25 °C achieved shown table 1. The radius of chitosans ranged from 219 nm to 3083 nm. The ultrasonic irradiation resulted in the increase of the ratio of macromolecules with low *Rh*. The CS-LMW sample showed a major proportion of macromolecules with *Rh* of 3007 nm (72%) and a smaller proportion of 425 nm macromolecules *Rh* (18%), after ultrasound. The ultrasonic irradiation of CS-LMW chitosan by 30 min generate the CS-LMW-30 macromolecules with 492 nm and 2794 nm *Rh* values, with intensity of 93 and 26%, respectively. The CS-MMW is composed macromolecules of *Rh* values between 403 and 3083 nm with intensity of 47 and 31%, respectively. After the ultrasound irradiation for 30 min, it was yielded the CS-MMW-30 sample containing small macromolecules with *Rh* ranging from 218 to 482 nm with intensity of 67 and 28%, respectively.

Table 1. Hydrodynamic radius (*Rh*), intensity percentage of light scattering (% Intensity), polydispersity index (% PdI) measures by DLS and zeta potential (ζ) of chitosan samples.

Sample	**CS-LMW**		**CS-LMW-30**		**CS-MMW**		**CS-MMW-30**	
ζ potential (mV)	24.51±1.29		26.12±0.85		26.52±2.4		24.78±2.4	
Radius (nm)	425	3007	492	2794	403	3083	219	482
% Intensity	18.8	71.9	93.1	26.4	46.9	31.8	67.0	28.8
% PdI	4.49	4.24	1.83	2.88	3.4	1.8	3.3	3.8

The chitosan samples measures before (shaded column) and after irradiation (non-shaded column).

The ζ-potential represents the electrical potential of solutions and can represent the particle stability influence in suspension, through the electrostatic repulsion between particles. When the ζ-potential is high (close 30 mV), the suspension is more stable avoid particles agglomeration, due a higher electrostatic repulsion when comparing suspensions with lower ζ-potential values. (ARORA; PADUA, 2010)

7.3.2 MIC and MBC determination

The antimicrobial activity potential of both fibrils and ultrasound treated nanoparticles was evaluated. The MIC and MBC for the pre (CS-MMW e CS-LMW) and the post (CS-MMW30 e CS-LMW30) irradiated chitosan samples were evaluated against *E. coli*. It was also evaluated the influence of pH of the culture medium at the inhibitory activities (Table 2).

The MBC values are similar or higher than MIC ones. The chitosan concentrations used to kill and inhibit bacteria are very close. The chitosans, pre and post sonicated samples showed bactericidal behavior, acting (i) by the lysis of cell wall and/or cell membrane of target bacteria or (ii) by inhibiting DNA or RNA, injuring the replication nuclear process and/or gene transcription (YANG, C. et al., 2014). MIC values are in the range of 0.2 and 0.4 mg/mL, depending on pH of medium. The sample that showed to be more effective was CS-LMW30 and the less effective ones were CS-MMW and CS-MM30. The superior activity of CS-LMW and CS-LMW30 corroborate data from literature, where the chitosan activity is dependent on MW and DA (PATEL, J.; JIVANI, 2009).

Chitosans show low solubility in few weak environments as sodium acetate, pKa near 6.0. When pKa values are higher, the solubility is decreased, and may occur polymers precipitation. At pH just below pKa, chitosan shows polyelectrolytic behavior because of its charged amine radical (CÖLFEN et al., 2001). The protonation of chitosan cause it dispersion and turn it more effective against *E. coli*. MIC values against *E. coli* showed pH dependent, for CS-MMW (0.47 and 0.4) CS-MMW30 (0.4 and 0.28) and for CS-LMW (0.3 and 0.33) and CS-LMW30 (0.3 and 0.2), for pH 7.0 and 5.0 respectively.

The results showed here demonstrated that the production of nanoparticles by modification of the polymer chain length by ultrasound irradiation is a simple method and

dispersed the addition of acid solvent. The MW modifications provoke satisfactory changes in the antimicrobial potential of the nanoparticles produced.

Table 2. MIC and MBC from different chitosan samples against *E. coli* cells. Pre-sonicated, medium molecular mass (CS-MMW) and low molecular mass chitosans (CS-LMW) and post-sonicated medium molecular mass (CS-MMW30) and low molecular mass (CS-LMW30) chitosan samples had the MIC and MBC measured against E. coli (DH5α).

Sample	MIC (mg/mL)		MBC (mg/mL)	
	pH 7.0	pH 5.0	pH 7.0	pH 5.0
CS-MMW	0.47 ± 0.06^{a}	0.4 ± 0.00^{a}	0.4	0.4
CS-MMW30	0.4 ± 0.00^{a}	$0.28\pm0.03^{b,c}$	0.4	0.3
CS-LMW	0.3 ± 0.00^{b}	0.33 ± 0.06^{c}	0.3	0.3
CS-LMW30	0.3 ± 0.00^{b}	0.2 ± 0.00^{b}	0.4	0.2

Mean values ± standard deviations. Superscripts in the same column with different letters indicate significant differences ($p < 0.05$).

Low MIC value of 0.2 mg/mL was observed in pH 5.0, as expected for a polyelectrolyte with positive charged amine radicals, improving the bind of macromolecule to the negative charged plasmatic membrane of bacteria and/or interfering the replication nuclear process and/or gene transcription, this explanation need more investigation (KRISHNAN, 2001; LIU, H. et al., 2004).

7.3.3 Integrity of target-cell membrane

It was observed an increased in the OD_{260} measures, suggesting the release of nucleic acid material from *E. coli* cells in when chitosans were added at different concentrations, 0.5 and 1.0 mg/mL. The concentration of release of nucleic acids was affected by both chitosan concentration and incubation time and the results were compared with the cellular growth) (Fig. 1).

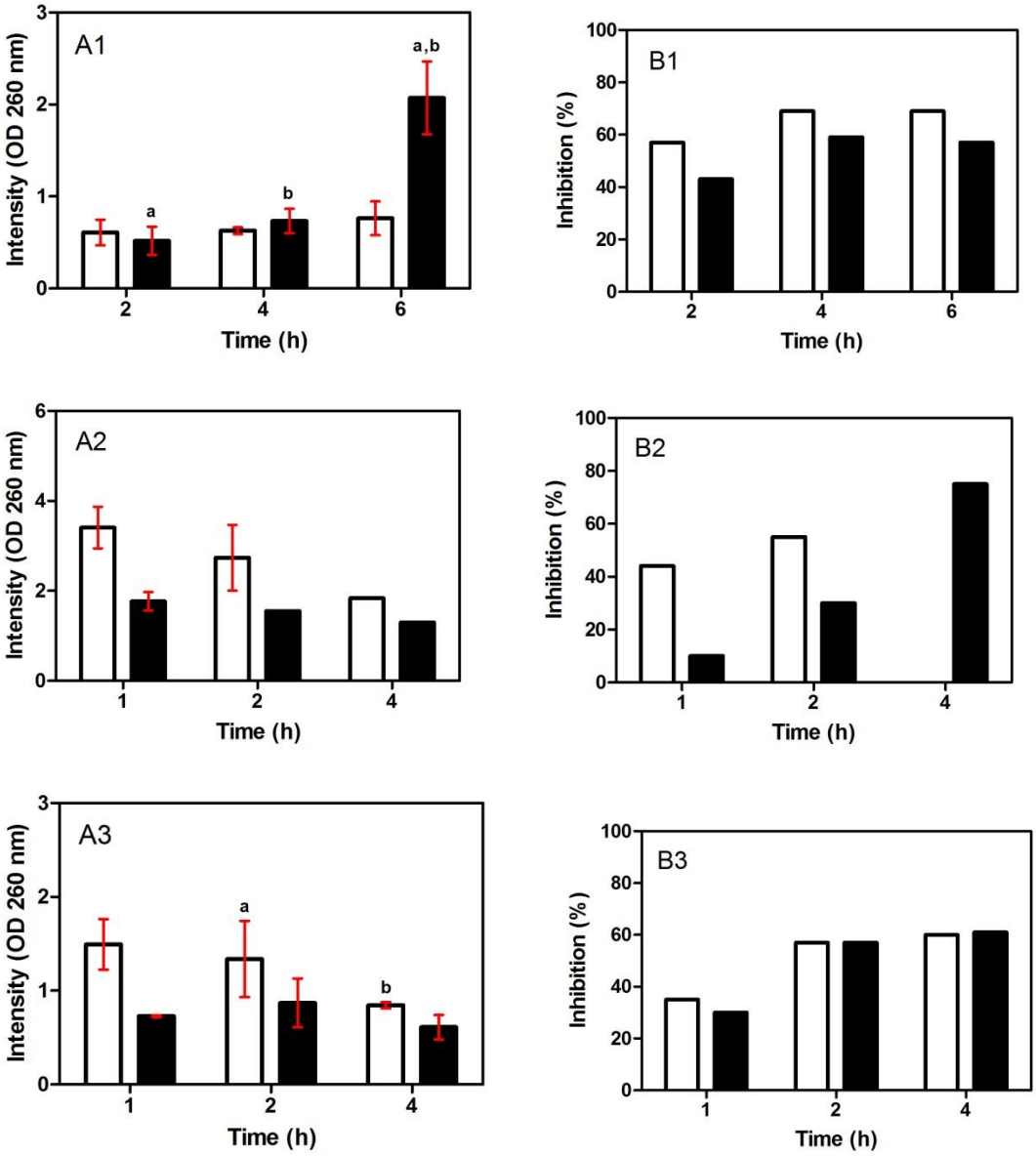

Figure. 1. The ratio release of nucleic acids and growth inhibition of *E. coli* cells. (A) Release of nucleic acids evaluated by increments in the absorbance at 260nm and (B) growth of inhibition (%) of *E. coli* cells harvested in LB medium at pH7.0. The white and black bars represent the growth inhibition at 0.5 and 1.0 mg/mL of chitosan solutions, respectively, in all panels. The numbers 1, 2 and 3 represent the CS-LMW, CS-MMW and CS-MMW30 in all panels, respectively. The samples with same letter showed significance difference, $p<0.05$.

The CS-LMW at the concentration of 0.5 mg/mL provoked a constant release of nucleic acids and the inhibition of cell growth near 70% after 4h of chitosan exposition (figure 1, panels A1 and B1). Chitosan treatment may cause minor damages to the cells keeping a constant inhibition. The release of nucleic acids and inhibition of growth by CS-MMW and CS-MMW30 seems to show similar and constant behavior (figure 1, panels A2, B2 and A3, B3). It seems that these samples form aggregates that interfere in the measurement of nucleic acids during the assay, because the encapsulation characteristic of chitosan aggregates nucleic acids molecules. The AGUDELO; KREPLAK; TAJMIR-RIAHI (2016) reported that linkage among DNA and chitosan occurs through electrostatic interactions between the polymer cationic charged NH_2 and negatively charged backbone phosphate groups. The phenomenon of aggregation can be deduced from the PdI and ζ-potential measures (Table 1) where it was observed a high % of inhibition but the concentration of nucleic acids is constant after 4 h of incubation.

In general, the highest increase in OD_{260}nm values provoked by CS-MMW and CS-MMW30 at both concentrations was obtained after 1h incubation (figure 1, panels A2 and A3), which is consistent with the results that was found under certain incubation times after treating the R22579 strains of *Xanthomonas* with chitosan (WANG, Y. et al., 2012). At the same time a growth inhibition was seen. After 4h incubation the % of inhibition is higher the 55% at all samples.

The difference in growth inhibition compared with the release of nucleic acids can be discussed considering the molecular weight. The smallest macromolecule can be enter through the plasmatic membrane altering the DNA transcription and killing more cells than the largermolecules that do not reduce the transit of nutrients from medium and kills the cells slowly but a relative growth of cells was detected.

Interestingly, the antibacterial mechanism of chitosan has been mainly attributed to the interaction between positive charge chitosan and the negative charge bacterial membrane, which may cause the leaking of low molecular weight compounds, nucleic acid and proteins (DINA RAAFAT et al., 2008; LI, X.-F. et al., 2010). Indeed, various studies performed recently have shown that this charge interaction can alter bacterial surface morphology and increase membrane permeability, causing leakage of intracellular substances. That phenomenon can reinforce the importance of the interaction between chitosan and bacterial

membrane (EATON et al., 2008; TANG, H. et al., 2010). The mode of action of chitosan against *E. coli* cells, may, at least partially, be attributed to this charge interaction between chitosan and bacteria. This indicated the complexity of the interactions between chitosan and bacterial membranes.

7.4 PARTIAL CONCLUSIONS

In this study, the physical and chemical characteristics of chitosan nanoparticles produced by ultrasound irradiation were evaluated and compared with its inhibition activity towards *E. coli in vitro*. Experimental figures and data presented have provided several evidences that chitosans NPs with low and medium molecular weights demonstrated strong inhibition activity against *E. coli*, but the inhibition activity differed in pH and MW, within the tested chitosans. The molecular weight and particle size/zeta potential allow an easy manipulation of physicochemical properties of nanoparticles suitable for its application. More experiments should help us go further to improve the understanding of the exact mode of action of chitosan nanoparticles and its antibacterial activity.

Acknowledgments

The authors acknowledge the financial support from Fundação Carlos Chagas Filho de Amparo à Pesquisa do Estado do Rio de Janeiro (FAPERJ, Rio de Janeiro, Brazil), Conselho Nacional de Desenvolvimento Científico e Tecnológico (CNPq, Brasília, Brazil), Coordenação de Aperfeiçoamento de Pessoal de Nível Superior (CAPES, Brasília, Brazil) and L.P.G. acknowledges CAPES (Programa Institucional de Bolsas de Doutorado Sanduíche no Exterior, PDSE; Proc nº 18935/12-5).

8 DISCUSSÃO

Nos últimos anos, o conceito de desenvolvimento sustentável tem obtido atenção política e social importante, devido à aplicação das "tecnologias verdes" e o uso de "produtos verdes", que contribuem para a sustentabilidade através da diminuição da degradação ambiental, estabelecendo melhores maneiras mais adequadas de sintetizar produtos necessários para o desenvolvimento em diferentes áreas, ao mesmo tempo reduzindo os impactos sobre o ambiente (DAHL et al., 2007).

A química verde explora técnicas de química e metodologias que reduzam ou eliminem o uso ou geração de matérias-primas, produtos, subprodutos, solventes, reagentes, etc., que são danosos à saúde humana ou ao ambiente (RAVEENDRAN et al., 2003).

Com isso vem crescendo a busca por alternativas mais ecológicas de produtos que se enquadrem no conceito da “tecnologia verde”, a fim de substituir produtos derivados de petróleo. As crescentes exigências da sociedade em matéria de sustentabilidade e proteção ambiental deverão desencadear uma profunda transformação na produção industrial. Neste sentido, o aproveitamento dos abundantes recursos de biomassa deverá preparar a sociedade para uma bioeconomia.

Biopolímeros naturais são recursos adequados para biofabricação de materiais ambientalmente adequados devido às características de biodegradabilidade, biocompatibilidade, e abundância. A quitosana é um polissacarídeo obtido por N-desacetilação da quitina, o seu precursor natural, que é extraído do exoesqueleto de crustáceos e insetos (DEL AGUILA et al., 2012) é considerada uma alternativa para substituição de derivados do petróleo na produção de embalagens, principalmente as destinadas à indústria de alimentos e cosméticos, devido à capacidade de serem processados como hidrogéis, membranas, micropartículas, nanopartículas coloidais (SHUKLA, SUDHEESH K. et al., 2013).

Na ultima década, a quitosana tem sido explorada como material para produção de nanopartículas, a fim de melhorar suas propriedades, devido as características diferenciadas que as moléculas nessa escala podem apresentar, tais como seu caráter único como o seu tamanho quântico pode resultar em nanopartículas de quitosana com atividades superiores, apresentando melhor potencial mucoadesivo de natureza hidrofílica e, por causa disso; podem

ser utilizadas para a encapsulação de drogas, controlando o tempo de liberação e conferindo maior estabilidade as drogas quando presentes no organismo.

Diante disso, novas formas de produção de nanopartículas vêm sendo desenvolvidas, sempre baseados no conceito da "tecnologia verde". A irradiação por ultrassom oferece um potencial importante para a conversão de biomassa polimérica, tais como carboidratos, em moléculas de menor massa molar (GOMES, LAIDSON P. et al., 2010; KANG et al., 2014; SAVITRI et al., 2014). O uso de ultrassom tem demonstrado ser uma ferramenta simples e econômica para a degradação de moléculas poliméricas. Através do controle da temperatura, frequência, intensidade, tempo de sonicação e da concentração polimérica em solução é possível controlar a extensão da degradação polimérica (KASAAI, MOHAMMAD R., 2008).

Nossos estudos exploraram o processo de sonicação a fim de produzir nanopartículas de quitosana de diferentes tamanhos usando as mesmas condições de sonicação, mas variando o tempo de irradiação de 5, 15 e 30 min.

As análises por DLS mostraram que a quitosana comercial,CHIT90 (NS), não tratada possui três tipos predominantes de moléculas com R_h = 0.02, 0.18 e 19.5 µm, com intensidades de 5.7, 46 e 48%, respectivamente. As imagens obtidas por AFM mostraram quitosanas com baixo peso molecular (LMCH-NPs), na forma de esferas de nanopartículas com diâmetros de 300 nm, sobre matriz com dimensões na escala micrométrica (HMCH-microfibras). Foi possível observar pela técnica de SEM, a coexistência das LMCH-NPs e HMCH-microfibras, nanofibras em torno de 150 nm e pequenas partículas esféricas variando entre 10-20 nm (não observadas por AFM) (SOUZA, H. K. S. et al., 2013). A distribuição de tamanhos de partículas observadas supõe a coexistência entre LMCH-NPs (R_h= 0.18 µm), HMCH-microfibras (R_h= 19.5 µm) e NPs (R_h=0.02 µm).

A partir da exposição gradual da CHIT90 (NS) à sonicação, foi observada degradação gradual da molécula de quitosana com o aumento do período de exposição à sonicação, verificando se uma diminuição da intensidade de HMCH-microfibras acompanhada do aumento concomitante na intensidade LMCH-NPs. As amostras NPs não apresentaram variação relevante durante os intervalos de sonicação e a contribuição das microfibras no espalhamento de luz diminuiu linearmente com o aumento do tempo de sonicação (*ts*). Concomitantemente, o aumento linear da % da intensidade das LMCH-NPs também pode ser notado confirmando que a degradação de HMCH-microfibra é responsável pelo aumento da população de LMCH-NPs.

A partir das soluções sonicadas (S) por *ts*= 5, 15 e 30 min foram feitas misturas entre elas e a amostra original CHIT90 (NS) em diferentes proporções NS/S(*ts*) 7:3, 1:1 e 3:7. As análises de AFM foram utilizadas para investigar as caraterísticas morfológicas das misturas NS:S(*ts*). A diferença na topografia das diferentes amostras está correlacionada com as diferentes misturas feitas e aos períodos de sonicação diferentes.

Em relação às misturas de *S*(5), a imagem da topografia da mistura 7:3 não se parece com uma imagem típica da base de mica. A presença de uma densa película de quitosana é sugerida, com uma espessura estimada em 2 nm a partir dos perfis de altura extraídos e acima desta camada pode ser distinguida estruturas semelhantes à fibras não ramificadas com o comprimento variando entre 0.5 e 1 μm, altura em torno de 4 nm e largura em torno de 40 nm. Aparentemente estas parecem formar feixes mais grossos de cerca de 100 nm que se organizam como redes. A alta densidade da película formada na camada inferior e a presença de fibras sobre essa camada são compatíveis com as análises de AFM e SEM reportadas para filmes constituídos apenas por *NS* CHIT90 e outros polímeros (SOUZA, H. K. S. et al., 2013) quando preparados a partir de soluções diluídas (<30 $\mu g \cdot mL^{-1}$).

Dois outros tipos de estruturas podem ser identificados na camada mais externa, partículas com diâmetro e altura em torno de 50 e 60 nm respectivamente e corpos de formas não definidas com tamanho maior que 150 nm e altura em tono de 10 nm na mistura 7:3 NS/S(5). A partir de dados obtidos da análise de DLS foi observado um aumento de 1,8 vezes no valor da % de intensidade dos picos referentes às partículas em torno de 200 nm LMCH-NPs, conforme o período exposição da CHIT90 a sonicação é aumentado. Comparando a altura individual das fibras e da película na camada inferior, supõe se que a última camada pode ser formada por uma monocamada de um amontanhado de HMCH-microfibras ou um conjugado de microfibras-NPs, sendo que a mistura avaliada (7:3 NS/S(5)) era constituída de 70% do material fibroso (*NS* CHIT90).

Pode ser visto nas imagens que as mudanças foram desencadeadas pelo aumento da quantidade de *S* (5) nas misturas. Duas tendências são bem evidentes nas imagens: (i) embora ocorra redução brusca das fibras, o aumento da presença de NPs esféricas na camada mais externa pode ser notado e (ii) a densidade da película inferior sofre uma significante redução. As análises de amplitude para as amostras S(15 e 30 min) não apresentam essas transições de fibras para LMCH-NPs de maneira evidente.

Essas transições ficam mais claras nas análises dos dados de R_{MS} e $H_{AV.}$ As amostras NS/S(5) apresentam pequenas mudanças com adição de S(5) na mistura 3:7 devido à presença

predominante das NPs na superfície, porém, as outras misturas 7:3 e 1:1 apresentaram uma distribuição mais homogênea entre NPs e fibras, o que explica as mudanças discretas nessas amostras.

Paras as amostras S(15 e 30 min) em contraste aos resultados obtidos por DLS, a altura das partículas observadas nas imagens topográficas (de AFM) apresenta um aumento ao ser acrescentado uma quantidade de S nas misturas. Tal aumento pode ser interpretado como ação do fenômeno de agregação na formação dos filmes, sendo que esse processo pode ocorrer em solução, antes da formação das películas ou através de um efeito dirigido a secagem, que envolve a formação de microgotículas (KRISHNAN, 2001; SOUZA, H. K. S. et al., 2013).

Em resumo foi observada uma transição morfológica a partir de um material rico em fibras microscópicas para outros com aspecto cada vez mais nanoparticulado, que é ocasionado pelo período de tempo (*ts*) crescente ou através da variação na proporção das misturas *NS:S*(t_S). A grande variedade de morfologias identificadas neste experimento mostra que este sistema é promissor para a fabricação de biofilmes de quitosana com propriedades ajustáveis.

A partir dessas misturas NS/S(*ts*) foram efetuados testes mecânicos durante o cisalhamento dinâmico 0 - 100 rad s^{-1} onde somente no caso da amostra NS os módulos de armazenamento (G') e de perda (G'') demonstram uma tendência a convergirem em valores acima do limite analisado, caracterizando um comportamento viscoelástico (HANAOR et al., 2012). Os dados obtidos para as amostras *S*(*ts*), de forma isolada, ilustram bem como o aumento do *ts* afeta a magnitude de ambos os módulos diminuindo em toda gama de frequências juntamente com o aumento da relação logG'' – log G'. Esses efeitos já foram avaliados em trabalho prévio e foi atribuído a continua diminuição na viscoelasticidade das soluções que ocorre em paralelo com o aumento do tempo de irradiação (SOUZA, H. K. S. et al., 2013). Esse comportamento indica uma diminuição contínua do emaranhado conforme a degradação progride. A redução do emaranhado polimérico é atribuída principalmente à diminuição da massa molar média, e aos efeitos correspondentes ao tamanho e morfologia dos coloides (o que já foi investigado por DLS).

Essas conclusões são mais evidentes após análise das curvas de $tan\ \delta$ *vs.* ω, que foram calculados a partir da relação $tan\ \delta = G''/G'$, onde os menores valores registrados foram obtidos para CHIT90 (*NS*) o que confirma a maior elasticidade dessa amostra. A partir do

aumento do *ts* de 0 a 30 min, a *tan* δ aumenta progressivamente refletindo a redução da elasticidade (aumentando o comportamento tipo liquido) das amostras sonicadas, sendo que S(30) mostrou o maior valor. Além disso, foram feitos cálculos para as diferentes misturas, as quais demonstraram que independente do *ts* aplicados, a redução da quantidade de CHIT90 (*NS*) nas misturas resultou na diminuição progressiva da elasticidade (aumentado o valor de *tan* δ) em toda gama de frequência e por consequência a diminuição da propriedade viscoelástica. Assim, dependendo da *ts* aplicada e da proporção de misturas *S* (*ts*), podem ser obtidas misturas exibindo diferentes propriedades viscoelástica, mas sempre dentro dos limites definidos pela resposta dos seus componentes puros.

Assim propriedades viscoelásticas da quitosana comercial podem ser ajustadas através da sua mistura com produtos da sua sonicação, verificando que a elasticidade das misturas resultantes pode ser eficazmente reduzida pelo aumento da fração do componente sonicado e/ou aumentando o tempo de exposição da CHIT90 sonicação.

A partir da combinação de dados de viscosidade aparente versus a taxa de cisalhamento foi possível evidenciar um comportamento independente do tempo, típico de fluidos não tixotrópicos, corroborando com o comportamento apresentado nos dados dinâmicos, os maiores valores da η_A em toda gama da taxa de cisalhamento foi exibido pela componente não sonicada, no caso das componentes sonicadas *S* (*ts*), a η_A mostrou uma redução a partir dos altos níveis da amostra *NS* com o aumento do *ts*.

Foi observado que na região inicial das analises de cisalhamento efetuado paras as amostras NS e S(*ts*), ocorre o rompimento dos entrelaçamentos intermoleculares por ação da força de cisalhamento é bem equilibrada pela formação de novos entrelaçamentos, de modo a não ocorrer mudança e a viscosidade no cisalhamento inicial é mantida. Entretanto o aumento da $\dot{\gamma}$, a perturbação do emaranhado torna se predominante sobre a formação e as moléculas tendem a se alinhar na direção do fluxo o que resulta na diminuição da viscosidade. O aumento do *ts* resulta em uma mudança dessa transição para valores mais elevados de $\dot{\gamma}$ e também reduz progressivamente a contribuição da pseudoplasticidade. Isso está bem ilustrado pela resposta quase que puramente Newtoniana registrada para a amostra *S* (30). Este comportamento ocorre devido à diminuição significativa no tamanho dos coloídes de quitosana (CHUNG et al., 2004; COTTER et al., 2005).

A pseudoplasticidade também foi diminuída nas misturas, conforme a diminuição da contração da amostra CHIT90 (*NS*) nas mesmas. Em particular, enquanto as misturas de *S* (5)

e (15) ainda exibiram algum tipo de decaimento da Lei das Potências, a mistura rica em *S* (30) demonstrou uma pseudoplasticidade quase insignificante. De maneira geral, esses resultados foram compatíveis com as conclusões descritas acima.

Fluidos poliméricos submetidos a transições de comportamento Newtoniano para pseudoplástico podem ser modelados segundo as equações de Cross e Carreau (CHIELLINI; SOLARO, 1996; SOUSA et al., 2013; TOMASIK; ZARANYIKA, 1995). Os dados coletados durante a execução da taxa de cisalhamento estacionária foram ajustados aos modelos simplificados acima. Em geral foi encontrado um bom ajuste para ambos os modelos, que apresentaram baixos valores de RSS e MRD. Os valores ligeiramente menores apresentados para o ajuste com o modelo de Cross, são um indicativo da melhor adequação deste para descrever os sistemas estudados. Fluidos Newtonianos são tipicamente caracterizados por valores de *M* e *N* que tendem a zero. Por tanto, a pseudoplasticidade decrescente está associada ao aumento do *ts*, coincidindo perfeitamente com a diminuição dessas constantes nas amostras sonicadas *S* (*ts*). No caso das misturas, as constantes diminuem em paralelo ao aumento da fração nanoparticulada nas misturas.

Por outro lado, os parâmetros τ e λ podem ser considerados constantes de relaxação, o que indica o aparecimento da pseudoplasticidade. A redução drástica destes parâmetros nas componentes sonicadas (em relação aos valores máximos registrados para amostras *NS*) confirma o efeito do tratamento ultrassônico sobre a resposta viscoelástica das soluções coloidais estudadas, refletindo a redução progressiva da resposta pseudoplástica caracterizando o aumento do comportamento tipo Newtoniano. No caso das misturas, os valores registrados foram sempre menores do que os valores apresentados para a componente pura sonicada e não sonicada.

Apesar de não existir uma ligação teórica entre os dados provenientes dos ensaios mecânicos de cisalhamento estacionário e dinâmico, Cox e Merz descreveram uma boa correlação empírica entre eles para certos sistemas. Mais especificamente apresentaram uma boa correlação entre a viscosidade aparente (η) no cisalhamento estacionário e a viscosidade complexa ($|\eta^*|$) no cisalhamento oscilatório, em comparação a valores iguais de taxa de cisalhamento e frequência, em soluções de polissacarídeos *random-coil* e de alguns polímeros sintéticos (TANG, H. et al., 2010). No entanto, mesmo nesses casos, a regra não é aplicada a altas frequências. A fim de estudar a aplicabilidade desta adaptação para investigar a relação entre as viscosidades aparente (η_A), complexa ($|\eta^*|$) e dinâmica (η'), essa regra foi aplicada

nas amostras *NS, S*(*ts*) e nas misturas 1:1. Esta regra não pode ser aplicada na amostra 1:1 *NS S* (5), onde um desvio entre as viscosidade pode ser observado em toda gama de cisalhamento analisada, o qual pode ser ocasionado pela deterioração da estrutura devido: (i) ao efeito da tensão de deformação aplicada ao sistema ou (ii) a diferentes tipos de rearranjos moleculares que ocorrem através do cisalhamento aplicado que pode ser ocasionado por interações de cadeia interpolímero específica, além da formação dos emaranhados (WRZYSZCZYNSKI et al., 1995).

As diferenças entre as viscosidades sob o cisalhamento oscilatório e estacionário foram claramente atenuadas quando *ts* foi aumentado. Por conseguinte, uma boa correlação foi encontrada para *S* (15) e (30) e suas misturas correspondentes, dento do intervalo de 0,1-10 s^{-1}. Estes resultados demonstram que o comportamento observado, ou seja, soluções/dispersões de quitosana com caráter fortemente Newtoniano parecem seguir a regra de Cox-Merz melhor do que aqueles que apresentam propriedades viscoelásticas maiores. Embora neste trabalho caso essas diferenças pareçam ser principalmente determinadas pelas mudanças da massa molar induzidas pelo tratamento com ultrassom.

Na ultima década, houve um grande interesse no desenvolvimento de utilização de películas ativas de origem biológica, que são caracterizadas por possuírem atividade antimicrobiana e antifúngica, a fim de melhorar a conservação de alimentos reduzindo a utilização de conservantes químicos. Moléculas biologicamente ativas como a quitosana e seus derivados tem um potencial significativo na indústria de alimentos. A fim de explorar essa possibilidade, a partir das amostras NS, S(*ts*) e as misturas NS/S(*ts*) 7:3, 1:1 e 3:7, foram produzidos filmes poliméricos homogêneos sem a adição de aditivos e plastificantes, através do método *knife coating.*

A influência da composição dos filmes NS, S(*ts*) e NS/S(*ts*) sobre seu comportamento mecânico foi estudada. Os filmes NS apresentaram valores de *TS, E* e Y de 82.8±2.7 MPa, 2.9±0.1% e 35.2±0.9 MPa respectivamente, como já relatado em trabalhos anteriores (SOUZA, H. K. S. et al., 2013).

A incorporação de nanopartículas nas soluções de fibras leva a um resultado tal que os filmes preparados com NS/S(*ts*) apresentaram uma resistência mecânica melhorada quando comparada com os seus precursores S(*ts*). Diferentes comportamentos foram observados dependendo da proporção da mistura usada. As amostras NS/S(15) apresentaram um ganho de força na mistura com a proporção 7:3 e 1:1, a qual apresentou maior valor entre todas as amostras. As amostras NS/S(5) apresentaram um ganho de força com o aumento da razão S(5)

nas misturas, sendo que o a maior ganho foi na mistura com proporção 3:7, indicada pela evolução do valor de TS. As formulações NS/S(30) não apresentaram variações expressivas.

As medidas de elasticidade (E) também sofreram variações dentre as formulações testadas. As misturas NS/S(5 e 15) apresentaram valores de E maiores que seus precursores NS e S(5 e 15), porém entre as misturas NS/S(15 e 30) não houve mudança significativa. Comportamento diferente do observado nas misturas NS/S(5) que apresentaram valores variados dentre as misturas.

O filme 7:3 e 1:1 NS/S(15) apresentaram melhor relação entre TS e E, apresentando valores maiores que de CHIT90 e duas vezes maiores que seu percursor S(15). A partir desses resultados pode se inferir que esse comportamento ocorre devido à característica da molécula obtida após esse período de sonicação (15 min), que contém um número maior de cadeias terminais livres que a amostra S(5), devido à fragmentação da cadeia pela sonicação. Esta fragmentação permite maior possibilidade de interação com a matriz do filme (CHIT90), e por ser um polímero com maior número de monômeros que as presentes na amostra S(30), possuem um número maior de ligações do tipo β→1,4, o que confere maior resistência ao filme (GOCHO et al., 2000).

Com relação ao Modulo de Young (Y) foram observadas propriedades distintas nos três grupos: (i) os filmes preparados com a mistura NS/S(5) apresentou valores de Y mais baixos do que os seus precursores NS e S; (ii) um comportamento oposto foi observado para os filmes obtidos com NS/S(15) e (iii) os filmes NS/S(30) apresentaram valores de Y mais baixos do que o filme NS e três vezes maior do que a amostra S(30). No entanto, para cada grupo, o aumento na proporção de nanopartículas nas formulações dos filmes não causa diferença em Y.

Estudos vêm demonstrando que nanopartículas de quitosana produzem novas interações através dos grupamentos amina e as cadeias terminais presentes na molécula da quitosana (ALBANNA et al., 2013; OSTROWSKA-CZUBENKO; GIERSZEWSKA-DRUŻYŃSKA, 2009). Em filmes produzidos a partir da mistura entre quitosana e alginato foi demonstrada a presença de uma rede tridimensional formada por reticulação química por ação das cadeias presentes na quitosana (OSTROWSKA-CZUBENKO; GIERSZEWSKA-DRUŻYŃSKA, 2009).

Os parâmetros avaliados confirmam a hipótese de que as misturas entre fibras e nanopartículas de quitosana resultam em filmes com melhores TS, E e Y. Neste sentido, nos filmes de quitosana NS/S(*ts*) produzidos, as nanopartículas parecem ter um contato maior com a matriz fibrosa dos filmes (CHIT90) devido a seu menor tamanho, favorecendo a possibilidade de ligações químicas cruzadas entra as mesmas e por consequência alterando as propriedades mecânicas dos filmes.

A possibilidade de controlar as características do filme que se deseja produzir através da variação do tempo de sonicação e da proporção de mistura, urge como uma alternativa para a substituição do uso de plastificantes, que podem ser transferidas da embalagem para o produto embalado, representando uma ameaça a saúde, e ainda sendo uma alternativa para substituição de produtos derivados de petróleo.

As propriedades de permeabilidade à água e absorção de água em filmes estão associadas à difusão de moléculas através da matriz do filme, representando a relação de equilíbrio entre o seu teor de umidade e da atividade da água (*aw*), que são necessários para prever as propriedades de filmes em diferentes ambientes. A amostra NS apresentou maior valor de WVP entre todas as amostras (14.2±1.1), seguido das amostras S(5), S(30) e S(15), 13.6±4.4, 7.8±2.0 e 7.9±0.7, respectivamente. Os valores apresentados para as misturas NS/S(*ts*) apresentaram redução quando comparados com a amostra NS, concluindo que com a adição das nanopartículas, independente do tempo de sonicação a WVP é melhorada.

Foi demonstrado recentemente que filmes preparados a partir de CHIT90, degradados por sonicação, exibem menor WVP, devido à formação de pequenas partículas esféricas de quitosana que devido aos seus domínios cristalinos aumentam a resistência à penetração do solvente (SOUZA, H. K. S. et al., 2013). Estes dados corroboram com os resultados aqui apresentados onde os filmes produzidos com amostras S(30), possuem a maior quantidade de partículas menores dentre as amostras estudadas, e apresentam os menores valores de WVP. Esse comportamento já foi observado em outros estudos, onde a adição de nanopartículas de quitosana foi efetiva no intuito de melhorar o efeito de barreira em filmes de poli(caprolactona) e metilcelulose (FABER et al., 2005; JANJARASSKUL; KROCHTA, 2010).

Isotermas de sorção são procedimentos importantes para avaliar o efeito da temperatura e da umidade relativa sobre propriedade dos filmes (LAI; PADUA, 1998). A adição e remoção de água podem causar alterações na estrutura macromolecular do filme (TORRES, 1994). O modelo de GAB foi usado para avaliação do comportamento das isotermas das amostras de filme NS, S e NS/S(*ts*). Todas as misturas avaliadas apresentaram um aumento de atividade de água 0,3-0,6 para os filmes produzidos com amostras puras. Os resultados apresentados pelos filmes NS e S (*ts*) apresentaram se semelhantes aos resultados já descritos por SOUZA, H. K. S. et al. (2013).

Como foi relatado nesse trabalho o processo de sonicação é capaz de produzir nanopartículas de quitosana com tamanhos variados, os quais apresentam três sítios de adsorção predominantes, os grupamentos hidroxila, amino e as cadeias terminais do polímero. Com a diminuição do tamanho de partícula ocorre um aumento do número de cadeias terminais por unidade de massa. Desse modo, novos sítios de adsorção são produzidos com a degradação do polímero (GOCHO et al., 2000).

A quantidade de água envolvida na adsorção de uma monocamada é quantitativamente (numa base seca) descrita pelos valores do parâmetro X_0 e o parâmetro C representa a energia entre a adsorção de uma ou mais monocamadas. As amostras NS/S(15 e 30) apresentaram valores maiores de X_0 que seus precursores, porem não apresentaram diferenças entre as misturas indicando que estes filmes apresentam o maior número de sítios de adsorção do que em uma monocamada de filmes secos.

Os resultados de sorção estão em linha com os resultados observados nas propriedades mecânicas. Uma vez que as nanopartículas presentes em S(15) apresentam um tamanho maior do que as presentes em S(30), e essa diferença de tamanho se reflete diretamente na quantidade de ligações β→1,4, logo quanto menor a partícula menos ligações desse tipo ela possui. Assim, a mistura de misturada NS com S(15) gera uma película mais resistente como já mencionado. Diferente de quando adicionado S(30) às misturas, foram produzidos filmes menos resistentes devido a essa deficiência de ligações β→1,4. Os filmes NS/S(30) apresentaram valores pequenos para C e esse comportamento pode ser definido pelo fato de as moléculas estarem menos fortemente ligadas aos sítios do polímero, como observado nas análises de SEM. Os filmes apresentaram uma morfologia homogênea em que essas partículas presentes em S(30) estão mais organizadas na matriz dos filmes, impedindo a ligação das

moléculas de água. Esse comportamento está de acordo com os resultados de WVP em que essas amostras apresentaram a maior redução desse parâmetro com adição das S(*ts*).

A determinação da cor é uma medida importante para a compreensão da imagem e descrição do objeto, utilizada para conferir a avaliação da qualidade e inspeção de produtos alimentares. Os filmes produzidos em geral, não apresentaram alterações de cor que comprometessem a sua transparência.

Com o intuito de explorar o potencial antimicrobiano da quitosana e de nanopartículas de quitosana, foi determinada a concentração mínima inibitória de amostras de quitosana comercial (de baixo e médio pesos moleculares) e as nanopartículas oriundas da sonicação das mesmas. O processo de sonicação foi eficaz na produção das nanopartículas como já foi demonstrado anteriormente. As amostras não apresentaram alteração no potencial zeta e tiveram uma polidispersividade variando entre 1.7 – 4.5 %. A atividade antimicrobiana foi testada contra *E. coli*, onde foi observado que o valor de pH do meio de cultura interfere na concentração mínima inibitória. A menor concentração inibitória observada foi conseguida para a amostra de menor massa molar (CS-LMW30) com mínimo de 0.2mg/mL. No ensaio *in vitro* foi possível observar que após 4 h de incubação com as diferentes amostras, todas apresentaram inibição do crescimento acima de 55%. Também pode ser observada, a integridade da membrana plasmática das células, quando foi testada a amostra CS-LMW, que apresentou um aumento na liberação de ácidos nucléicos com o decorrer do tempo experimental. Esses resultados são um indicativo de que a quitosana pode estar rompendo a membrana plasmática da célula e expondo o material genético da mesma, corroborando com os resultados apresentados pela cinética de inibição.

9 CONLUSÕES

A ultrassonicação demonstrou ser capaz de degradar a quitosana através do controle do tempo (*ts*) e da proporção de misturas (S(ts)/CHIT90) das soluções, resultando na formação de soluções coloidais, sob condições controladas, sendo possível com isso ajustar as propriedades viscoelásticas e a morfologia das soluções;

A partir das análises de AFM foi possível observar a presença de fibras e nanopartículas nas amostras estudas, além de observar a morfologia dos filmes formados;

A mistura (NS/S) na proporção 1:1 preparada com quitosana sonicada por 15 min se destaca como o sistema mais promissor devido à sua viscoelasticidade e morfologia homogênea;

Os filmes biofilmes produzidos a partir das misturas coloidais são, flexíveis com transparência e morfologia homogênea sem a adição de plastificantes.

As características mecânicas dos filmes e a permeabilidade ao vapor de água foram ajustadas através do controle das proporções NS/S(*ts*), onde os filmes produzidos com as proporções 7:3 e 1:1 NS/S(15) apresentaram um melhor equilíbrio entre as propriedades mecânicas avaliadas.

Os filmes reforçados com as amostras S(30) apresentaram melhor propriedades de permeabilidade ao vapor de água, sugerindo que essas moléculas menores se dispersão de forma mais homogênea entre a matriz do filme formada por CHIT90, preenchendo os espaços vazios e impedindo assim a passagem do vapor de água.

As preparações de misturas de quitosanas com distintas morfologias e massas moleculares mostraram-se adequados como precursores alternativos para a fabricação de filmes, com propriedades ajustáveis, para a embalagem de alimentos;

As concentrações mínimas inibitórias sofreram alterações com a mudança no pH do meio de cultivo de *E. coli*.

Os valores do MBC são iguais ou maiores aos valores encontrados para MIC, para *E. coli*, sendo a amostra CS-LMW30 apresentou maior atividade antimicrobiana, com MIC de 0.2 mg/mL em pH 5.0.

10 PESPECTIVAS FUTURAS

Determinar o potencial antimicrobiano dos filmes;

Determinar as mínimas concentrações inibitórias das nanopartículas (NPs) para microrganismos Gram positivos (ex. *Staphylococcus aureus*);

Avaliar a expressão genica através de qPCR dos genes envolvidos na síntese da membrana plasmática de patógenos alimentares (*Escherichia coli* e *Staphylococcus aureus*) ;

Determinar a massa molar das NPs por cromatografia de gel permeação associada aos detectores de índice de refração, viscosidade capilar e espalhamento de luz de duplo laser (15° e 90°);

Estudos dos mecânicos de inibição de crescimento de bactérias pela quitosana po ensaios de agregação celular, acompanhados por microscopia ótica e de fluorescência;

Analisar a integridade da membrana celular dos microrganismos por microscopia eletrônica de transmissão;

Associar as nanopartículas à moléculas com atividades biológicas, tais como quinonas e peptídeos com atividade antimicrobiana;

Determinar a eficiência de carreamento e liberação das moléculas associadas às NPs, (ex quinonas, peptídeos e ácidos nucleicos).

11 REFERÊNCIAS

ABUGOCH, L. E. et al. Characterization of quinoa protein–chitosan blend edible films. **Food Hydrocolloids,** v. 25, n. 5, p. 879-886, 7// 2011.

AGNIHOTRI, S. A.; MALLIKARJUNA, N. N.; AMINABHAVI, T. M. Recent advances on chitosan-based micro-and nanoparticles in drug delivery. **Journal of controlled release,** v. 100, n. 1, p. 5-28, 2004.

AGUDELO, D.; KREPLAK, L.; TAJMIR-RIAHI, H. A. Microscopic and spectroscopic analysis of chitosan–DNA conjugates. **Carbohydrate Polymers,** v. 137, p. 207-213, 2/10/ 2016.

AI, H. et al. Antioxidant, antifungal and antiviral activities of chitosan from the larvae of housefly, Musca domestica L. **Food Chemistry,** v. 132, n. 1, p. 493-498, 5/1/ 2012.

AIDER, M. Chitosan application for active bio-based films production and potential in the food industry: Review. **LWT - Food Science and Technology,** v. 43, n. 6, p. 837-842, 7// 2010.

AIEDEH, K.; TAHA, M. O. Synthesis of iron-crosslinked chitosan succinate and iron-crosslinked hydroxamated chitosan succinate and their in vitro evaluation as potential matrix materials for oral theophylline sustained-release beads. **European Journal of Pharmaceutical Sciences,** v. 13, n. 2, p. 159-168, 5// 2001.

AL-MUHTASEB, A. H.; MCMINN, W. A. M.; MAGEE, T. R. A. Water sorption isotherms of starch powders: Part 1: mathematical description of experimental data. **Journal of Food Engineering,** v. 61, n. 3, p. 297-307, 2// 2004.

ALBANNA, M. Z. et al. Chitosan fibers with improved biological and mechanical properties for tissue engineering applications. **Journal of the Mechanical Behavior of Biomedical Materials,** v. 20, n. 0, p. 217-226, 4// 2013.

ALBERTENGO, L. et al. Physico-chemical studies and emulsifying properties of N-propyl-N-methylene phosphonic chitosan. **Carbohydrate Polymers,** v. 92, n. 2, p. 1641-1646, 2/15/ 2013.

ANTONIOU, J. et al. Characterization of tara gum edible films incorporated with bulk chitosan and chitosan nanoparticles: A comparative study. **Food Hydrocolloids,** v. 44, n. 0, p. 309-319, 2// 2015.

ARGÜELLES-MONAL, W. et al. Rheological study of the chitosan/glutaraldehyde chemical gel system. **Polymer Gels and Networks,** v. 6, n. 6, p. 429-440, 1998.

ARORA, A.; PADUA, G. Review: nanocomposites in food packaging. **Journal of Food Science,** v. 75, n. 1, p. R43-R49, 2010.

ASHOKKUMAR, M.; GRIESER, F. Ultrasound assisted chemical processes. **Reviews in Chemical Engineering,** v. 15, n. 1, p. 41-83, 1999.

AZEVEDO, E. P. et al. Mechanical properties of cellulose: chitosan blends for potential use as a coronary artery bypass graft. **Journal of Biomaterials Science, Polymer Edition,** v. 24, n. 3, p. 239-252, 2013.

AZIZ, M. A. et al. Antimicrobial properties of a chitosan dextran-based hydrogel for surgical use. **Antimicrobial Agents and Chemotherapy,** v. 56, n. 1, 2012.

BASTOS, D. S. et al. Characterization of a chitosan sample extracted from Brazilian shrimps and its application to obtain insoluble complexes with a commercial whey protein isolate. **Food Hydrocolloids,** v. 24, n. 8, p. 709-718, 2010.

BAXTER, S.; ZIVANOVIC, S.; WEISS, J. Molecular weight and degree of acetylation of high-intensity ultrasonicated chitosan. **Food Hydrocolloids,** v. 19, n. 5, p. 821-830, 9// 2005.

BAYER, M. E.; SLOYER, J. L. The electrophoretic mobility of Gram-negative and Gram positive bacteria: an electrokinetic analysis. **Journal of General Microbiology** v. 136, p. 8, 1990.

BEANEY, P.; LIZARDI-MENDOZA, J.; HEALY, M. Comparison of chitins produced by chemical and bioprocessing methods. **Journal of Chemical Technology & Biotechnology,** v. 80, n. 2, p. 145-150, 2005.

BERNE, B. J.; PECORA, R. Dynamic light scattering with application to chemistry, biology and physics. **Courier Dover, New York**, 1976.

BITTELLI, M. et al. Reduction of transpiration through foliar application of chitosan. **Agricultural and Forest Meteorology,** v. 107, n. 3, p. 167-175, 4/2/ 2001.

BLAGODATSKIKH, I. V. et al. Influence of glucosamine on oligochitosan solubility and antibacterial activity. **Carbohydrate Research,** v. 381, n. 0, p. 28-32, 11/15/ 2013.

BODEK, K. H. Study on the rheological properties of microcrystalline chitosan hydrogels used as drug carriers. **Polimery,** v. 45, n. 11-12, p. 818-825, 2000.

BODMEIER, R.; MAINCENT, P. Polymeric dispersions as drug carriers. **Pharmaceutical dosage forms,** v. 3, p. 87-128, 1998.

BORGES, J.; CAMPIÑA, J. M.; SILVA, A. F. Chitosan biopolymer–F (ab′) 2 immunoconjugate films for enhanced antigen recognition. **Journal of Materials Chemistry B,** v. 1, n. 4, p. 500-511, 2013.

BORMAN, S. Push for new materials, chemicals from biomass sparks active R and D. **Chemical and Engineering News;(USA),** v. 68, n. 37, 1990.

BRUGNEROTTO, J. et al. Overview on structural characterization of chitosan molecules in relation with their behavior in solution. **Macromolecular Symposia,** v. 168, n. 1, p. 1-20, 2001.

BRUICE, T. C. A View at the Millennium: the Efficiency of Enzymatic Catalysis. **Accounts of Chemical Research,** v. 35, n. 3, p. 139-148, 2002/03/01 2002.

BRUNETTI, F. **Mecânica dos Fluidos**. São Paulo: Pearson Prentice Hall, 2008.

CARREAU, P. J. Rheological equations from molecular network theories. **Transactions of The Society of Rheology (1957-1977),** v. 16, n. 1, p. 99-127, 1972.

CARREAU, P. J.; DE KEE, D.; CHHABRA, R. P. **Rheology of polymeric systems: principles and applications**. Hanser Publishers Munich, 1997. ISBN 1569902186.

CHAMBERLAIN, E.; RAO, M. Rheological properties of acid converted waxy maize starches in water and 90% DMSO/10% water. **Carbohydrate Polymers,** v. 40, n. 4, p. 251-260, 1999.

CHANTARASATAPORN, P. et al. Water-based nano-sized chitin and chitosan as seafood additive through a case study of Pacific white shrimp (Litopenaeus vannamei). **Food Hydrocolloids,** v. 32, n. 2, p. 341-348, 8// 2013.

CHENG, G. X. et al. Studies on dynamic behavior of water in crosslinked chitosan hydrogel. **Journal of applied polymer science,** v. 67, n. 6, p. 983-988, 1998.

CHIBU, H. Effects of chitosan applications on the growth of several crops. 한국키틴키토산학회지**,** v. 5, n. 3, p. 182-182, 2000.

CHIELLINI, E.; SOLARO, R. Biodegradable polymeric materials. **Advanced Materials,** v. 8, n. 4, p. 305-313, 1996.

CHO, J. et al. Viscoelastic properties of chitosan solutions: Effect of concentration and ionic strength. **Journal of Food Engineering,** v. 74, n. 4, p. 500-515, 2006.

CHO, K. et al. Therapeutic nanoparticles for drug delivery in cancer. **Clinical cancer research,** v. 14, n. 5, p. 1310-1316, 2008.

CHO, S. Y.; RHEE, C. Sorption characteristics of soy protein films and their relation to mechanical properties. **LWT-Food Science and Technology,** v. 35, n. 2, p. 151-157, 2002.

CHOI, B.-K. et al. In vitro antimicrobial activity of a chitooligosaccharide mixture against Actinobacillus actinomycetemcomitans and Streptococcus mutans. **International Journal of Antimicrobial Agents,** v. 18, n. 6, p. 553-557, 2001.

CHUNG, Y.-C. et al. Relationship between antibacterial activity of chitosan and surface characteristics of cell wall. **Acta Pharmacologica Sinica,** v. 25, p. 932-936, 2004.

CHUNG, Y.-C.; YEH, J.-Y.; TSAI, C.-F. Antibacterial Characteristics and Activity of Water-Soluble Chitosan Derivatives Prepared by the Maillard Reaction. **Molecules,** v. 16, n. 10, p. 8504, 2011.

CIANNAMEA, E. M.; STEFANI, P. M.; RUSECKAITE, R. A. Physical and mechanical properties of compression molded and solution casting soybean protein concentrate based films. **Food Hydrocolloids,** v. 38, n. 0, p. 193-204, 7// 2014.

CÖLFEN, H.; BERTH, G.; DAUTZENBERG, H. Hydrodynamic studies on chitosans in aqueous solution. **Carbohydrate Polymers,** v. 45, n. 4, p. 373-383, 8// 2001.

COLINET, I. et al. Effect of chitosan coating on the swelling and controlled release of a poorly water-soluble drug from an amphiphilic and pH-sensitive hydrogel. **International Journal of Biological Macromolecules,** v. 47, n. 2, p. 120-125, 8/1/ 2010.

CONG, Y. et al. Importance of characterizing nanoparticles before conducting toxicity tests. **Integrated Environmental Assessment and Management,** v. 7, n. 3, p. 502-503, 2011.

COOKSEY, K. Effectiveness of antimicrobial food packaging materials. **Food Additives & Contaminants,** v. 22, n. 10, p. 980-987, 2005/10/01 2005.

COTTER, P. D.; HILL, C.; ROSS, R. P. Bacteriocins: developing innate immunity for food. **Nature Reviews Microbiology,** v. 3, n. 10, p. 777-788, 2005.

COX, W. P.; MERZ, E. H. Correlation of dynamic and steady flow viscosities. **Journal of Polymer Science,** v. 28, n. 118, p. 619-622, 1958.

CROSS, M. M. Rheology of non-Newtonian fluids: a new flow equation for pseudoplastic systems. **Journal of colloid science,** v. 20, n. 5, p. 417-437, 1965.

CRUZ-ROMERO, M.; KERRY, J. Packaging of cooked meats and muscle-based convenience-style food products. In: JOSEPH P. KERRY e JOHN F. KERRY (Ed.). **Processed Meats: Improving Safety, Nutrition and Quality**. July 2011: Elsevier, 2011. p.666. ISBN 978-1-84569-466-1.

CUERO, R. G.; OSUJI, G.; WASHINGTON, A. N-carboxymethylchitosan inhibition of aflatoxin production: Role of zinc. **Biotechnology Letters,** v. 13, n. 6, p. 441-444, 1991/06/01 1991.

CZECHOWSKA-BISKUP, R. et al. Degradation of chitosan and starch by 360-kHz ultrasound. **Carbohydrate Polymers,** v. 60, n. 2, p. 175-184, 2005.

DAHL, J. A.; MADDUX, B. L. S.; HUTCHISON, J. E. Toward Greener Nanosynthesis. **Chemical Reviews,** v. 107, n. 6, p. 2228-2269, 2007/06/01 2007.

DAVIDOVICH-PINHAS, M. et al. Modified chitosan: A step toward improving the properties of antibacterial food packages. **Food Packaging and Shelf Life,** v. 1, n. 2, p. 160-169, 6// 2014.

DE MOURA, M. R. et al. Improved barrier and mechanical properties of novel hydroxypropyl methylcellulose edible films with chitosan/tripolyphosphate nanoparticles. **Journal of Food Engineering,** v. 92, n. 4, p. 448-453, 6// 2009.

DE MOURA, M. R. et al. Highly Stable, Edible Cellulose Films Incorporating Chitosan Nanoparticles. **Journal of Food Science,** v. 76, n. 2, p. N25-N29, 2011.

DEBEAUFORT, F.; QUEZADA-GALLO, J.-A.; VOILLEY, A. Edible Films and Coatings: Tomorrow's Packagings: A Review. **Critical Reviews in Food Science and Nutrition,** v. 38, n. 4, p. 299-313, 1998/05/01 1998.

DEGROIS, M. et al. The effects of ultrasound on starch grains. **Ultrasonics,** v. 12, n. 3, p. 129-131, 5// 1974.

DEL AGUILA, E. M. et al. Biocatalytic production of chitosan polymers from shrimp shells, using a recombinant enzyme produced by pichia pastoris. **American Journal of Molecular Biology,** v. 2, p. 9, 2012.

DEVLIEGHERE, F.; VERMEULEN, A.; DEBEVERE, J. Chitosan: antimicrobial activity, interactions with food components and applicability as a coating on fruit and vegetables. **Food Microbiology,** v. 21, n. 6, p. 703-714, 12// 2004.

DINA RAAFAT et al. Insights into the Mode of Action of Chitosan as an Antibacterial Compound. **Applied and Environmental Microbiology,** v. 74, n. 12, 2008.

DUTTA, P. K. et al. Perspectives for chitosan based antimicrobial films in food applications. **Food Chemistry,** v. 114, n. 4, p. 1173-1182, 6/15/ 2009.

EATON, P. et al. Atomic force microscopy study of the antibacterial effects of chitosans on Escherichia coli and Staphylococcus aureus. **Ultramicroscopy,** v. 108, n. 10, p. 1128-1134, 9// 2008.

EISSA, H. A. Effect of chitosan coating on shelf life and quality of fresh-cut mushroom. **Journal of food quality,** v. 30, n. 5, p. 623-645, 2007.

EL-SAWY, N. M. et al. Radiation-induced degradation of chitosan for possible use as a growth promoter in agricultural purposes. **Carbohydrate Polymers,** v. 79, n. 3, p. 555-562, 2/11/ 2010.

EL-SHARIF, A. A.; HUSSAIN, M. H. M. Chitosan-EDTA new combination is a promising candidate for treatment of bacterial and fungal infections. **Current Microbiology,** v. 62, n. 3, 2011.

EL GHAOUTH, A. et al. Antifungal activity of chitosan on post-harvest pathogens: induction of morphological and cytological alterations in Rhizopus stolonifer. **Mycological Research,** v. 96, n. 9, p. 769-779, 9// 1992.

ELPINER, I. Action of ultrasonic waves on biomacromolecules. **Ultrasound, Physical, chemical and biological effects**, p. 149-230, 1964.

ELSABEE, M. Z.; ABDOU, E. S. Chitosan based edible films and coatings: A review. **Materials Science and Engineering: C,** v. 33, n. 4, p. 1819-1841, 5/1/ 2013.

FABER, C. et al. In vivo comparison of Dhvar-5 and gentamicin in an MRSA osteomyelitis prevention model. **Journal of Antimicrobial Chemotherapy,** v. 54, n. 6, p. 1078-1084, 2004.

FABER, C. et al. Comparable efficacies of the antimicrobial peptide human lactoferrin 1-11 and gentamicin in a chronic methicillin-resistant Staphylococcus aureus osteomyelitis model. **Antimicrobial agents and chemotherapy,** v. 49, n. 6, p. 2438-2444, 2005.

FAN, J.-M. et al. Preparation and characterization of kidney bean protein isolate (KPI)–chitosan (CH) composite films prepared by ultrasonic pretreatment. **Food Hydrocolloids,** v. 36, n. 0, p. 60-69, 5// 2014.

FERNANDES, S. C. et al. Novel transparent nanocomposite films based on chitosan and bacterial cellulose. **Green Chemistry,** v. 11, n. 12, p. 2023-2029, 2009.

FERNANDEZ, J. G.; INGBER, D. E. Manufacturing of Large-Scale Functional Objects Using Biodegradable Chitosan Bioplastic. **Macromolecular Materials and Engineering,** v. 299, n. 8, p. 932-938, 2014.

G, D. Effect of rosemary extract, chitosan and α-tocopherol on lipid oxidation and colour stability during frozen storage of beef burgers **Meat Science,** v. 75, n. 2, p. 256-264, 2007.

GARCíA-OLMEDO, F. et al. Antibiotic activities of peptides, hydrogen peroxide and peroxynitrite in plant defence. **FEBS letters,** v. 498, n. 2, p. 219-222, 2001.

GAVHANE, Y.; GURAV, A.; YADAV, A. Chitosan and its applications: a review of literature. **Int. J. Biomed. Pharm. Sci,** v. 4, p. 312-331, 2013.

GOCHO, H. et al. Effect of polymer chain end on sorption isotherm of water by chitosan. **Carbohydrate Polymers,** v. 41, n. 1, p. 87-90, 1// 2000.

GOMES, L. P. et al. Green Synthesis and Physical and Chemical Characterization of Chitosans with a High Degree of Deacetylation, Produced by a Binary Enzyme System. **Journal of Life Sciences,** v. 8, n. 3, p. 7, 2014.

GOMES, L. P. et al. Purificação e caracterização da quitinase de uva (Vitis vinífera L. cv Red Globe) para a produção de quitosana a partir de quitina de camarão. **Quimica nova,** v. 33, n. 9, p. 4, 2010.

GOMES, L. P. et al. Tweaking the mechanical and structural properties of colloidal chitosans by sonication. **Food Hydrocolloids,** v. 56, p. 29-40, 5// 2016.

HAMDINE, M.; HEUZEY, M.-C.; BÉGIN, A. Effect of organic and inorganic acids on concentrated chitosan solutions and gels. **International Journal of Biological Macromolecules,** v. 37, n. 3, p. 134-142, 2005.

HAN, C. et al. Edible coatings to improve storability and enhance nutritional value of fresh and frozen strawberries (Fragaria × ananassa) and raspberries (Rubus ideaus). **Postharvest Biology and Technology,** v. 33, n. 1, p. 67-78, 7// 2004.

HANAOR, D. et al. The effects of carboxylic acids on the aqueous dispersion and electrophoretic deposition of ZrO 2. **Journal of the European Ceramic Society,** v. 32, n. 1, p. 235-244, 2012.

HELANDER, I. M. et al. Chitosan disrupts the barrier properties of the outer membrane of Gram-negative bacteria. **International Journal of Food Microbiology,** v. 71, n. 2–3, p. 235-244, 12/30/ 2001.

HERNÁNDEZ-LAUZARDO, A. N. et al. Antifungal effects of chitosan with different molecular weights on in vitro development of Rhizopus stolonifer (Ehrenb.:Fr.) Vuill. **Carbohydrate Polymers,** v. 73, n. 4, p. 541-547, 9/5/ 2008.

HIRANO, S. et al. Chitinase Activity in Seeds Coated with Chitosan Derivatives. **Agricultural and Biological Chemistry,** v. 54, n. 10, p. 2719-2720, 1990.

HOMAYONI, H.; RAVANDI, S. A. H.; VALIZADEH, M. Influence of the molecular weight of chitosan on the spinnability of chitosan/poly (vinyl alcohol) blend nanofibers. **Journal of applied polymer science,** v. 113, n. 4, p. 2507-2513, 2009.

HONG, K. et al. Effects of chitosan coating on postharvest life and quality of guava (Psidium guajava L.) fruit during cold storage. **Scientia Horticulturae,** v. 144, n. 0, p. 172-178, 9/6/ 2012.

HOSOKAWA, J. et al. Biodegradable film derived from chitosan and homogenized cellulose. **Industrial & engineering chemistry research,** v. 29, n. 5, p. 800-805, 1990.

HWANG, K. T. et al. Properties of chitosan-based biopolymer films with various degrees of deacetylation and molecular weights. **Journal of Applied Polymer Science,** v. 89, n. 13, p. 3476-3484, 2003.

IKEDA, I. et al. Effects of chitosan hydrolyzates on lipid absorption and on serum and liver lipid concentration in rats. **Journal of Agricultural and Food Chemistry,** v. 41, n. 3, p. 431-435, 1993.

ING, L. Y. et al. Antifungal Activity of Chitosan Nanoparticles and Correlation with Their Physical Properties. **International Journal of Biomaterials**, p. 9, 2012.

IZIDORO, D. R. et al. Physical and chemical properties of ultrasonically, spray-dried green banana (Musa cavendish) starch. **Journal of Food Engineering,** v. 104, n. 4, p. 639-648, 6// 2011.

JANJARASSKUL, T.; KROCHTA, J. M. Edible Packaging Materials. **Annual Review of Food Science and Technology,** v. 1, n. 1, p. 415-448, 2010.

JAVANMARD, M. SHELF LIFE OF WHEY PROTEIN-COATED PISTACHIO KERNEL (PISTACIA VERA L.). **Journal of food process engineering,** v. 31, n. 2, p. 247-259, 2008.

JAYAKUMAR, R. et al. Chitosan conjugated DNA nanoparticles in gene therapy. **Carbohydrate Polymers,** v. 79, n. 1, p. 1-8, 2010.

JIA, Z.; SHEN, D.; XU, W. Synthesis and antibacterial activities of quaternary ammonium salt of chitosan. **Carbohydrate Research,** v. 333, n. 1, p. 1-6, 6/22/ 2001.

JONES, J. B. Enzymes in organic synthesis. **Tetrahedron,** v. 42, p. 3351-3403, 1986.

JUNG, B.-O. et al. Preparation of amphiphilic chitosan and their antimicrobial activities. **Journal of Applied Polymer Science,** v. 72, n. 13, p. 1713-1719, 1999.

KAHHAT, R.; WILLIAMS, E. Materials flow analysis of e-waste: Domestic flows and exports of used computers from the United States. **Resources, Conservation and Recycling,** v. 67, p. 67-74, 2012.

KANG, L.-X.; LIANG, Y.-X.; MA, L.-X. Novel characteristics of chitin deacetylase from Colletotrichum lindemuthianum: Production of fully acetylated chitooligomers, and hydrolysis of deacetylated chitooligomers. **Process Biochemistry,** v. 49, n. 11, p. 1936-1940, 11// 2014.

KASAAI, M. R. Calculation of Mark–Houwink–Sakurada (MHS) equation viscometric constants for chitosan in any solvent–temperature system using experimental reported viscometric constants data. **Carbohydrate Polymers,** v. 68, n. 3, p. 477-488, 4/5/ 2007.

_____. A review of several reported procedures to determine the degree of N-acetylation for chitin and chitosan using infrared spectroscopy. **Carbohydrate Polymers,** v. 71, n. 4, p. 497-508, 3/7/ 2008.

KASAAI, M. R.; ARUL, J.; CHARLET, G. Fragmentation of chitosan by ultrasonic irradiation. **Ultrasonics sonochemistry,** v. 15, n. 6, p. 1001-1008, 2008.

KATIYAR, D. et al. Future Perspective in Crop Protection: Chitosan and its Oligosaccharides. **Advances in Plants & Agriculture Research,** v. 1, n. 3, 2014.

KEAN, T.; THANOU, M. Biodegradation, biodistribution and toxicity of chitosan. **Advanced Drug Delivery Reviews,** v. 62, n. 1, p. 3-11, 1/31/ 2010.

KENDRA, D. F.; HADWIGER, L. A. Characterization of the smallest chitosan oligomer that is maximally antifungal toFusarium solani and elicits pisatin formation inPisum sativum. **Experimental Mycology,** v. 8, n. 3, p. 276-281, 9// 1984.

KHALID, M. et al. Swelling properties and mechanical characterization of a semi-interpenetrating chitosan/polyethylene oxide network: comparison with a chitosan reference gel. **STP pharma sciences,** v. 9, n. 4, p. 359-364, 1999.

KHUNAWATTANAKUL, W. et al. Novel chitosan−magnesium aluminum silicate nanocomposite film coatings for modified-release tablets. **International Journal of Pharmaceutics,** v. 407, n. 1–2, p. 132-141, 4/4/ 2011.

KIM, B. et al. Bactericidal effect of TiO2 photocatalyst on selected food-borne pathogenic bacteria. **Chemosphere,** v. 52, n. 1, p. 277-281, 7// 2003.

KIM, I.-Y. et al. Chitosan and its derivatives for tissue engineering applications. **Biotechnology advances,** v. 26, n. 1, p. 1-21, 2008.

KIM, K. M. et al. Properties of Chitosan Films as a Function of pH and Solvent Type. **Journal of Food Science,** v. 71, n. 3, p. E119-E124, 2006.

KIM, S.-K.; RAJAPAKSE, N. Enzymatic production and biological activities of chitosan oligosaccharides (COS): A review. **Carbohydrate Polymers,** v. 62, n. 4, p. 357-368, 12/14/ 2005.

KIM, S. et al. Chitosan–lignosulfonates sono-chemically prepared nanoparticles: Characterisation and potential applications. **Colloids and Surfaces B: Biointerfaces,** v. 103, n. 0, p. 1-8, 3/1/ 2013.

KITTUR, F. S.; VISHU KUMAR, A. B.; THARANATHAN, R. N. Low molecular weight chitosans—preparation by depolymerization with Aspergillus niger pectinase, and characterization. **Carbohydrate Research,** v. 338, n. 12, p. 1283-1290, 6/16/ 2003.

KNORR, D. Nutritional quality, food processing, and biotechnology aspects of chitin and chitosan: a review. **Process biochemistry.,** v. 21, n. 3, p. 90-92, 1986/06// 1986.

KOBAYASHI, S.; MAKINO, A. Enzymatic Polymer Synthesis: An Opportunity for Green Polymer Chemistry. **Chemical Reviews,** v. 109, n. 11, p. 5288-5353, 2009/11/11 2009.

KOBAYASHI, S.; SAKAMOTO, J.; KIMURA, S. In vitro synthesis of cellulose and related polysaccharides. **Progress in Polymer Science,** v. 26, n. 9, p. 1525-1560, 11// 2001.

KOBAYASHI, S.; UYAMA, H.; KIMURA, S. Enzymatic Polymerization. **Chemical Reviews,** v. 101, n. 12, p. 3793-3818, 2001/12/01 2001.

KONG, M. et al. Preparation and antibacterial activity of chitosan microshperes in a solid dispersing system. **Frontiers of Materials Science in China,** v. 2, n. 2, p. 214-220, 2008/06/01 2008.

KONG, M. et al. Antimicrobial properties of chitosan and mode of action: A state of the art review. **International Journal of Food Microbiology,** v. 144, n. 1, p. 51-63, 11/15/ 2010.

KRAJEWSKA, B. Membrane-based processes performed with use of chitin/chitosan materials. **Separation and Purification Technology,** v. 41, n. 3, p. 305-312, 2/15/ 2005.

KRISHNAN, H. B. Biochemistry and molecular biology of soybean seed storage proteins. **Journal of New Seeds,** v. 2, n. 3, p. 1-25, 2001.

KROCHTA, J. M.; MULDER-JOHNSTON, D. Edible and biodegradable polymer films: challenges and opportunities. **Food technology (USA)**, 1997.

KUMAR, H. N. et al. Compatibility studies of chitosan/PVA blend in 2% aqueous acetic acid solution at 30 C. **Carbohydrate Polymers,** v. 82, n. 2, p. 251-255, 2010.

KUMIRSKA, J. et al. Application of Spectroscopic Methods for Structural Analysis of Chitin and Chitosan. **Marine Drugs,** v. 8, n. 5, p. 1567, 2010.

KURITA, K.; KAMIYA, M.; NISHIMURA, S.-I. Solubilization of a rigid polysaccharide: Controlled partial N-Acetylation of chitosan to develop solubility. **Carbohydrate Polymers,** v. 16, n. 1, p. 83-92, // 1991.

KUZMA, J.; ROMANCHEK, J.; KOKOTOVICH, A. Upstream Oversight Assessment for Agrifood Nanotechnology: A Case Studies Approach. **Risk Analysis,** v. 28, n. 4, p. 1081-1098, 2008.

LAI, H.-M.; PADUA, G. W. Water Vapor Barrier Properties of Zein Films Plasticized with Oleic Acid. **Cereal Chemistry Journal,** v. 75, n. 2, p. 194-199, 1998/03/01 1998.

LAPLANTE, S.; TURGEON, S. L.; PAQUIN, P. Emulsion-stabilizing properties of chitosan in the presence of whey protein isolate: Effect of the mixture ratio, ionic strength and pH. **Carbohydrate polymers,** v. 65, n. 4, p. 479-487, 2006.

LAUTEN, R. A.; NYSTRÖM, B. Linear and nonlinear viscoelastic properties of aqueous solutions of cationic polyacrylamides. **Macromolecular Chemistry and Physics,** v. 201, n. 6, p. 677-684, 2000.

LECETA, I. et al. Characterization and antimicrobial analysis of chitosan-based films. **Journal of Food Engineering,** v. 116, n. 4, p. 889-899, 6// 2013.

LEUBA, J. L.; STOSSEL, P. Chitosan and Other Polyamines: Antifungal Activity and Interaction with Biological Membranes. In: MUZZARELLI, R.;JEUNIAUX, C., *et al* (Ed.). **Chitin in Nature and Technology**: Springer US, 1986. cap. 29, p.215-222. ISBN 978-1-4612-9277-7.

LI, J.; CAI, J.; FAN, L. Effect of sonolysis on kinetics and physicochemical properties of treated chitosan. **Journal of Applied Polymer Science,** v. 109, n. 4, p. 2417-2425, 2008.

LI, X.-F. et al. Chitosan kills Escherichia coli through damage to be of cell membrane mechanism. **Carbohydrate Polymers,** v. 79, n. 3, p. 493-499, 2010.

LINDEN, J. et al. Organic Disease Control Elicitors. **Agro FOOD Industry Hi Tech,** v. Oct, p. 12-15, 2000.

LIU, H. et al. Chitosan kills bacteria through cell membrane damage. **International Journal of Food Microbiology,** v. 95, n. 2, p. 147-155, 9/1/ 2004.

LIU, X. D. et al. Chitosan coated cotton fiber: preparation and physical properties. **Carbohydrate Polymers,** v. 44, n. 3, p. 233-238, 3// 2001.

LIU, Z. et al. Effects of chitosan molecular weight and degree of deacetylation on the properties of gelatine-based films. **Food Hydrocolloids,** v. 26, n. 1, p. 311-317, 2012.

LOPEZ, O. et al. Thermo-compression of biodegradable thermoplastic corn starch films containing chitin and chitosan. **LWT - Food Science and Technology,** v. 57, n. 1, p. 106-115, 6// 2014.

LORBER, B. et al. Protein analysis by dynamic light scattering: methods and techniques for students. **Biochemistry and Molecular Biology Education,** v. 40, n. 6, p. 372-382, 2012.

LU, Y. et al. Fabrication and characterisation of Î±-chitin nanofibers and highly transparent chitin films by pulsed ultrasonication. **Carbohydrate Polymers,** v. 98, n. 2, p. 1497-1504, 2013a.

_____. Fabrication and characterisation of α-chitin nanofibers and highly transparent chitin films by pulsed ultrasonication. **Carbohydrate Polymers,** v. 98, n. 2, p. 1497-1504, 11/6/ 2013b.

MADHUMATHI, K. et al. Development of novel chitin/nanosilver composite scaffolds for wound dressing applications. **Journal of Materials Science: Materials in Medicine,** v. 21, n. 2, p. 807-813, 2010.

MADUREIRA, A. R. et al. Production of antimicrobial chitosan nanoparticles against food pathogens. **Journal of Food Engineering,** v. 167, Part B, p. 210-216, 12// 2015.

MAEZAKI, Y. et al. Hypocholesterolemic Effect of Chitosan in Adult Males. **Bioscience, Biotechnology, and Biochemistry,** v. 57, n. 9, p. 1439-1444, 1993/01/01 1993.

MAGREZ, A. et al. Cellular Toxicity of Carbon-Based Nanomaterials. **Nano Letters,** v. 6, n. 6, p. 1121-1125, 2006/06/01 2006.

MARTÍNEZ-CAMACHO, A. P. et al. Chitosan composite films: Thermal, structural, mechanical and antifungal properties. **Carbohydrate Polymers,** v. 82, n. 2, p. 305-315, 9/5/ 2010.

MARTINS, A. F. et al. Characterization of N-trimethyl chitosan/alginate complexes and curcumin release. **International Journal of Biological Macromolecules,** v. 57, p. 174-184, 6// 2013.

MATE, J. I.; KROCHTA, J. M. Whey protein coating effect on the oxygen uptake of dry roasted peanuts. **Journal of Food Science,** v. 61, n. 6, p. 1202-1207, 1996.

MCHUGH, T. H.; KROCHTA, J. M. Sorbitol-vs glycerol-plasticized whey protein edible films: integrated oxygen permeability and tensile property evaluation. **Journal of Agricultural and Food Chemistry,** v. 42, n. 4, p. 841-845, 1994.

MEGHA AGARWAL et al. Chitosan Nanoparticles based Drug Delivery: an Update. **International Journal of Advanced Multidisciplinary Research,** v. 2, n. 4, p. 1-13, 2015.

MELO, K. C. D. Avaliação e modelagem reológica de fluido de perfuração base água. 2008.

MIMA, S. et al. Highly deacetylated chitosan and its properties. **Journal of Applied Polymer Science,** v. 28, n. 6, p. 1909-1917, 1983.

MIZRAHY, S.; PEER, D. Polysaccharides as building blocks for nanotherapeutics. **Chemical Society Reviews,** v. 41, n. 7, p. 2623-2640, 2012.

MOHANRAJ, V.; CHEN, Y. Nanoparticles-a review. **Tropical Journal of Pharmaceutical Research,** v. 5, n. 1, p. 561-573, 2007.

MOREIRA, M. D. R. et al. Antimicrobial Effectiveness of Bioactive Packaging Materials from Edible Chitosan and Casein Polymers: Assessment on Carrot, Cheese, and Salami. **Journal of Food Science,** v. 76, n. 1, p. M54-M63, 2011.

MOREIRA, M. D. R.; ROURA, S. I.; PONCE, A. Effectiveness of chitosan edible coatings to improve microbiological and sensory quality of fresh cut broccoli. **LWT - Food Science and Technology,** v. 44, n. 10, p. 2335-2341, 12// 2011.

MUZZARELLI; A, R. Chitosan composites with inorganics, morphogenetic proteins and stem cells, for bone regeneration. **Carbohydrate Polymers,** v. 83, n. 4, p. 1433-1445, 2011.

MUZZARELLI, R. A. A.; TOMASETTI, M.; ILARI, P. Deploymerization of chitosan with the aid of papain. **Enzyme and Microbial Technology,** v. 16, n. 2, p. 110-114, 2// 1994.

NADANATHANGAM VIGNESHWARAN et al. Functional finishing of cotton fabrics using zinc oxide–soluble starch nanocomposites. **Nanotechmology,** v. 17, n. 20, p. 5087-5095, 2006.

NADARAJAH, K. **Development and characterization of antimicrobial edible films from crawfish chitosan**. 2005. University of Peradeniya

NADARAJAH, K. et al. Sorption behavior of crawfish chitosan films as affected by chitosan extraction processes and solvent types. **Journal of Food Science,** v. 71, n. 2, p. E33-E39, 2006.

NAGPAL, K.; SINGH, S. K.; MISHRA, D. N. Chitosan Nanoparticles: A Promising System in Novel Drug Delivery. **Chemical and Pharmaceutical Bulletin,** v. 58, n. 11, p. 1423-1430, 2010.

NEL, A. et al. Toxic Potential of Materials at the Nanolevel. **Science,** v. 311, p. 5, 2006.

NIKOLAEV, A. et al. **THERMODYNAMICS OF SORPTION OF WATER-VAPOR BY FILMS OF CHITOSAN AND ITS DERIVATIVES**: PLENUM PUBL CORP CONSULTANTS BUREAU 233 SPRING ST, NEW YORK, NY 10013. 60**:** 209-210 p. 1987.

NO, H. K. et al. Stability and antibacterial activity of chitosan solutions affected by storage temperature and time. **Carbohydrate Polymers,** v. 65, n. 2, p. 174-178, 7/25/ 2006.

OBERDÖRSTER, G.; OBERDÖRSTER, E.; OBERDÖRSTER, J. Nanotoxicology: an emerging discipline evolving from studies of ultrafine particles. **Environmental health perspectives**, p. 823-839, 2005.

OCHEKPE, N. A.; OLORUNFEMI, P. O.; NGWULUKA, N. C. Nanotechnology and drug delivery part 2: nanostructures for drug delivery. **Tropical Journal of Pharmaceutical Research,** v. 8, n. 3, 2009.

OLABARRIETA, I. et al. Transport properties of chitosan and whey blended with poly (ε-caprolactone) assessed by standard permeability measurements and microcalorimetry. **Polymer,** v. 42, n. 9, p. 4401-4408, 2001.

OLIVAS, G.; BARBOSA-CÁNOVAS, G. Edible coatings for fresh-cut fruits. **Critical Reviews in Food Science and Nutrition,** v. 45, n. 7-8, p. 657-670, 2005.

OSTROWSKA-CZUBENKO, J.; GIERSZEWSKA-DRUŻYŃSKA, M. Effect of ionic crosslinking on the water state in hydrogel chitosan membranes. **Carbohydrate Polymers,** v. 77, n. 3, p. 590-598, 7/11/ 2009.

PAN, Y. et al. Bioadhesive polysaccharide in protein delivery system: chitosan nanoparticles improve the intestinal absorption of insulin in vivo. **International Journal of Pharmaceutics,** v. 249, n. 1, p. 139-147, 2002.

PAPINEAU, A. M. et al. Antimicrobial effect of water-soluble chitosans with high hydrostatic pressure. **Food Biotechnology,** v. 5, n. 1, p. 45-57, 1991/01/01 1991.

PARK, H. J.; CHINNAN, M. S. Gas and water vapor barrier properties of edible films from protein and cellulosic materials. **Journal of Food Engineering,** v. 25, n. 4, p. 497-507, // 1995.

PATEL, J.; JIVANI, N. Chitosan based nanoparticles in drug delivery. **Int J Pharmaceut Sci Nanotech,** v. 2, p. 517-522, 2009.

PATEL, M. P.; PATEL, R. R.; PATEL, J. K. Chitosan mediated targeted drug delivery system: a review. **Journal of Pharmacy & Pharmaceutical Sciences,** v. 13, n. 4, p. 536-557, 2010.

PAYNE, G. F.; RAGHAVAN, S. R. Chitosan: a soft interconnect for hierarchical assembly of nano-scale components. **Soft Matter,** v. 3, n. 5, p. 521-527, 2007.

PENG, Y.; LI, Y. Combined effects of two kinds of essential oils on physical, mechanical and structural properties of chitosan films. **Food Hydrocolloids,** v. 36, n. 0, p. 287-293, 5// 2014.

PERERA, U.; RAJAPAKSE, N. Chitosan Nanoparticles: Preparation, Characterization, and Applications. In: (Ed.). **Seafood Processing By-Products**: Springer, 2014. p.371-387. ISBN 146149589X.

PETERSEN, K. et al. Potential of biobased materials for food packaging. **Trends in Food Science & Technology,** v. 10, n. 2, p. 52-68, 1999.

PILLAI, C.; PAUL, W.; SHARMA, C. P. Chitin and chitosan polymers: Chemistry, solubility and fiber formation. **Progress in polymer science,** v. 34, n. 7, p. 641-678, 2009.

PITTS, K. F. et al. Co-effect of salt and sugar on extrusion processing, rheology, structure and fracture mechanical properties of wheat–corn blend. **Journal of Food Engineering,** v. 127, p. 58-66, 4// 2014.

QI, L. et al. Preparation and antibacterial activity of chitosan nanoparticles. **Carbohydrate Research,** v. 339, n. 16, p. 2693-2700, 11/15/ 2004.

RAMOS, Ó. L. et al. Effect of whey protein purity and glycerol content upon physical properties of edible films manufactured therefrom. **Food Hydrocolloids,** v. 30, n. 1, p. 110-122, 1// 2013.

RAO, V.; JOHNS, J. Mechanical properties of thermoplastic elastomeric blends of chitosan and natural rubber latex. **Journal of applied polymer science,** v. 107, n. 4, p. 2217-2223, 2008.

RATKOVICH, N. et al. Activated sludge rheology: a critical review on data collection and modelling. **Water research,** v. 47, n. 2, p. 463-482, 2013.

RAVEENDRAN, P.; FU, J.; WALLEN, S. L. Completely "Green" Synthesis and Stabilization of Metal Nanoparticles. **Journal of the American Chemical Society,** v. 125, n. 46, p. 13940-13941, 2003/11/01 2003.

REN, G. et al. Characterisation of copper oxide nanoparticles for antimicrobial applications. **International Journal of Antimicrobial Agents,** v. 33, n. 6, p. 587-590, 6// 2009.

RENAULT, F. et al. Chitosan for coagulation/flocculation processes – An eco-friendly approach. **European Polymer Journal,** v. 45, n. 5, p. 1337-1348, 5// 2009.

RESIN, F. **Analise da variabilidade de melhoria em um ferramental de conformação**. 2010. (Graduação). Universidade do estado de santa catariana.

REVERCHON, E.; ADAMI, R. Nanomaterials and supercritical fluids. **The Journal of Supercritical Fluids,** v. 37, n. 1, p. 1-22, 2// 2006.

RICHARDSON, R. K.; ROSS-MURPHY, S. B. Non-linear viscoelasticity of polysaccharide solutions. 1: Guar galactomannan solutions. **International Journal of Biological Macromolecules,** v. 9, n. 5, p. 250-256, 1987.

ROLLAND, J. P. et al. Direct Fabrication and Harvesting of Monodisperse, Shape-Specific Nanobiomaterials. **Journal of the American Chemical Society,** v. 127, n. 28, p. 10096-10100, 2005/07/01 2005.

ROLLER, S.; COVILL, N. The antifungal properties of chitosan in laboratory media and apple juice. **International Journal of Food Microbiology,** v. 47, n. 1–2, p. 67-77, 3/1/ 1999.

RONCAL, T. et al. High yield production of monomer-free chitosan oligosaccharides by pepsin catalyzed hydrolysis of a high deacetylation degree chitosan. **Carbohydrate Research,** v. 342, n. 18, p. 2750-2756, 12/28/ 2007.

ROSA, G. S.; MORAES, M. A.; PINTO, L. A. Moisture sorption properties of chitosan. **LWT-Food Science and Technology,** v. 43, n. 3, p. 415-420, 2010.

RUNGSARDTHONG, V. et al. Application of fungal chitosan for clarification of apple juice. **Process Biochemistry,** v. 41, n. 3, p. 589-593, 3// 2006.

S. SEKIGUCHI; Y. MIURA; H. KANEKO. **Molecular weight dependency of antimicrobial activity by chitosan oligomers**. Food Hydrocolloids: Structures, Properties, and Functions. New York, NY, USA: Plenum**:** 5 p. 1994.

SATO, A. C. K. et al. Food grade nanoparticles obtained from natural source ingredients. 2011.

SATO, H. et al. Determination of the Degree of Acetylation of Chitin/Chitosan by Pyrolysis-Gas Chromatography in the Presence of Oxalic Acid. **Analytical Chemistry,** v. 70, n. 1, p. 7-12, 1998/01/01 1998.

SAVITRI, E. et al. Degradation of chitosan by sonication in very-low-concentration acetic acid. **Polymer Degradation and Stability,** v. 110, n. 0, p. 344-352, 12// 2014.

SCHIFFMAN, J. D.; SCHAUER, C. L. Cross-Linking Chitosan Nanofibers. **Biomacromolecules,** v. 8, n. 2, p. 594-601, 2007/02/01 2007.

SCHIRMER, B. C. et al. A novel packaging method with a dissolving CO2 headspace combined with organic acids prolongs the shelf life of fresh salmon. **International Journal of Food Microbiology,** v. 133, n. 1–2, p. 154-160, 7/31/ 2009.

SCHRAMM, G. **A practical approach to rheology and rheometry**. Haake Karlsruhe, 1994.

SEBTI, I. et al. Water sensitivity, antimicrobial, and physicochemical analyses of edible films based on HPMC and/or chitosan. **Journal of Agricultural and Food Chemistry,** v. 55, n. 3, p. 693-699, 2007.

SESHADRI, R. et al. Ultrasonic processing influences rheological and optical properties of high-methoxyl pectin dispersions. **Food Hydrocolloids,** v. 17, n. 2, p. 191-197, 2003.

SHAO, X. et al. A Combination of heat treatment and chitosan coating delays ripening and reduces decay in. 2012.

SHELDON, R. A. Green solvents for sustainable organic synthesis: state of the art. **Green Chemistry,** v. 7, n. 5, p. 267-278, 2005.

SHUKLA, S. K. et al. Chitosan-based nanomaterials: A state-of-the-art review. **International journal of biological macromolecules,** v. 59, p. 46-58, 2013.

SHUKLA, S. K. et al. Chitosan-based nanomaterials: A state-of-the-art review. **International Journal of Biological Macromolecules,** v. 59, n. 0, p. 46-58, 8// 2013.

SIMPSON, B. K. et al. Utilization of chitosan for preservation of raw shrimp (Pandalus borealis). **Food Biotechnology,** v. 11, n. 1, p. 25-44, 1997/03/01 1997.

SINHA, V. R. et al. Chitosan microspheres as a potential carrier for drugs. **International Journal of Pharmaceutics,** v. 274, n. 1–2, p. 1-33, 4/15/ 2004.

SORLIER, P. et al. Relation between the Degree of Acetylation and the Electrostatic Properties of Chitin and Chitosan. **Biomacromolecules,** v. 2, n. 3, p. 765-772, 2001/09/01 2001.

SORLIER, P. et al. Light Scattering Studies of the Solution Properties of Chitosans of Varying Degrees of Acetylation. **Biomacromolecules,** v. 4, n. 4, p. 1034-1040, 2003/07/01 2003.

SOTHORNVIT, R. et al. Tensile properties of compression-molded whey protein sheets: Determination of molding condition and glycerol-content effects and comparison with solution-cast films. **Journal of Food Engineering,** v. 78, n. 3, p. 855-860, 2// 2007.

SOTHORNVIT, R.; RHIM, J.-W.; HONG, S.-I. Effect of nano-clay type on the physical and antimicrobial properties of whey protein isolate/clay composite films. **Journal of Food Engineering,** v. 91, n. 3, p. 468-473, 2009.

SOUSA, A. M. et al. Shaping the molecular assemblies of native and alkali-modified agars in dilute and concentrated aqueous media via microwave-assisted extraction. **Soft Matter,** v. 9, n. 11, p. 3131-3139, 2013.

SOUZA, B. W. S. et al. Influence of electric fields on the structure of chitosan edible coatings. **Food Hydrocolloids,** v. 24, n. 4, p. 330-335, 6// 2010.

SOUZA, H. K. S. et al. Ultrasound-assisted preparation of size-controlled chitosan nanoparticles: Characterization and fabrication of transparent biofilms. **Food Hydrocolloids,** v. 31, n. 2, p. 227-236, 6// 2013.

SOWJANYA, N. T. et al. Potential Applications of Chitosan Nanoparticles as Novel Support in Enzyme Immobilization. **Research Journal of Engineering and Technology,** v. 4, n. 4, p. 14, 2013.

SRINIVASA, P. C.; RAMESH, M. N.; THARANATHAN, R. N. Effect of plasticizers and fatty acids on mechanical and permeability characteristics of chitosan films. **Food Hydrocolloids,** v. 21, n. 7, p. 1113-1122, 10// 2007.

SUDARSHAN, N.; HOOVER, D.; KNORR, D. Antibacterial action of chitosan. **Food Biotechnology,** v. 6, n. 3, p. 257-272, 1992.

SUDARSHAN, N. R.; HOOVER, D. G.; KNORR, D. Antibacterial action of chitosan. **Food Biotechnology,** v. 6, n. 3, p. 257-272, 1992/01/01 1992.

SUN, X. et al. The antimicrobial, mechanical, physical and structural properties of chitosan–gallic acid films. **LWT - Food Science and Technology,** v. 57, n. 1, p. 83-89, 6// 2014.

SUSLICK, K. S.; PRICE, G. J. APPLICATIONS OF ULTRASOUND TO MATERIALS CHEMISTRY. **Annual Review of Materials Science,** v. 29, n. 1, p. 295-326, 1999/08/01 1999.

TAKAHASHIA, T. et al. Growth inhibitory effect on bacteria of chitosan membranes regulated by the deacetylation degree. **Biochemical Engineering Journal** v. 40, p. 6, 2008.

TAN, T. S. et al. Structural alterations, pore generation, and deacetylation of α- and β-chitin submitted to steam explosion. **Carbohydrate Polymers,** v. 122, n. 0, p. 321-328, 5/20/ 2015.

TANG, E. S. K.; HUANG, M.; LIM, L. Y. Ultrasonication of chitosan and chitosan nanoparticles. **International Journal of Pharmaceutics,** v. 265, n. 1–2, p. 103-114, 10/20/ 2003.

TANG, H. et al. Antibacterial action of a novel functionalized chitosan-arginine against Gram-negative bacteria. **Acta Biomaterialia,** v. 6, n. 7, p. 2562-2571, 2010.

TEZOTTO-ULIANA, J. V. et al. Chitosan applications pre- or postharvest prolong raspberry shelf-life quality. **Postharvest Biology and Technology,** v. 91, n. 0, p. 72-77, 5// 2014.

THAKHIEW, W.; DEVAHASTIN, S.; SOPONRONNARIT, S. Physical and mechanical properties of chitosan films as affected by drying methods and addition of antimicrobial agent. **Journal of Food Engineering,** v. 119, n. 1, p. 140-149, 11// 2013.

THATAI, S. et al. Nanoparticles and core–shell nanocomposite based new generation water remediation materials and analytical techniques: A review. **Microchemical Journal,** v. 116, n. 0, p. 62-76, 9// 2014.

TIKHONOV, V. E. et al. Bactericidal and antifungal activities of a low molecular weight chitosan and its N-/2(3)-(dodec-2-enyl)succinoyl/-derivatives. **Carbohydrate Polymers,** v. 64, n. 1, p. 66-72, 4/19/ 2006.

TOKURA, S. et al. Molecular weight dependent antimicrobial activity by Chitosan. **Macromolecular Symposia,** v. 120, n. 1, p. 1-9, 1997.

TOMASIK, P.; ZARANYIKA, M. F. Nonconventional methods of modification of starch. **Advances in carbohydrate chemistry and biochemistry,** v. 51, p. 243-318, 1995.

TORRES, J. A. Edible coatings and ®lms from proteins. **Protein functionality in food systems**, p. 467-507, 1994.

TSAI, G. J.; SU, W. H. Antibacterial activity of shrimp chitosan against Escherichia coli. **Journal of Food Protection** v. 62, p. 5, 1999.

TSIGOS, I. et al. Chitin deacetylases: new, versatile tools in biotechnology. **Trends in Biotechnology,** v. 18, n. 7, p. 305-312, 7/1/ 2000.

UCHIDA, Y.; M. IZUME; A. OHTAKARA. **Preparation of chitosan oligomers with purified chitosanase and its application,**. London, UK, : 1989. 9

USDA; EPA, N. A. **Rule on Chitosan**. Rules and Regulation: Federal Register. 72 2007.

VARGAS, M.; ALBORS, A.; CHIRALT, A. Application of chitosan-sunflower oil edible films to pork meat hamburgers. **Procedia Food Science,** v. 1, p. 39-43, 2011.

VASYUKOVA, N. et al. Modulation of plant resistance to diseases by water-soluble chitosan. **Applied Biochemistry and Microbiology,** v. 37, n. 1, p. 103-109, 2001.

VELICKOVA, E. et al. Impact of chitosan-beeswax edible coatings on the quality of fresh strawberries (Fragaria ananassa cv Camarosa) under commercial storage conditions. **LWT - Food Science and Technology,** v. 52, n. 2, p. 80-92, 7// 2013.

VU, K. D. et al. Development of edible bioactive coating based on modified chitosan for increasing the shelf life of strawberries. **Food Research International,** v. 44, n. 1, p. 198-203, 1// 2011.

WANG, R. H.; XIN, J. H.; TAO, X. M. UV-Blocking Property of Dumbbell-Shaped ZnO Crystallites on Cotton Fabrics. **Inorganic Chemistry,** v. 44, n. 11, p. 3926-3930, 2005/05/01 2005.

WANG, W. et al. A new green technology for direct production of low molecular weight chitosan. **Carbohydrate Polymers,** v. 74, n. 1, p. 127-132, 10/1/ 2008.

WANG, X.; DU, Y.; LIU, H. Preparation, characterization and antimicrobial activity of chitosan–Zn complex. **Carbohydrate Polymers,** v. 56, n. 1, p. 21-26, 5/17/ 2004.

WANG, Y. et al. Action of chitosan against Xanthomonas pathogenic bacteria isolated from Euphorbia pulcherrima. **Molecules,** v. 17, n. 6, p. 7028-7041, 2012.

WONG, C.-H.; WHITESIDES, G. M. **Enzymes in synthetic organic chemistry**. Academic Press, 1994. ISBN 0080359418.

WRZYSZCZYNSKI, A. et al. Blends of poly (ethylene oxide) with chitosane acetate salt and with dibuturylchitin: Structure and morphology. **Polymer Bulletin,** v. 34, n. 4, p. 493-500, 1995.

WU, D.; SUN, D.-W. Colour measurements by computer vision for food quality control – A review. **Trends in Food Science & Technology,** v. 29, n. 1, p. 5-20, 1// 2013.

XIA, W. et al. Biological activities of chitosan and chitooligosaccharides. **Food Hydrocolloids,** v. 25, n. 2, p. 170-179, 3// 2011.

XIE, W. et al. Preparation and antibacterial activity of a water-soluble chitosan derivative. **Carbohydrate Polymers,** v. 50, n. 1, p. 35-40, 10/1/ 2002.

YAMAN, Ö.; BAYOINDIRLI, L. Effects of an edible coating and cold storage on shelf-life and quality of cherries. **LWT-Food science and Technology,** v. 35, n. 2, p. 146-150, 2002.

YANG, C. et al. Inhibitory effect and mode of action of chitosan solution against rice bacterial brown stripe pathogen Acidovorax avenae subsp. avenae RS-1. **Carbohydrate Research,** v. 391, p. 48-54, 6/4/ 2014.

YANG, T.-C.; CHOU, C.-C.; LI, C.-F. Antibacterial activity of N-alkylated disaccharide chitosan derivatives. **International Journal of Food Microbiology,** v. 97, n. 3, p. 237-245, 1/1/ 2005.

YANG, Y. et al. Effect of chitosan on physiological activities in germinating seed and seedling leaves of maize. **Journal of Hebei Vocationtechnical Teachers College,** v. 15, n. 4, p. 9-12, 2000.

ZENG, D.; WU, J.; KENNEDY, J. F. Application of a chitosan flocculant to water treatment. **Carbohydrate Polymers,** v. 71, n. 1, p. 135-139, 1/5/ 2008.

ZHANG, L. et al. Development of nanoparticles for antimicrobial drug delivery. **Current Medicinal Chemistry,** v. 17, n. 6, 2010.

ZHANG, Y. et al. Determination of the degree of deacetylation of chitin and chitosan by X-ray powder diffraction. **Carbohydrate Research,** v. 340, n. 11, p. 1914-1917, 8/15/ 2005.

ZHONG, Z. et al. Synthesis of acyl thiourea derivatives of chitosan and their antimicrobial activities in vitro. **Carbohydrate Research,** v. 343, n. 3, p. 566-570, 2/25/ 2008.

ZIANI, K. et al. Antifungal activity of films and solutions based on chitosan against typical seed fungi. **Food Hydrocolloids,** v. 23, n. 8, p. 2309-2314, 12// 2009.

ZIANI, K. et al. Effect of the presence of glycerol and Tween 20 on the chemical and physical properties of films based on chitosan with different degree of deacetylation. **LWT - Food Science and Technology,** v. 41, n. 10, p. 2159-2165, 12// 2008.

ZOON, P. et al. Rheological properties of skim milk gels at various temperatures; interrelation between the dynamic moduli and the relaxation modulus. **Rheologica Acta,** v. 29, n. 3, p. 223-230, 1990.

ANEXO I

Hindawi Publishing Corporation

Hindawi

Eduardo Mere Del Aguila Update My Account Logout

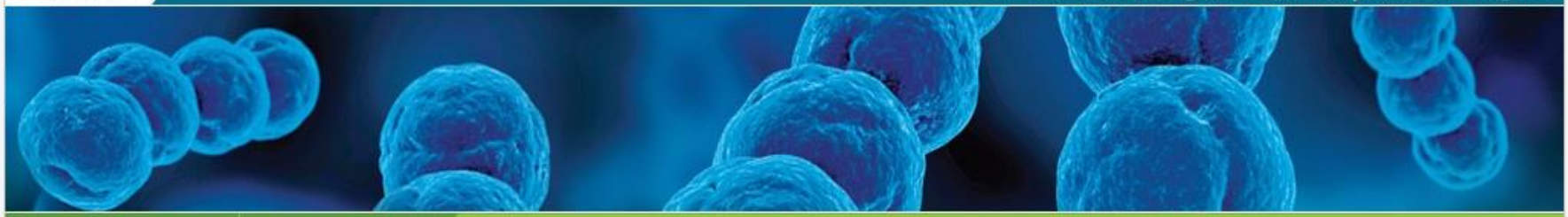

Submit a Manuscript | Author Activities

705378.v1 (Review Article)

Title	Chitosan nanoparticles: production by green chemistry, physicochemical properties and applications in food preservation
Journal	International Journal of Polymer Science
Issue	Polymers from Biomass: Characterization, Modification, Degradation, and Applications (PBCMDA)
Additional Files	Cover Letter
Manuscript Number	705378 (Review Article)
Submitted On	2015-08-28
Author(s)	Laidson Paes Gomes, Vânia M. F. Paschoalin, **Eduardo Mere Del Aguila**
Editor	Pratheep K. Annamalai
Status	Under Review

ANEXO II

CIQUP
Chemistry Research Unit
University of Porto

Dept. de Química e Bioquímica da Universidade do Porto
Rua do Campo Alegre, 687, 4169-007, Porto, Portugal

23th September 2015

Dear Dr. Fiszman,

Attached to this letter you may find our response to the concerns raised by the reviewers in the assessment of manuscript FOODHYD-D-15-00339. In the first place, we would like to thank the reviewers for their excellent job and interesting suggestions which will certainly contribute to improve the final quality of the manuscript. We agree with most of their claims and the relevant changes have been introduced in the manuscript (please, see the attached list of amendments).

In the attached rebuttal letter we reply to each specific claim, explaining the amendments made to the original manuscript or why we did not found it necessary. For clarity, the list of amendments is supplemented by a manuscript file with highlighted changes. A last revision was also applied in terms of the English usage to make it further easier to the reader.

I do hope that, after the changes, the manuscript is now ready for publication in Food Hydrocolloids

Sincerely yours,

Dr. José M. Campiña, Phone: (+351) 220402643,
Fax: (+351) 2260832959,
E-mail: jpina@fc.up.pt